NASA CR-72418

N68-33321
(ACCESSION NUMBER) 46
(PAGES) CR-72418
(NASA CR OR TMX OR AD NUMBER)
(THRU) 1
(CODE) 24
(CATEGORY)
FACILITY FORM 602

POLYMERIC POSITIVE EXPULSION BLADDERS FOR LIQUID OXYGEN SYSTEMS

by

J. T. Hoggatt

Prepared for

NATIONAL AERONAUTICS AND SPACE ADMINISTRATION

Lewis Research Center

Contract NAS 3-7952

SEP 1968
RECEIVED
NASA STI FACILITY
INPUT BRANCH

THE BOEING COMPANY

NOTICE

This report was prepared as an account of Government sponsored work. Neither the United States, nor the National Aeronautics and Space Administration (NASA), nor any person acting on behalf of NASA:

A.) Makes any warranty or representation, expressed or implied, with respect to the accuracy, completeness, or usefulness of the information contained in this report, or that the use of any information, apparatus, method, or process disclosed in this report may not infringe privately owned rights; or

B.) Assumes any liabilities with respect to the use of, or for damages resulting from the use of any information, apparatus, method or process disclosed in this report.

As used above, "person acting on behalf of NASA" includes any employee or contractor of NASA, or employee of such contractor, to the extent that such employee or contractor of NASA, or employee of such contractor prepares, disseminates, or provides access to any information pursuant to his employment or contract with NASA, or his employment with such contractor.

Requests for copies of this report should be referred to:

National Aeronautics and Space Administration
Office of Scientific and Technical Information
Attention: AFSS-A
Washington, D. C. 20546

NASA CR-72418

FINAL REPORT - PART I

POLYMERIC POSITIVE EXPULSION BLADDERS FOR LIQUID OXYGEN SYSTEMS

by
John T. Hoggatt

Prepared for
NATIONAL AERONAUTICS AND SPACE ADMINISTRATION
Lewis Research Center

June 1968

CONTRACT NAS 3-7952

Technical Management
NASA Lewis Research Center
Cleveland, Ohio
Liquid Rocket Technology Branch
Chemical Rocket Division
R. F. Lark

THE BOEING COMPANY
Aerospace Group
Seattle, Washington

FOREWORD

This report was prepared by The Boeing Company, Space Division, under NASA Contract NAS 3-7952. The work was administered by the Lewis Research Center, Liquid Rocket Technology Branch, Chemical Rocket Division, Cleveland, Ohio with Mr. Raymond F. Lark as program manager.

Contract NAS 3-7952, "Development of Liquid Oxygen Positive Expulsion Bladders" was a 23-month program (July 1966 to June 1968) consisting of three separate but related tasks. This final report covers the work performed under Task II and III (January 1967 to June 1968) of that program. Task I was reported in NASA document NASA-CR-72134, in January 1967.

In July 1968 a 6-month additional task, Task IV "Development of LOX Compatible Adhesives", was awarded and will be reported as Part II of this report at its completion.

Performance of this contract was under the direction of the Materials and Processes organization, Spacecraft Mechanics and Materials Technology, Space Division of The Boeing Company. Mr. C. D. Burns was Program Supervisor and Mr. J.T. Hoggatt Program Manager and Principal Investigator. Principal contributors to the program were:

Bladder Fabrication:	C. L. Lofgren R. E. Nelsen
Tank Design:	W. P. Haese R. V. Biegert
Tank Fabrication:	D. E. Gieseking
Testing:	F. O. Gray E. B. Kracht
Bladder Analysis:	A. D. VonVolkli

POLYMERIC POSITIVE EXPULSION BLADDERS FOR LIQUID OXYGEN SYSTEMS

by
John T. Hoggatt

ABSTRACT

This report covers the evaluation of eighteen polymeric expulsion bladders for the containment of liquid oxygen. The bladders, 10 of Mylar film and 8 of Kapton film construction, were evaluated for expulsion capability and endurance, and response to dynamic loading conditions in a liquid oxygen environment. Ten of the bladders were subjected to expulsion cycling with 25 complete cycles as the endurance goal. The remaining eight bladders experienced slosh, vibration, impact and burst type loadings to study their structural integrity and LOX compatibility.

CONTENTS

LIST OF TABLES

LIST OF ILLUSTRATIONS

LIST OF ILLUSTRATIONS (Continued)

LIST OF ILLUSTRATIONS (Continued)

LIST OF ILLUSTRATIONS (Continued)

1.0 INTRODUCTION

The development of a reliable and light-weight expulsion bladder is highly desireable for use in applications such as reaction control systems, multiple engine restarts, life support systems, and orbiting vehicle refueling. Of primary interest is the development of an expulsion system for cryogenic propellants to operate in a zero gravity environment to replace existing systems which utilize heavy and cumbersome pump and valve components for fluid transportation.

Metallic bellows and diaphragms have proven capable of repeated cycles at cryogenic temperatures, but these incur weight and volumetric efficiency penalties as well as shape limitations. Metallic bladders do not withstand repeated folding particularly three-corner folding, without pinholing or tearing.

Under NASA contracts polymeric expulsion bladders and diaphragms (References 4, 6 and 8) have been investigated for liquid nitrogen (-320°F) and liquid hydrogen (-423°F) service. These programs have shown that Mylar film and Kapton film are the best potential materials for polymeric bladders for cryogens. The feasibility of the polymeric bladders concept was also demonstrated.

Since polymeric bladders did demonstrate feasibility at temperatures of -320°F and -423°F, it is apparent that they should be functional at -297°F for liquid oxygen service.

With a liquid oxygen environment, the impact sensitivity of the bladder materials must be a prime consideration in addition to the bladders functional characteristics. Unfortunately both materials which have demonstrated the best potential for cryogenic bladders, Mylar and Kapton film, are considered LOX impact sensitive according to the Army Ballistic Missile Agency (ABMA)

liquid-oxygen impact sensitivity test (Kapton is marginal). In this test, an aluminum cup containing the specimen is placed on anvil; a striker pin is then placed on the specimen, and the cup filled with liquid oxygen. The impact energy of a calibrated weight falling on the striker pin is expended in deformation of the specimen. The energy level at which local heating is sufficient to cause the material and liquid oxygen to react is recorded. A minimum of 20 drops at 72 foot-pounds of energy without detonation or discoloration of the specimen is the generally accepted criteria for liquid-oxygen insensitivity.

Although Mylar and Kapton will react above 35 to 65 foot-pounds respectively in the ABMA test (Reference 3), it is quite possible that this level of energy will never be imposed on bladders in actual space systems during launch, in space, or during re-entry. Also, there is no certainty that the mode of application of the energy in an actual system will duplicate the results of the ABMA test. For example, impact energy received from a blow on the exterior of a propellant tank would be dissipated mostly in the outer plies of the bladder, which are not in contact with the liquid oxygen. It is probable that a higher level of impact energy can be tolerated in this case. In all but a completely filled tank, the entire bladder would not be forced into intimate contact with the tank wall. Also, vibration, rapid sloshing, and rapid expulsion type of excitations are not simulated in the ABMA test. It was the purpose of this program to determine the capability of polymeric materials as expulsion bladders to satisfy typical system requirements in a liquid oxygen environment and to establish whether or not the ABMA test is a reliable method of rating a material for LOX bladder useage.

This program was composed of the three following tasks:

TASK I - IMPACT SENSITIVITY TESTING
TASK II - STATIC EXPULSION TESTING
TASK III - DYNAMIC EXCITATION

Task I was completed in January 1967 and the work reported in NASA report CR-72134 "Compatibility of Polymeric Films with Liquid Oxygen" (Reference 1). Tasks II and III have been completed and are reported herein.

A 6-month extension contract was awarded The Boeing Company in July 1968 for the "Development of LOX Compatible Adhesives". The objective of the investigation, which will be reported as Task IV of this contract, is to develop an adhesive system for bonding Kapton which is insensitive to liquid oxygen. The results of the investigation will be reported as NASA report NASA CR-72418, "Final Report - Part II" at its conclusion.

2.0 SUMMARY

Ten polymeric expulsion bladders were evaluated for expulsion endurance and efficiency using liquid oxygen (-297°F) as the expelling fluid. In the expulsion tests two basic barrier films were evaluated in conjunction with three basic specimen configurations. The configurations were (1) 10 ply, 12-gore concept, (2) 5 ply, 12-gore concept and (3) a 5 ply, 6-gore concept. The two basic barrier ply materials were Mylar and Kapton polymeric films. Two of the bladders reached the program developmental goal of 25 expulsion cycles without failure. These were both 10 ply, 12-gore bladders fabricated from 1/2 mil Kapton polyimide film. Similar bladders fabricated from 1/4 mil Mylar polyester film reach a maximum of 17 cycles at -297°F before the tests were terminated due to excessive leakage.

The 5-ply, 12-gore and the 5-ply, 6 gore concepts did not perform well. Five cycles was the maximum number of expulsions achieved with 5-ply bladders.

The expulsion and fill efficiencies of the ten bladders averaged 82 and 84% respectively.

Following the expulsion tests, eight additional bladders, four of Kapton and four of Mylar film, were subjected to dynamic modes of excitation to study the structural capabilities and liquid oxygen compatibility of the materials in simulated service. The bladders were subject to sloshing and vibration, in both the horizontal and vertical mode, blunt impact, ballistic penetration and burst type loadings in a liquid oxygen environment. With exception of the ballistic penetration test, none of the loadings caused an extraneous reaction between the bladder materials with the propellant. The penetration tests which were conducted by firing a 30.06 caliber projectile into the propellant tank, did cause ignition of the polymeric bladders. The Mylar bladder merely charred

upon penetration but the Kapton bladder supported combustion and was completely consumed.

Both the expulsion and the dynamic tests demonstrated that it is very difficult to get sufficient energy into a polymeric bladder which is contained in a propellant tank to cause ignition or violent reaction of the bladder, even under abnormally high (216 ft-lb) impact loads.

3.0 TEST PROGRAM

3.1 TASK I - MATERIAL COMPATIBILITY TESTS

The prime objective of Task I was to select polymeric film materials and material configurations, for bladder fabrication in Task II and III, using the ABMA LOX impact sensitivity test as the initial screening criteria. The liquid oxygen impact energy threshold values of twenty different polymeric sample configurations were determined. The samples consisted of four basic polymeric films: 1/4-mil and 1/2-mil Mylar, 1/2-mil Kapton and 1/2-mil Kapton film coated both sides with 1/2-mil FEP Teflon; each in single and multi-ply configurations. TFE Teflon fabric was placed between the film plies of selected samples to investigate the possible decrease of the laminate impact sensitivity by increasing its energy absorbing capabilities. Each ply of the sample, including the fabric, contained a butt seam with an adhesive bonded reinforcing doubler on each side. The effects of a multi-ply sample, the influence of Teflon fabric as an energy absorbing media, and the effects of long term liquid oxygen exposure on the impact sensitivity level of a given material were determined. The impact sensitivity tests were conducted per the standard ABMA specification pertaining thereto (Reference 3) since this test method was determined to be the most reliable test for initial material screening. The material selection and specimen configurations were based solely on impending usage in expulsion bladder applications.

A detailed description of the Task I test program was published in NASA Report NASA CR-72134, "Compatibility of Polymeric Films with Liquid Oxygen", Reference 1. A summary of the impact test results are shown in Tables I and II and the pertinent conconclusions are stated below.

A. The program demonstrated that the ABMA test method for impact sensitivity determinations, which was designed for single-ply materials, could be adapted for multi-ply sample testing. However, the impact sensitivity results from multi-ply and single-ply tests do not appear to have a direct correlation. Multi-ply testing of a given material results in a greater "indicated" LOX

TABLE I - RESULTS - LOX IMPACT SENSITIVITY TESTS

Configuration	Barrier Film	No. of Barrier Plies	No. of Substrate Plies	Impact Energy Level [1] - kg-m									
				10	9	8	7	6	5	4	3	2	1
1	1/4-mil Mylar	1	-	1						1	0	0	0
2	1/4-mil Mylar	10	-	10						9		13	0
3	1/4-mil Mylar	20	-	20						9		4	0
4	1/4-mil Mylar	10	11	4	8	0		0		0			
5	1/4-mil Mylar	20	21	7				8		9	3	0	
6	1/2-mil Mylar	1	-	5				3		3	1	0	
7	1/2-mil Mylar	10	-	20						20		19	15
8	1/2-mil Mylar	20	-	20						19		16	3
9	1/2-mil Mylar	10	11	17						15		8	3
10	1/2-mil Mylar	20	21	20						7		6	0
11	1/2-mil Kapton	1	-	5				4	3	0		0	
12	1/2-mil Kapton	10	-	20						20		20	9
13	1/2-mil Kapton	20	-	20						20		2	2
14	1/2-mil Kapton	10	11	20						18		8	0
15	1/2-mil Kapton	20	21	20						11	2	0	
16	1/2-mil FEP-coated Kapton	1	-	1				1	5	0			
17	"	10	-	9						9	7	0	
18	"	20	-	9						9	9	0	
19	"	10	11	5				4	7	3	0		
20	"	20	21	18				8	13	0			
1-A [2]	1/4-mil Mylar	1	-							9	6	0	
6-A	1/2-mil Mylar	1	-							9		2	0
11-A	1/2-mil Kapton	1	-					16		10		1	
16-A	1/2-mil FEP-coated Kapton	1	-					12		3		0	

[1] Number of reactions out of 20 drops.

[2] -A denotes samples submerged 14 days in LOX.

TABLE II - RESULTS - LOX IMPACT SENSITIVITY TESTS ON PLAIN POLYMERIC MATERIALS

Material	Treatment	Impact Energy Level [3] - kg-m					
		10	8	6	4	2	1
1/4-mil Mylar	As-Received				1	0	
1/2-mil Mylar	As-Received (Lot 1)			1	0		
1/2-mil Mylar	As-Received (Lot 2)	2	0				
1/2-mil Kapton	Aged 24 hrs. at 450°F	0					
1/2-mil Kapton	As-Received [2]	0					
1/2-mil FEP on 1/2-mil Kapton	As-Received	0					
1/2-mil FEP on 1/2-mil Kapton	Aged 24 hrs. at 450°F	0					
TFE Fabric	Bleached	0					
Teflon-Kapton Laminate [1]	Aged 24 hrs. at 450°F	0					

[1] 1/2-mil FEP-1/2-mil Kapton film press laminated to both sides 1/2-mil FEP-1/2-mil Kapton-1/2-mil FEP film.

[2] Film sample supplied by NASA-LeRC.

[3] Number of reactions out of 20 test drops.

impact sensitivity than does the same material in single-ply form. Additional testing with a wider variety of materials is required to establish a limit of acceptability for multi-ply samples.

B. None of the twenty laminated configurations tested passed the ABMA impact acceptability requirement of 72 ft-lbs, even though in some samples all the individual material components are rated as LOX compatible. In subsequent tests it was verified that single plies of plain Kapton film, FEP coated Kapton and TFE Teflon fabric are LOX compatible (Table II).

C. The effects of long term LOX exposure upon the impact sensitivity of polymeric materials was established by submerging selected laminated samples in LOX for a period of 14 days and then testing. The exposure resulted in both a greater reactivity and a greater sensitivity to impact.

3.2 TASK II - POSITIVE EXPULSION TESTING

The objective of this task was to determine the cyclic expulsion performance of selected polymeric bladders in a liquid oxygen environment. The contract established a goal of 25 expulsion cycles (50 reversals) at -297°F without failure. The failure criteria was set at either a maximum leakage rate of 200 std cc/minute of gaseous helium at 1 psi differential or a fill/expulsion efficiency of less than 50%.

Ten polymeric film bladders were evaluated in this task, comparing two barrier film materials and three different construction configurations. Of prime concern in the evaluation were cyclic endurance, expulsion efficiency, LOX compatibility, and failure mode (if any) of each bladder.

3.2.1 MATERIAL SELECTION

For the Task II bladder construction, 1/4-mil Mylar and 1/2-mil Kapton films were selected as the barrier ply materials (Table III). This selection was based on the liquid oxygen impact tests conducted in Task I. It was first proposed that the barrier ply

TABLE III MATERIAL SELECTION

Material	Thickness	Description	Source
	Mils		
Mylar Film Type C	.25	Poly(ethylene terephthalate) film	E. I. DuPont
Kapton Film Type H	.50	Polyimide film	E. I. DuPont
GT-100 Adhesive	.50	Polyester Adhesive	G. T. Schjeldahl
GT-300 Adhesive	1.0	0.5 mil polyester adhesive on 0.5 mil mylar film	G. T. Schjeldahl
Teflon Fabric Style T-138	3.0	TFE Teflon fabric	Stern & Stern, Inc.

materials for Task II be selected from the LOX compatible specimen configurations from Task I. That is, the barrier film selections would qualify to the ABMA LOX impact test. Unfortunately none of the seamed configurations tested in Task I successfully met the 72 ft-lb ABMA test requirement. Therefore, one Kapton and one Mylar film seamed configuration was chosen for Task II by selecting the configuration of the respective materials having (1) the highest impact threshold level, and (2) the best known cryogenic flexibility. One-fourth mil Mylar was chosen because it had a higher threshold level and also possessed greater cryogenic flexibility (References 4 and 7) than 1/2-mil Mylar. The better cryogenic flexibility (Reference 7) of 1/2-mil Kapton film over Teflon (FEP) coated Kapton was the governing factor in its selection.

Heat cleaned and dimensionally stabilized Style T-138 Teflon fabric (Table III) was chosen as the abrasion (substrate) ply material. This material is flexible at -297°F and LOX impact insensitive (Table II).

Polyester tape adhesives, GT-100 and GT-300, were used as the adhesive systems (Table III) for bladder fabrication. GT-100 is a thermoplastic tape adhesive without a film carrier, while GT-300 is the same adhesive applied to one side of a Mylar film which serves as a carrier. Both are excellent adhesives for bladder fabrication, but are LOX impact sensitive (Reference 1). They represent a poor choice for use in a liquid oxygen system, but unfortunately there were no other commercially available adhesive systems with improved LOX compatibility which possessed the desired characteristics for bladder fabrication. The polyester adhesives were then used realizing the choice as a compromising one.

The material selections in Table III were concurred with and approved by the NASA program manager.

3.2.2 SPECIMEN CONFIGURATION

The test bladders for Task II consisted of ten polymeric bladders; comparing two basic barrier ply materials, and three configurations. Mylar (1/4-mil) and Kapton (1/2-mil)

films were the barrier ply materials, while the three configurations consisted of: (1) 10-ply with 12-gores per ply; (2) 5-ply with 6-gores per ply and (3) 5-ply with 12-gores per ply. A typical bladder is illustrated in Figure 1.

Each bladder was nominally 12" in diameter with two stems geometrically opposed to one another. Definition of each major component of the bladder is as follows:

Barrier Ply - A layer of polymeric film used to separate the cryogen from the pressurizing gas. This is the structural film of the bladder. Each barrier ply is constructed from individual gores, adhesively bonded together.

Abrasion Ply - The abrasion plies are a layer of Teflon fabric placed on the interior and exterior of the bladder to protect the barrier plies and to prevent the bladder from sealing against the tank wall during filling and against the standpipe during expulsion. The abrasion plies are not structural members of the bladder.

Substrate Ply - The substrate plies are of the same material and construction as the abrasion plies except they are located between barrier plies and serve to structurally reinforce the bladder and to minimize sharp folding in the bladder.

Specimens No. 2, 3, 4, 5, 6 and 7 were 10 ply-12 gore bladders with 2 abrasion plies and 1 substrate ply (Table IV). Bladders 4, 5, 6, and 8 were made with Kapton film as the barrier ply material while bladders 1, 2, 3, 7, 9 and 10 used Mylar film.

Specimens No. 1, 8 and 9 were 5 ply-12 gore bladders used to evaluate the effect or reducing the number of barrier film plies from 10 to 5. The bladders had two abrasion plies, one on each the interior and exterior surfaces. No substrate plies were used.

Specimen No. 10 represented a radical change in that its configuration consisted of 5 plies with only 6 gores per ply. This bladder compared the performance of a 12-gore bladder with that of a 6-gore bladder. By reducing the number of gores, the

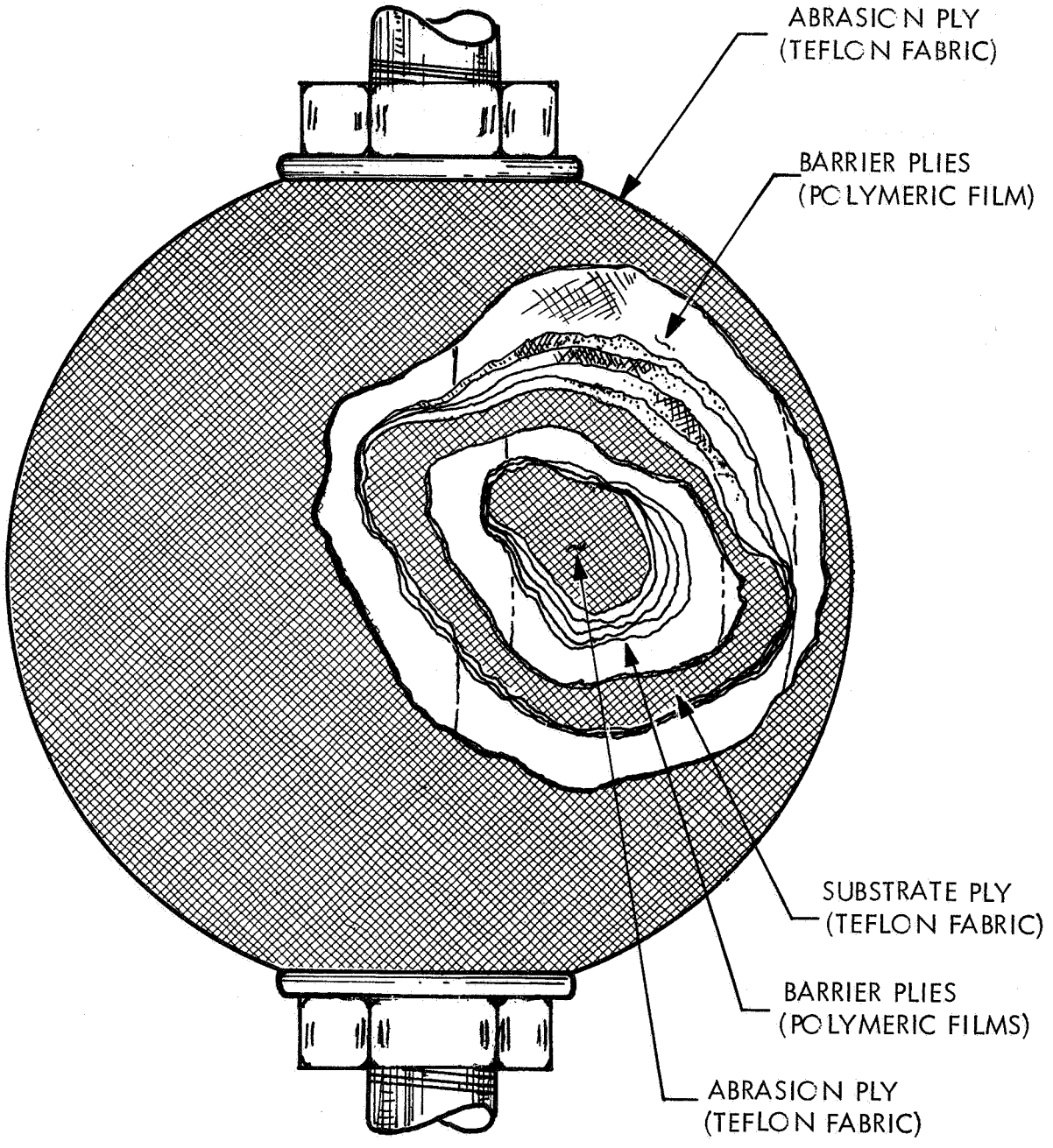

FIGURE 1 TYPICAL EXPULSION BLADDER

TABLE IV EXPULSION BLADDER CONFIGURATIONS - TASK II

BLADDER NUMBER	BARRIER FILM PLIES				NUMBER OF ABRASION PLIES	NUMBER OF ▷ SUBSTRATE PLIES
	Material	Thickness (mils)	No. of Plies	Gores per ply		
1	Mylar	0.25	5	12	2	0
2	Mylar	0.25	10	12	2	1
3	Mylar	0.25	10	12	2	1
4	Kapton	0.50	10	12	2	1
5	Kapton	0.50	10	12	2	1
6	Kapton	0.50	10	12	2	1
7	Mylar	0.25	10	12	2	1
8	Kapton	0.50	5	12	2	0
9	Mylar	0.25	5	12	2	0
10	Mylar	0.25	5	6	2	0

▷ Located between 5th and 6th barrier film plies

adhesive buildup in the stem area is reduced, thus increasing the flexibility in that region. To make a spherical 6-gore bladder it was necessary to thermoform the Mylar film into 60° arc segments of a sphere. The procedure used for thermoforming is discussed in Section 3.2.3.

Permeability tests were conducted on samples of thermoformed Mylar and it was observed that a 2 to 3 fold increase in the helium permeability rate occurred due to the forming operation (Reference 7). There was some concern that this increase would cause substantial inner-ply inflation of the bladder but as it turned out this did not affect the bladder (see Section 3.2.6 for test results).

3.2.3 SPECIMEN FABRICATION

A total of 18 bladders, 10 for Task II and 8 for Task III, were fabricated in this program. Each bladder was nominally 12" in diameter with two fittings (Figure 1). Although the material construction, number of plies and sequence varied, the basic fabrication techniques were the same and are as follows:

3.2.3.1 Materials - The materials used for bladder fabrication are shown in Table III. All materials were standard commercial grades and inspected for quality by The Boeing Company prior to use.

3.2.3.2 Mandrel - The bladder mandrels were hollow slosh-cast soluble plaster spheres as shown in Figure 2. Enclosed within the sphere, during its fabrication, were the bladder attachment stems (Figure 3). The stems were LOX cleaned per Reference 12 and then sealed on the mandrel support rod in an "Aclar"* film bag for protection.

After the plaster was completely dry, the mandrel was removed from the mold and covered with a Mylar protective film to keep the interior plies of the expulsion bladder from being contaminated with plaster dust. This protective layer was made by forming 1/2-mil Mylar

*Allied Chemical Corporation

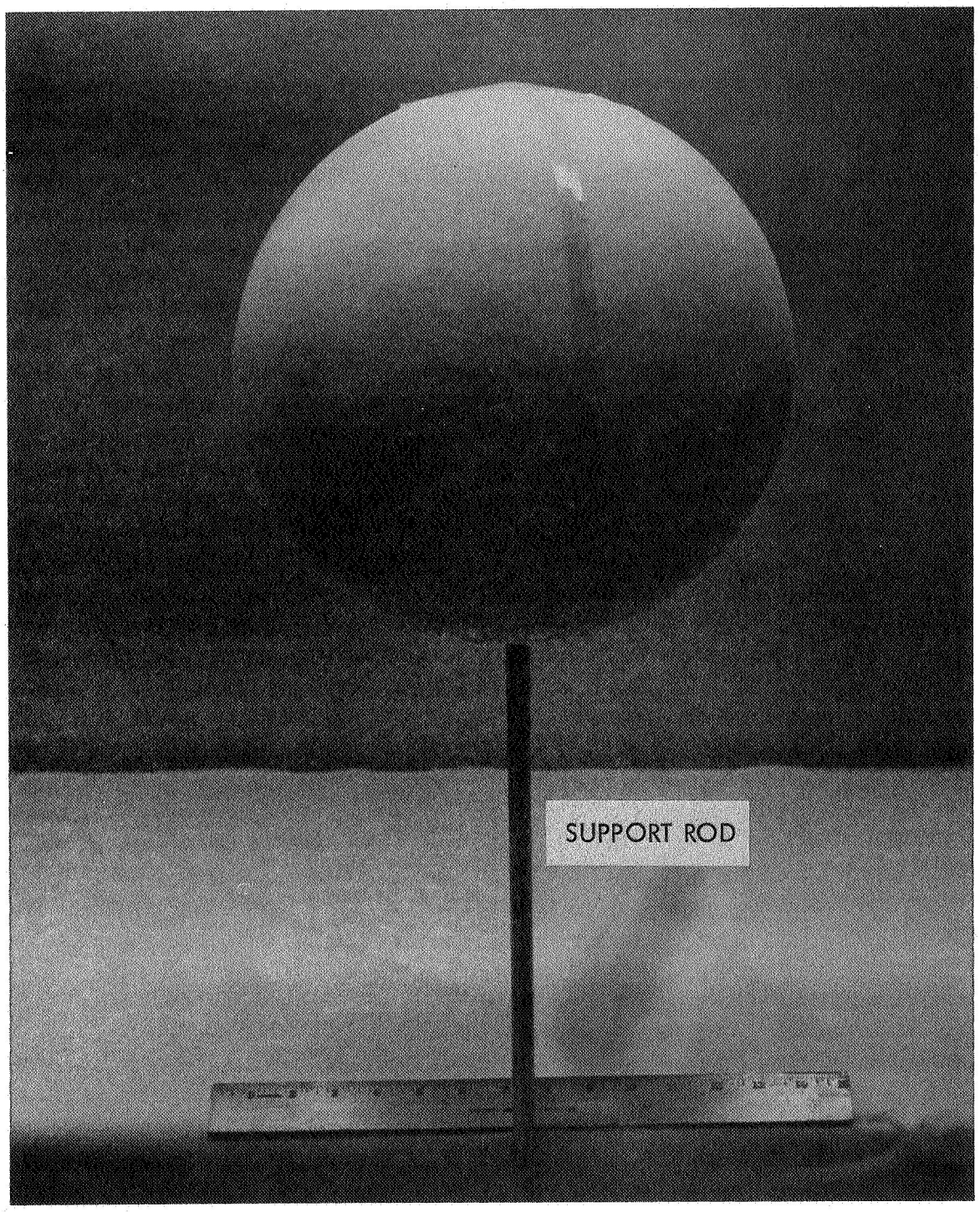

FIGURE 2 MANDREL ASSEMBLY WITH PROTECTIVE FILM

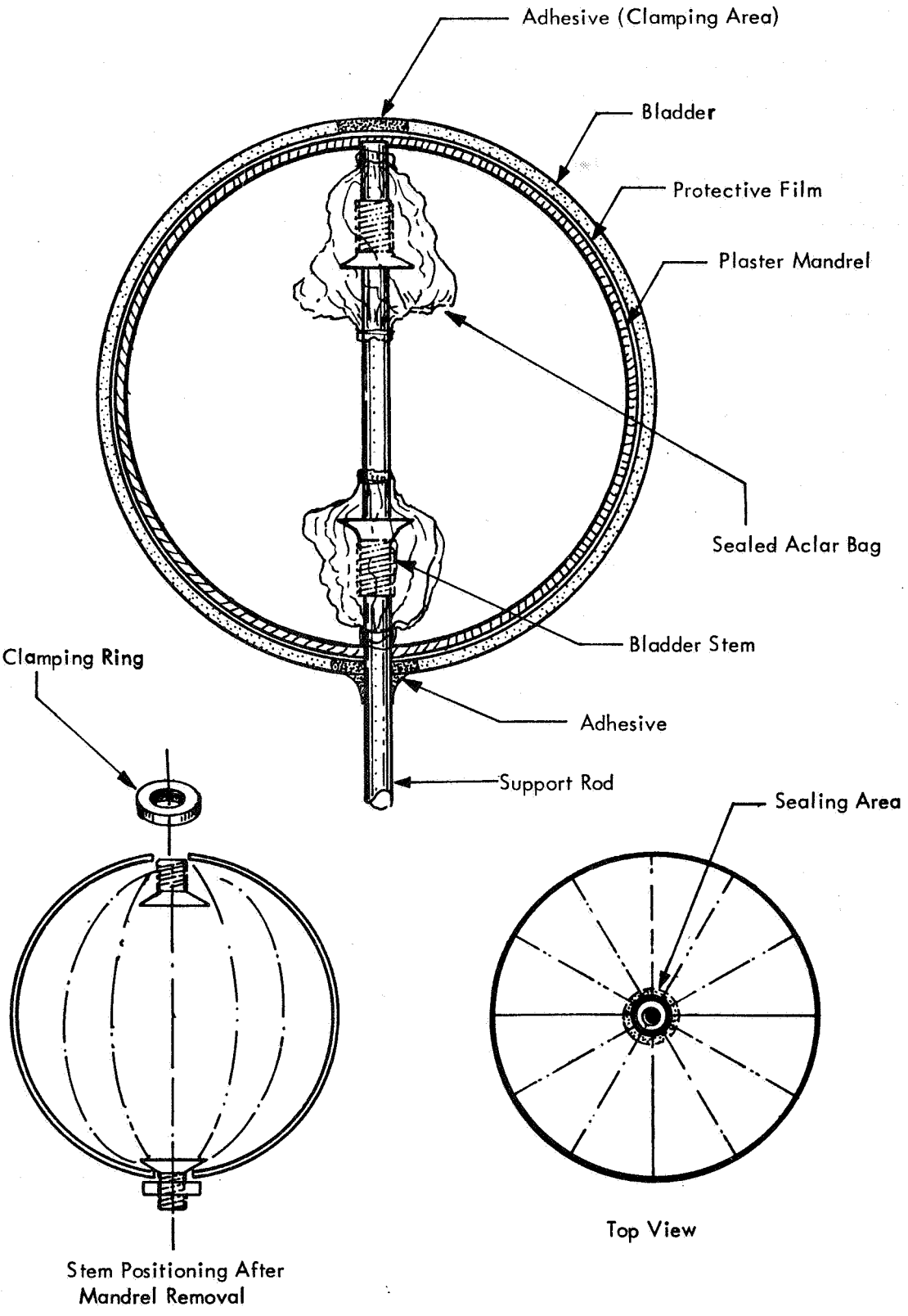

FIGURE 3 MANDREL ASSEMBLY

(Type A) into one-quarter spherical sections and then sealing the sections together on the mandrel using GT-300 adhesive. The completed mandrels had a diameter of 12 ±.030 inches. At this point the mandrel was ready for bladder fabrication.

3.2.3.3 Abrasion Plies - The first ply to be placed on the mandrel was the inner abrasion ply which was made from heat stabilized and bleached T-138 TFE Teflon fabric. Teflon fabric which has not been heat stabilized and bleached is brown in color due to surface contaminants and as a result is LOX impact sensitive. By heating the fabric in a ventilated air circulating oven for 4 hours at 475°F followed by a 24 hour hold at 575°F (Reference 13) the contaminants are removed. The resulting material is LOX compatible and white in color. The heat-cycle causes approximately a 25% surface area shrinkage.

The Teflon fabric for the abrasion ply was vacuum formed into one-quarter spherical sections to eliminate wrinkles when the material was placed on the mandrel. For the forming operation a sheet of 1-mil Teflon film was placed on each side of the fabric and placed in the forming tool (Figure 4) with the weave of the fabric running ±45° to the longitudinal axis of the mold. A vacuum was slowly drawn (approximately 5 psi per minute) while heat was applied with a hot air gun (300-350°F fabric temperature). When the fabric contacted the mold surface, the heat was removed and the formed fabric taken from the mold. The quarter-segments were then trimmed to size and sealed together on the mandrel with GT-300 adhesive. A butt seam was used with adhesive applied to both sides of the joint, forming a mechanical interlock with the Teflon fabric rather than a true adhesive bond.

On the 10-ply bladders a substrate ply which was constructed in the same manner as the abrasion ply, was placed between the 5th and 6th barrier film ply. All bladders contain another abrasion ply on their exterior. The abrasion and substrate plies were attached in the stem area as shown in Figure 5. This is a critical seal since the fabric represents a potential leak path if it extends too far into the stem area or is improperly installed.

3.2.3.4 Barrier Plies - Individual barrier plies which were made from individual 12-gore segments were first fabricated into hemispheres on a plaster mandrel as shown in

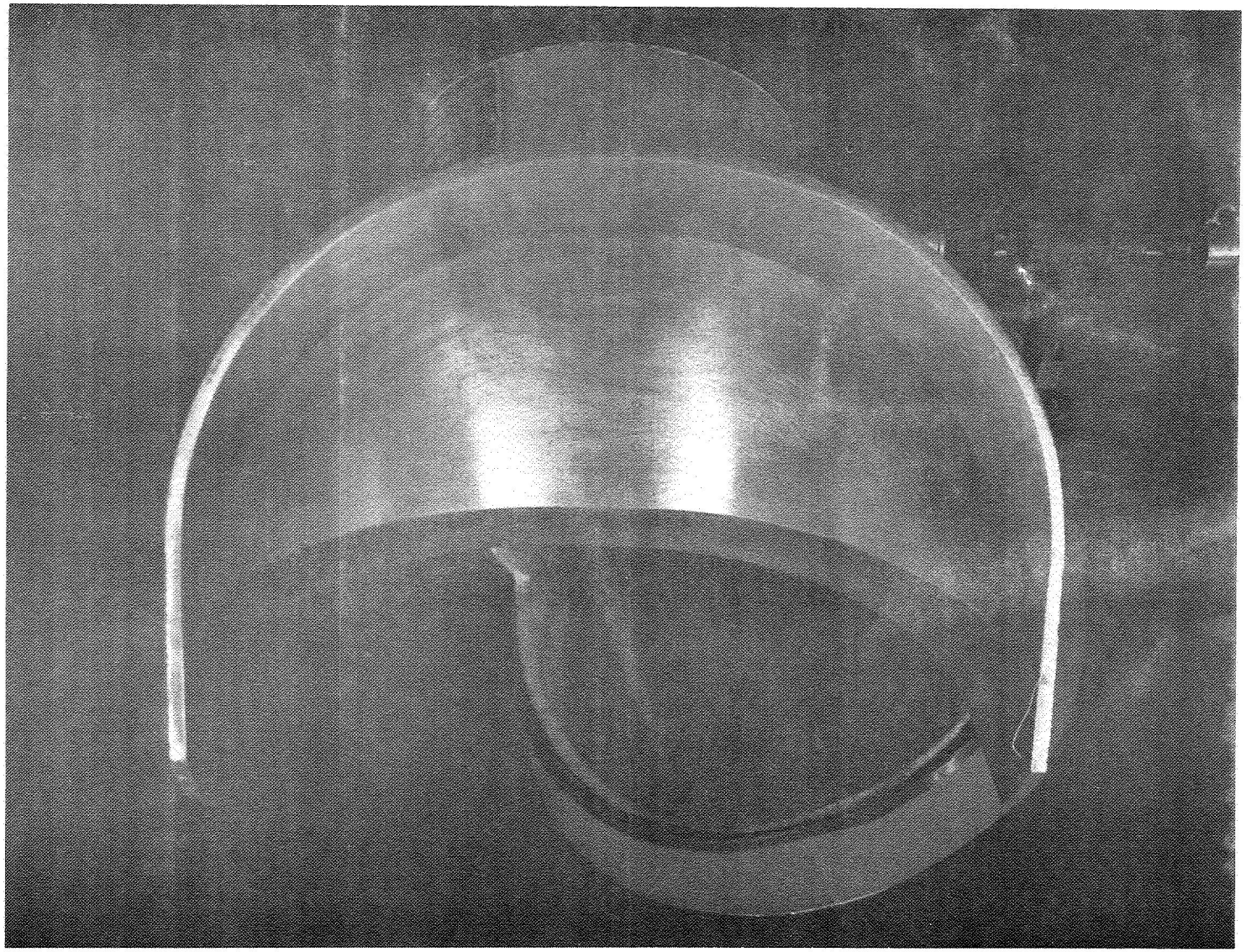

FIGURE 4 TEFLON FABRIC FORMING TOOL

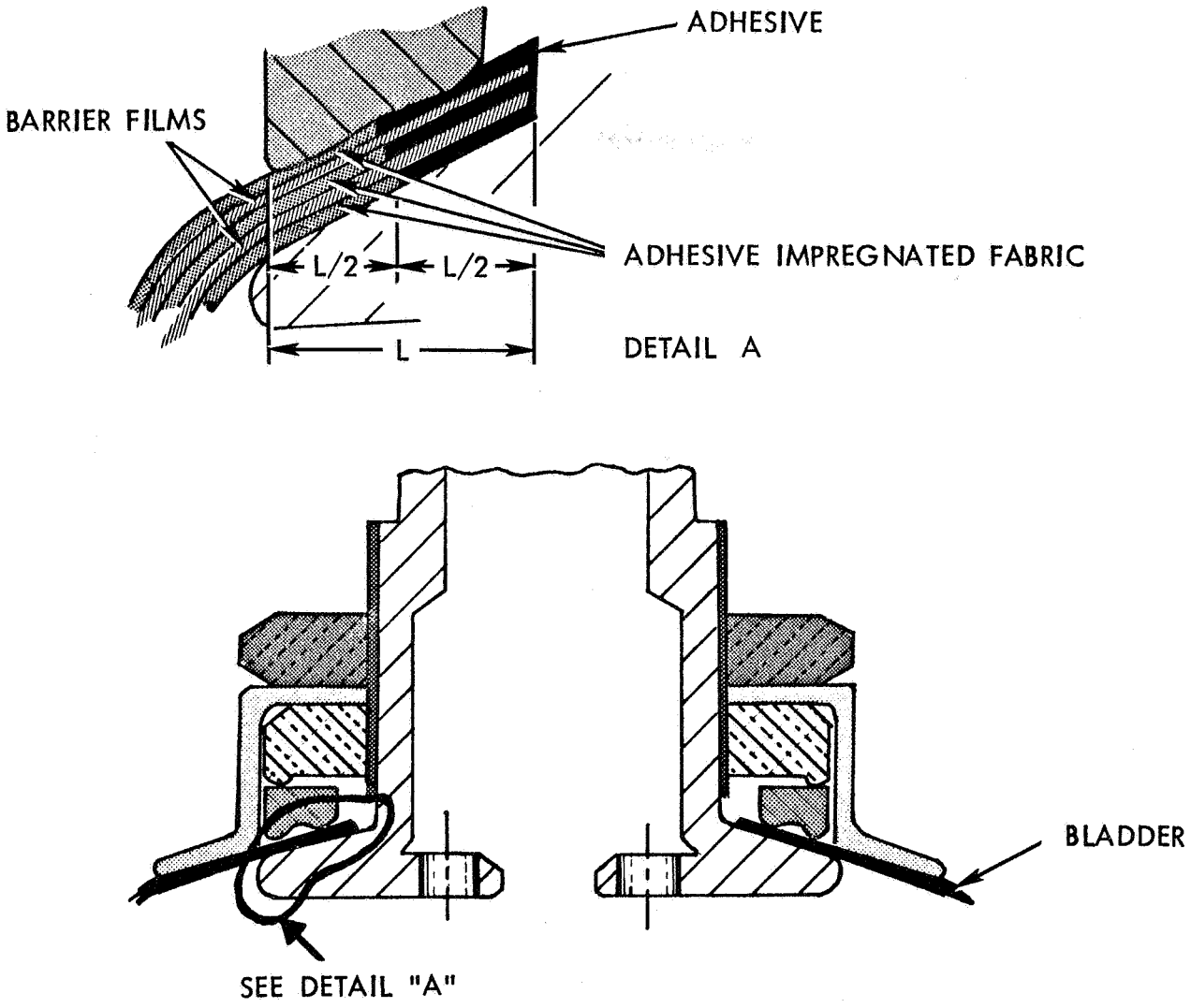

FIGURE 5 BLADDER ATTACHMENT DETAILS

Figures 6 and 7. The hemispherical mandrel had six flat sections as shown, one for each gore. The flat section enabled the fabricator to apply the tape adhesive without wrinkling either the barrier film or the adhesive thus minimizing adhesive ridges, stress concentrations and possible leak paths. The gores were sealed using GT-300 adhesive on both sides of a butt joint. The sealing iron was set at 310 ±10°F. The completed film hemispheres were then placed on the main spherical mandrel and sealed together with GT-300. All seams were butt joints with adhesive on both sides.

The individually formed gores for the 6-gore bladders were fabricated in the tooling shown in Figure 4. The procedure specified for the Teflon fabric forming (Section 3.2.3.3) was used except the forming temperature was reduced to 100-125°F. The barrier plies were fabricated directly on a spherical mandrel. In constructing the barrier ply, two hemispherical sections consisting of 3-gores each were prefabricated on a spherical mandrel and then transferred to the final bladder mandrel.

The attachment methods and all remaining fabrication procedures were the same for both the 6- and 12-gore bladders.

The abrasion ply was sealed to the first barrier ply with GT-100 adhesive in the peripheral area just inside the clamping area of the bladder attachment stems (Figure 5). The adhesive extended over the entire clamping area (for the abrasion ply seal only) to prevent a leak path around the stem. After completing the first ply, it was leak checked prior to assembling subsequent plies (see paragraph below on leak checking procedures).

Each subsequent barrier ply was fabricated in the same manner as the first and sealed to the adjacent plies with GT-100 adhesive in the attachment stem area at each end of the bladder. While the abrasion plies only extended partially into the clamping area, the barrier films extend over the entire clamping area. The adhesive was located only in the clamping area.

Following the fabrication and checking of the appropriate number of barrier film plies (and inserting the substrate ply when prescribed), an outer abrasion ply was applied.

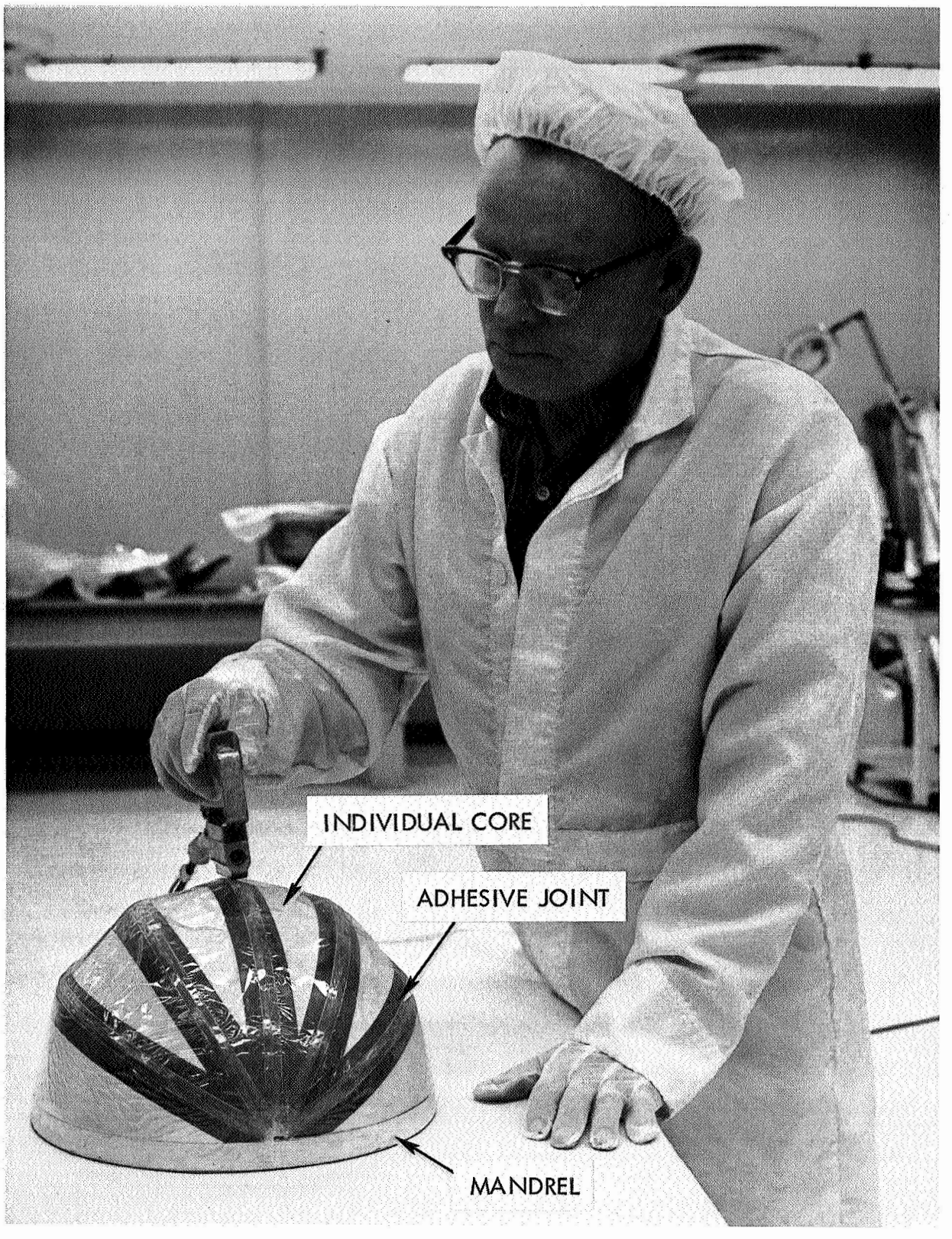

FIGURE 6 FABRICATING HEMISPHERICAL SECTION FOR BARRIER FILM PLY

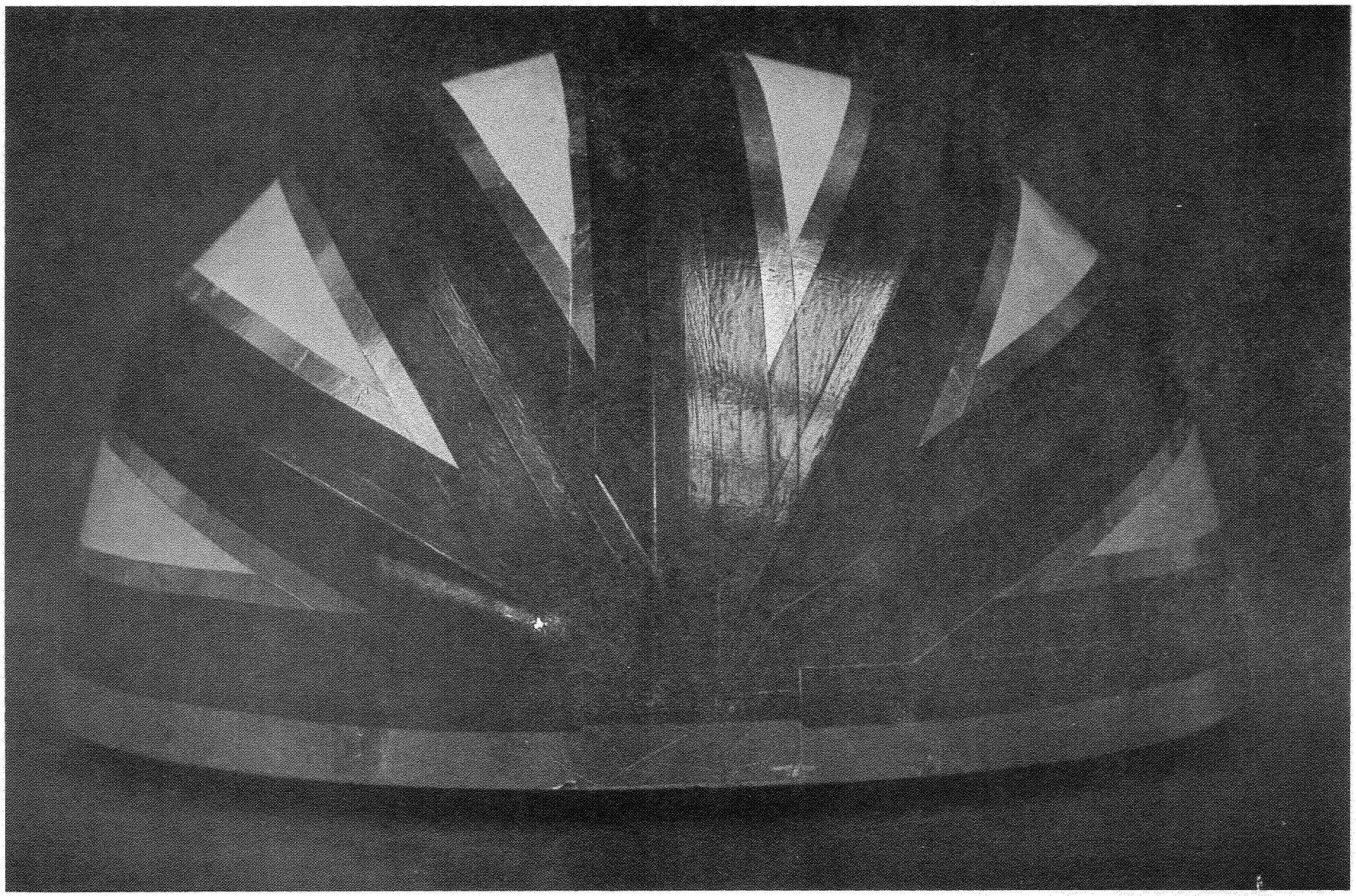

FIGURE 7 GORE SEALING MANDREL

It was fabricated in the same manner as the inner abrasion ply and again bonded just inside the clamping area. At this point the bladder was essentially complete, with only the placement of the stems remaining.

A 1" diameter hole was cut at each end of the bladder for the stems, taking care not to cut the inner protective Mylar film on the mandrel. Now another protective cover of 1/2-mil Mylar (Type A) film was applied over the entire bladder. This film was sealed to the inner protective film within the periphery of the pole trim area, thereby forming a closed envelope containing the bladder. With the bladder protected from contamination, the mandrel was removed.

3.2.3.5 Mandrel Removal - The bladder-mandrel assembly was secured in a foam cushioned nesting fixture to further protect the bladder. A hole was drilled through the plaster shell at the stem location, and water injected. After the plaster had softened, it was removed and the interior flushed clean with water.

After drying, both the inner protective liner and the bags covering the bladder stems were removed, leaving the outer protective film in place. The stem area was then trimmed to net size.

The bladder attachment stems were positioned, bonded in place with Type 46971 adhesive*, and clamped. After allowing the adhesive to dry for 16 to 24 hours, the outer protective film was removed and a helium leak check was performed (paragraph below). If acceptable, the bladder was then installed in the test tank. (See Section 3.2.5). The entire bladder fabrication sequence is illustrated in Figure 8 and a completed bladder shown in Figure 9.

3.2.3.6 Leak Checks - Each individual barrier ply was checked for leaks with a helium mass spectrometer (Figure 10). To perform this check, a flanged stem was sealed into the film ply in the center of the bladder attachment area at the top of the mandrel (Figure 11)

*E. I. duPont polyester adhesive.

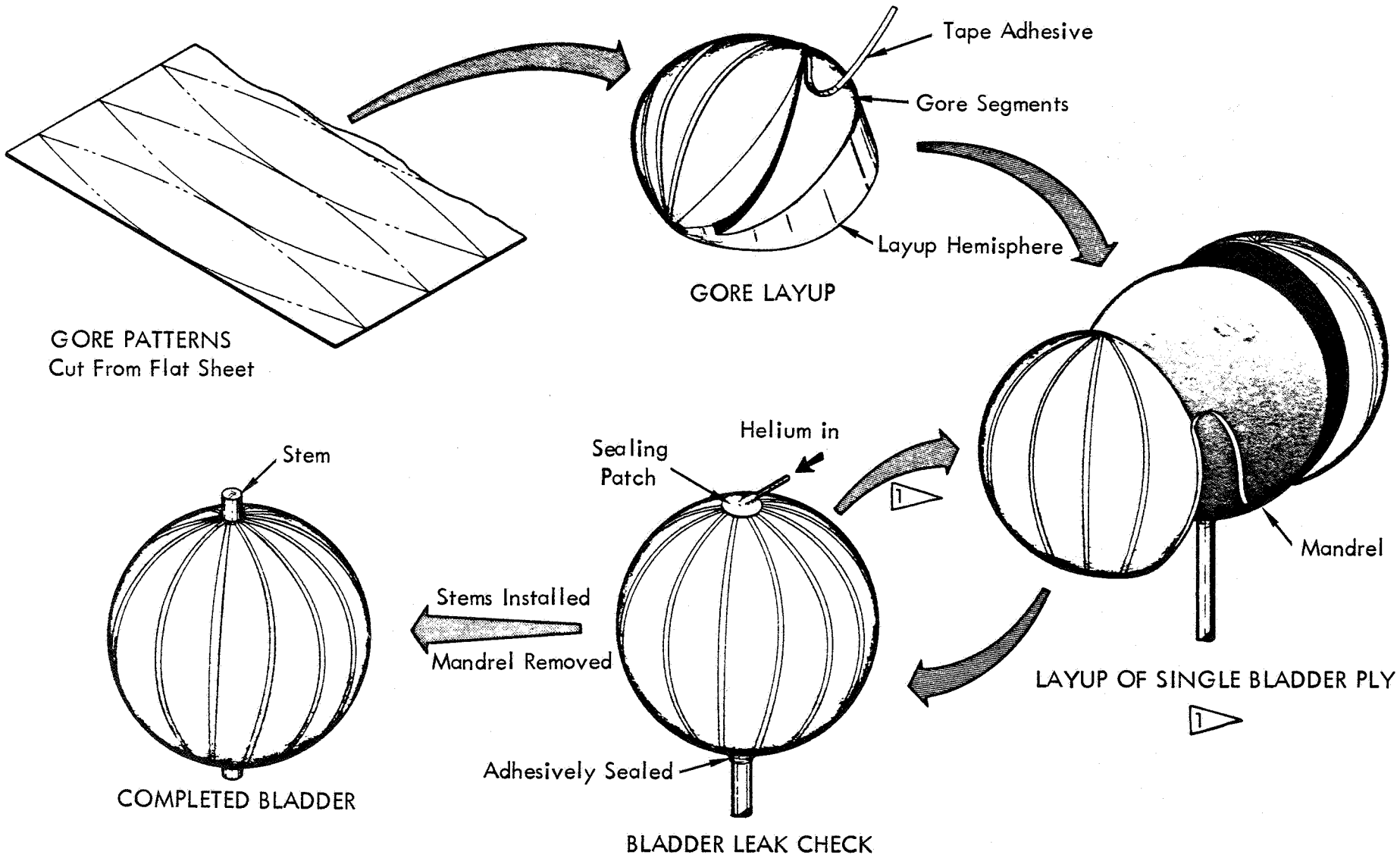

FIGURE 8 BLADDER FABRICATION SEQUENCE

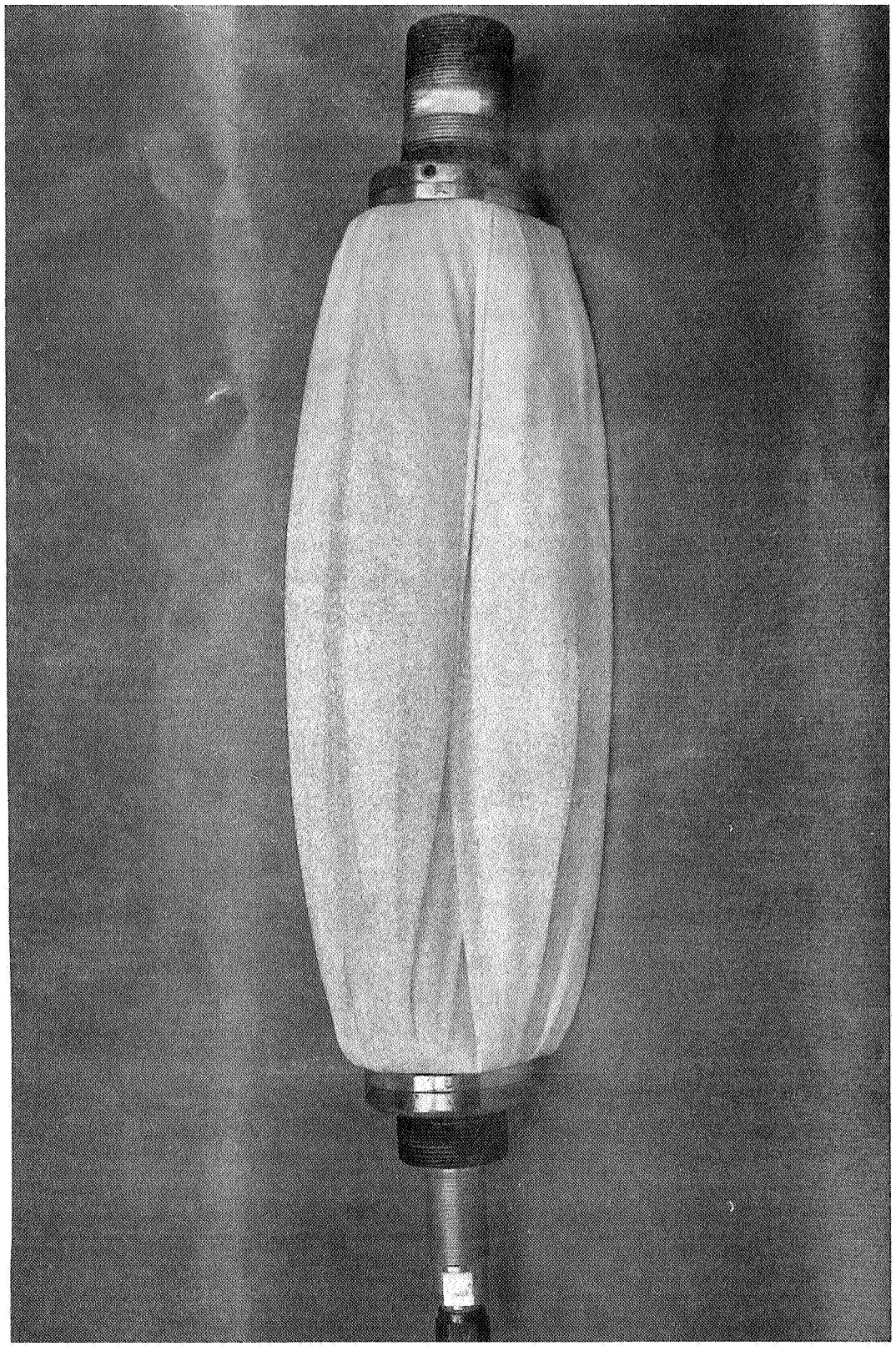

FIGURE 9 ASSEMBLED BLADDER

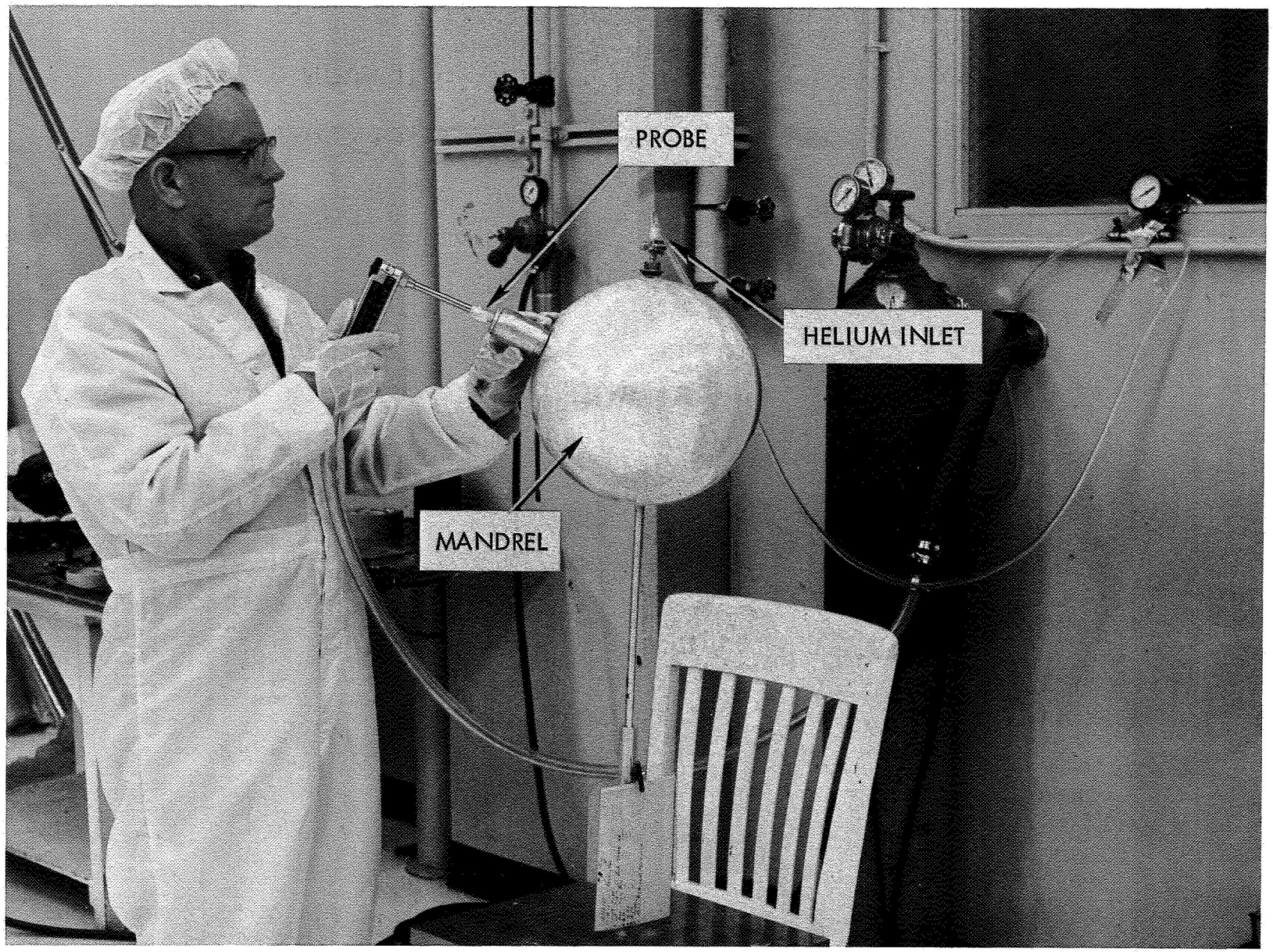

FIGURE 10 LEAK CHECKING OF BARRIER FILM PLY

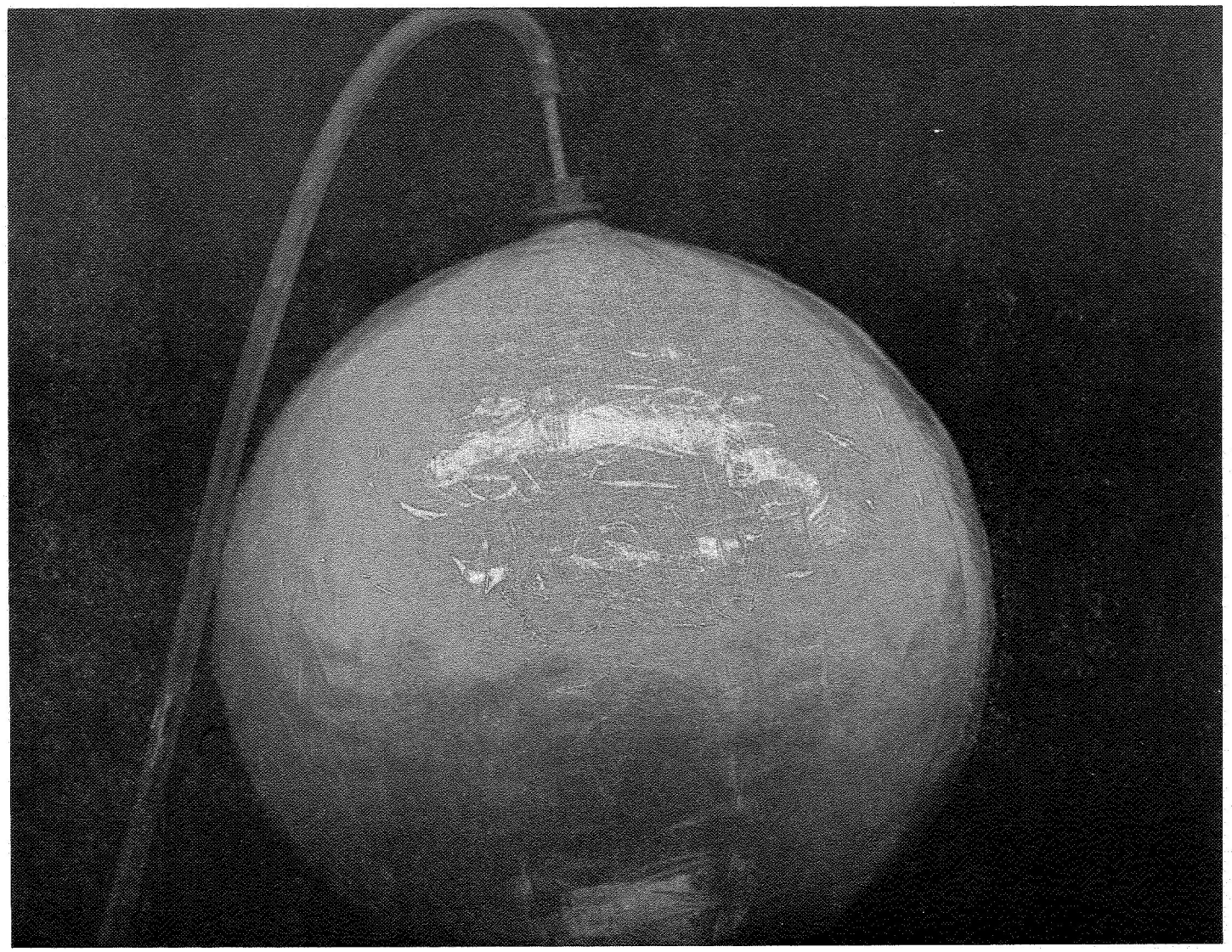

FIGURE 11 LEAK CHECKING MYLAR PLY (UNPRESSURIZED)

for the injection of helium. At the opposite pole the film was sealed to the mandrel support rod. The annulus between the bladder plies was pressurized with helium to 1/2 psi differential pressure and the entire bladder surface checked with a helium leak detector.

To perform the leak checks, a standard mass spectrometer, Model 24-120A, manufactured by Consolidated Electrodynamics Corporation was used. A zero division rise on the X-1 scale (or less than 2×10^{-10} std cc/sec) was used for acceptance. The probe was modified by adding a cup to the end of the probe as shown in Figure 12. The cup, 1.25 in^2 in cross-sectional area, enabled the operator to measure the helium leakage rate over a known surface area. Consequently, with the known area, the mass spectrometer measured to an acceptance level of 1.6×10^{-10} cc/sec/in^2. The cup was held in one location for 1 to 3 seconds during the checks. If held for extended period of time, the equipment would begin to register the gaseous permeability of the film material.

The ply was accepted if no leaks were detected which exceeded 1.6×10^{-10} std cc/sec/in^2. If a leak was detected it was patched with GT-300 or if in a seam, resealed. No more than two patches per ply were permitted. A ply was scrapped and replaced if it did not pass a leak check and could not be satisfactorily repaired.

A completed bladder was pressurized to 1.0 psi and permitted to stabilize for a period of 20 to 30 minutes. After this waiting period, the entire surface was probed with the leak detector. To be acceptable the leakage could not exceed 1.6×10^{-10} std cc/sec/in^2.

3.2.4 TEST EQUIPMENT

A schematic drawing of the test setups used in Task II for the static expulsion evaluation of the polymer bladders are shown in Figures 13 and 14. The set-up shown in Figure 13 was designed for outward expulsion. In this mode of expulsion the cryogen is between the tank wall and the bladder and expelled by inflating the bladder with helium. Outward expulsion was attempted on two bladders (No's. 1 and 2).

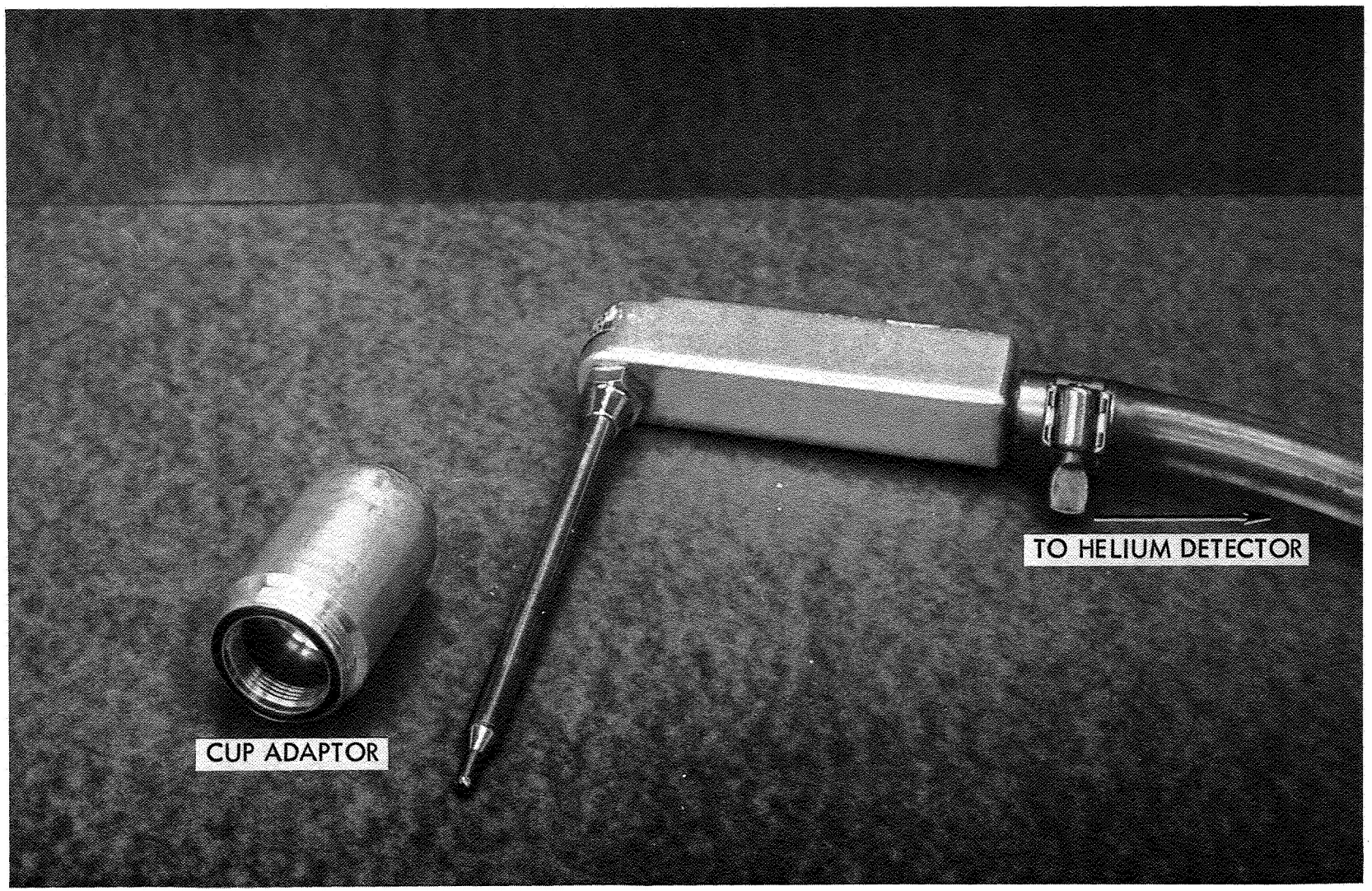

FIGURE 12 HELIUM LEAK DETECTOR NOZZLE HEAD

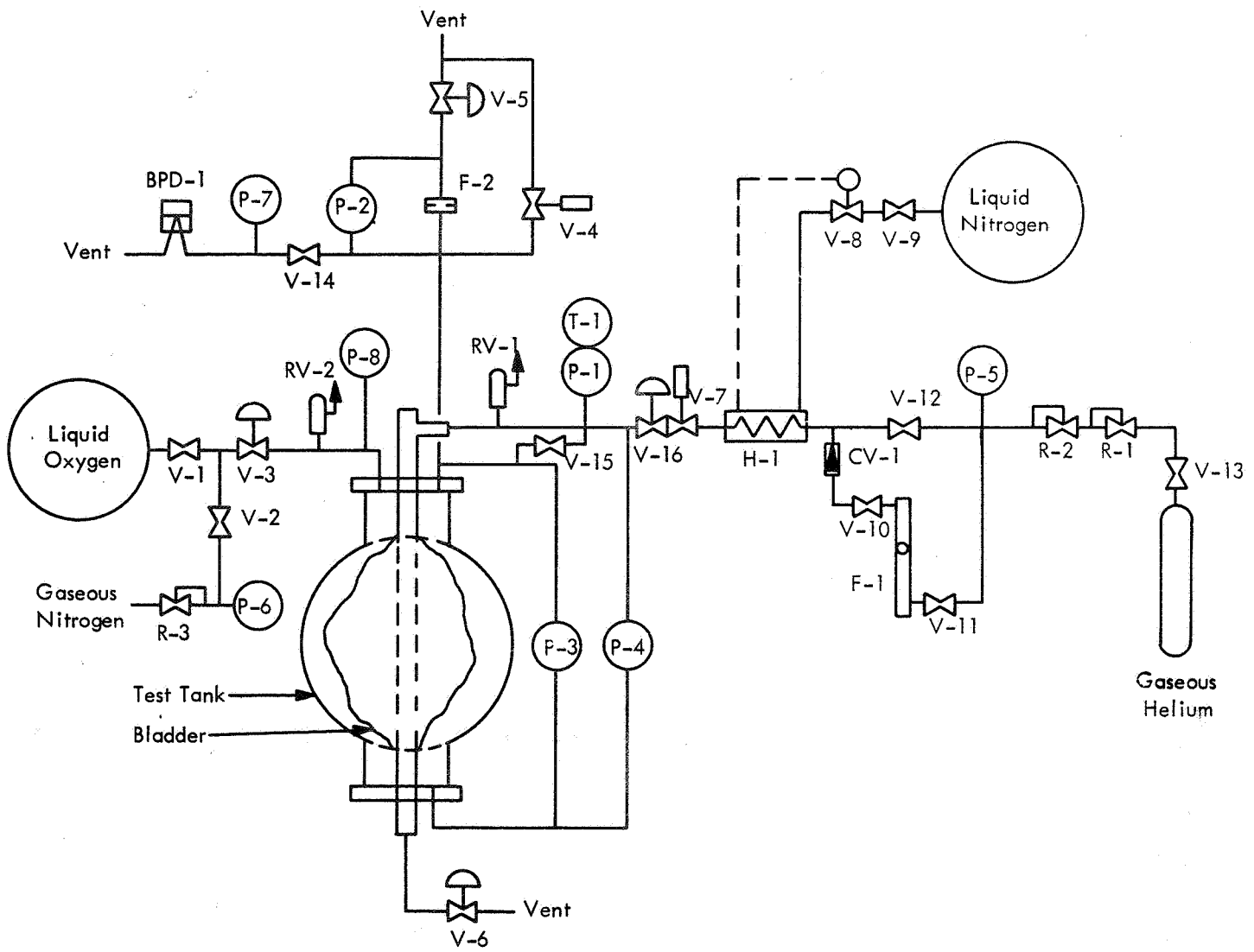

FIGURE 13 TEST SCHEMATIC FOR OUTWARD EXPULSION EVALUATIONS

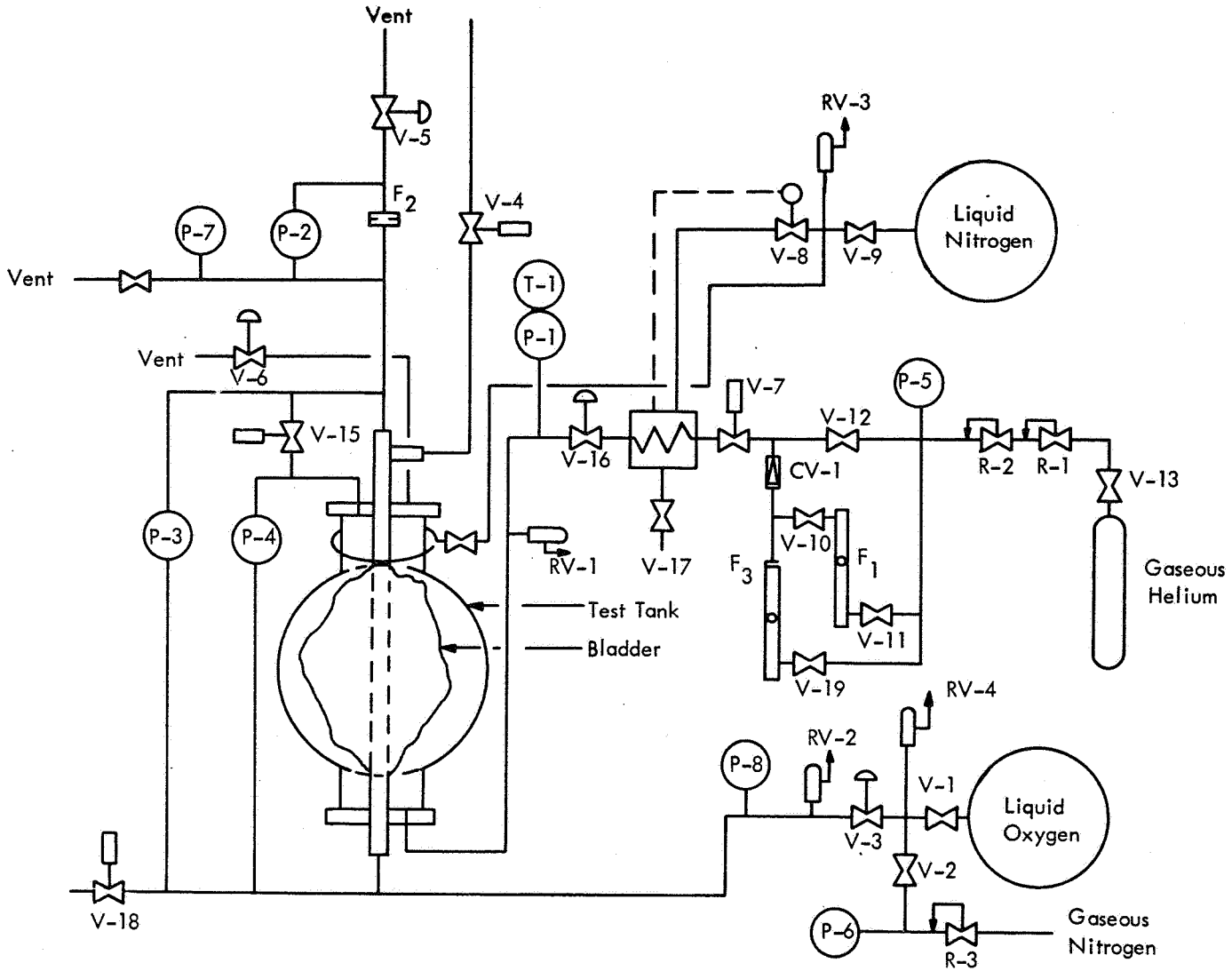

FIGURE 14 TEST SCHEMATIC FOR INWARD EXPULSION EVALUATIONS

Inward expulsion is where the cryogen is contained in the bladder and expelled by pressurizing the annulus between the bladder and the tank. The set-up for inward expulsion is shown in Figure 14. Bladders 2 through 10 were evaluated in this mode.

A list of the test equipment is tabulated in Table V for both test setups.

Figures 15 to 17 show the control console, recording charts, and the test area, respectively.

3.2.4.1 Test Tank - The test chamber was a spherical stainless steel (AISI 321 CRES) tank with an inside diameter of $12\ ^{+.030}_{-.000}$ inches and a minimum wall thickness of .07. The upper and lower flanges were 3003 aluminum alloy and the standpipe and all bladder fittings were 6061-T4 aluminum alloy. The tank was designed for a room temperature burst pressure of 265 psi. The tank was proof tested to 200 psi.

The tank (Figures 18 and 19) was designed for inward expulsion. It features provisions for filling from either the top or the bottom fitting; venting and expulsion from the top fitting; and helium pressurization and venting (to the exterior of the bladder) through the top flange. Teflon or Creavey seals were used at all flange areas to prevent leakage. The upper flange, bladder fitting and standpipe are shown in Figure 20.

3.2.4.2 Heat Exchanger - The purpose of the heat exchanger was to chill the helium pressurizing gas before it entered the test tank to minimize boil-off to the cryogen in the tank. The internal volume of the copper coils was slightly greater than that of the test tank. The exchanger consisted of a coil of copper tubing submerged in the liquid nitrogen dewar, which chilled the gas to -310° ±10°F.

During testing the test tank was suspended in a 600 gallon dewar and continuously sprayed with liquid nitrogen to minimize heat leakage into the tank since the tank itself was not insulated. Also the liquid nitrogen spray enabled the operator to maintain a relatively constant tank temperature for the leakage checks.

TABLE V — EQUIPMENT LIST — EXPULSION (TASK II)

SYMBOL	DESCRIPTION	SIZE	TYPE	SERVICE	REMARKS
-	Test Tank Assembly	12" dia.	Sph.	LO_2	
-	Dewar	600 gal.	-	"	
-	Dewar	600 gal.	-	LN_2	
-	Bottle Manifold	10 cyl.	-	GHe	
H-1	Heat Exchanger	1" dia.x120'	Cu. Tube	LN_2-GHe	
R-1	Pressure Regulator, High Pressure	0-3000 psi	Dome Loaded	GHe	
R-2	Pressure Regulator, Low Pressure	0-25 psi	Diaphragm	GHe	Grove
R-3	Pressure Regulator, Purge	0-150 psig	Diaphtagm	GN_2	Conoflow
R-4	Pressure Regulator, High Capacity				
RV-1	Heat Exchanger Relief Valve	1/2"	Poppet	GHe	Circle Seal, 35 psig
RV-2	Test Tank Relief Valve	1/2"	Poppet	LO_2	Circle Seal, 10 psig
RV-3	LN_2 Line Relief Valve	1/2"	Poppet	LN_2	Circle Seal, 35 psig
RV-4	LO_2 Line Relief Valve	1/2"	Poppet	LO_2	Circle Seal, 35 psig
F-1	Rotameter	4-232 scc/M	Sph. Float	GHe	Manostat no.36-541-04
F-2	Orifice Meter	.1 to 10 gpm			
F-3	Rotameter	100-500 scc/M	Sph. Float	GHe	
V-1	LO_2 Shut-off Valve	3/4"	Globe	LO_2	Powell, On Dewar
V-2	GN_2 Shut-off Valve	1/2"	Ball	GN_2	Jamesbury
V-3	LO_2 Control Valve	3/4"	Globe		Annin, C_v=1.5
V-4	LO_2 Vent Valve	1 1/2"	Ball	LO_2	Jamesbury
V-6	He Space Vent Valve	3/4"	Glove	GHe	Annin, C_v=1
V-8	LN_2 Control Valve	1/2"	Poppet	LN_2	Leslie MCR
V-9	LN_2 Shut-off Valve	1/2"	Globe	LN_2	Powell, On Dewar
V-11, 19	Flowmeter Shut-off Valve	1/2"	Needle	GHe	Hoke
V-12	Flowmeter By-pass Valve	1/2"	Ball	GHe	Jamesbury
V-13	GHe Shut-off Valve	1/2"	Ball	GHe	Jamesbury
V-15	Bladder By-pass Valve	1/2"	Ball	GO_2	Jamesbury
V-16	GHe Control Valve	3/4"	Globe	GHe	Annin, C_v=0.6
V-18	LO_2 Drain Valve	1/2"	Ball	LO_2	Jamesbury

TABLE V (cont'd) EQUIPMENT LIST — TASK II

SYMBOL	DESCRIPTION	RANGE	ACCURACY	INDICATOR
P_1	GHe Pressurization Pressure	0-15 psig	± 5%	Strip Chart & Panel Meter
P_3	P Liquid Level	-1.5 to +2.5 psid	± 5%	Strip Chart & Panel Meter
P_4	P Across Bladder	± 2.5 psid	± 5%	Strip Chart & Panel Meter
P_5	R_2 Output Pressure Gage	0-50 in. of H_2O	± 10%	Manometer
P_6	R_3 Output Pressure Gage	0-30 psig	± 10%	Gage
P_8	Test Tank Pressure	0-15 psig	± 5%	Strip Chart & Panel Meter
T_1	GHe Temperature	140 to 520°R	± 5°R	Strip Chart
F_1	Manostat Rotameter	4-232 scc/M He	± 10%	Rotameter
P_u	LO_2 Fill Line Pressure	0-15 psig	± 5%	Panel Meter
T_2	Test Tank Temperature	140-520°R	± 5°R	Strip Chart

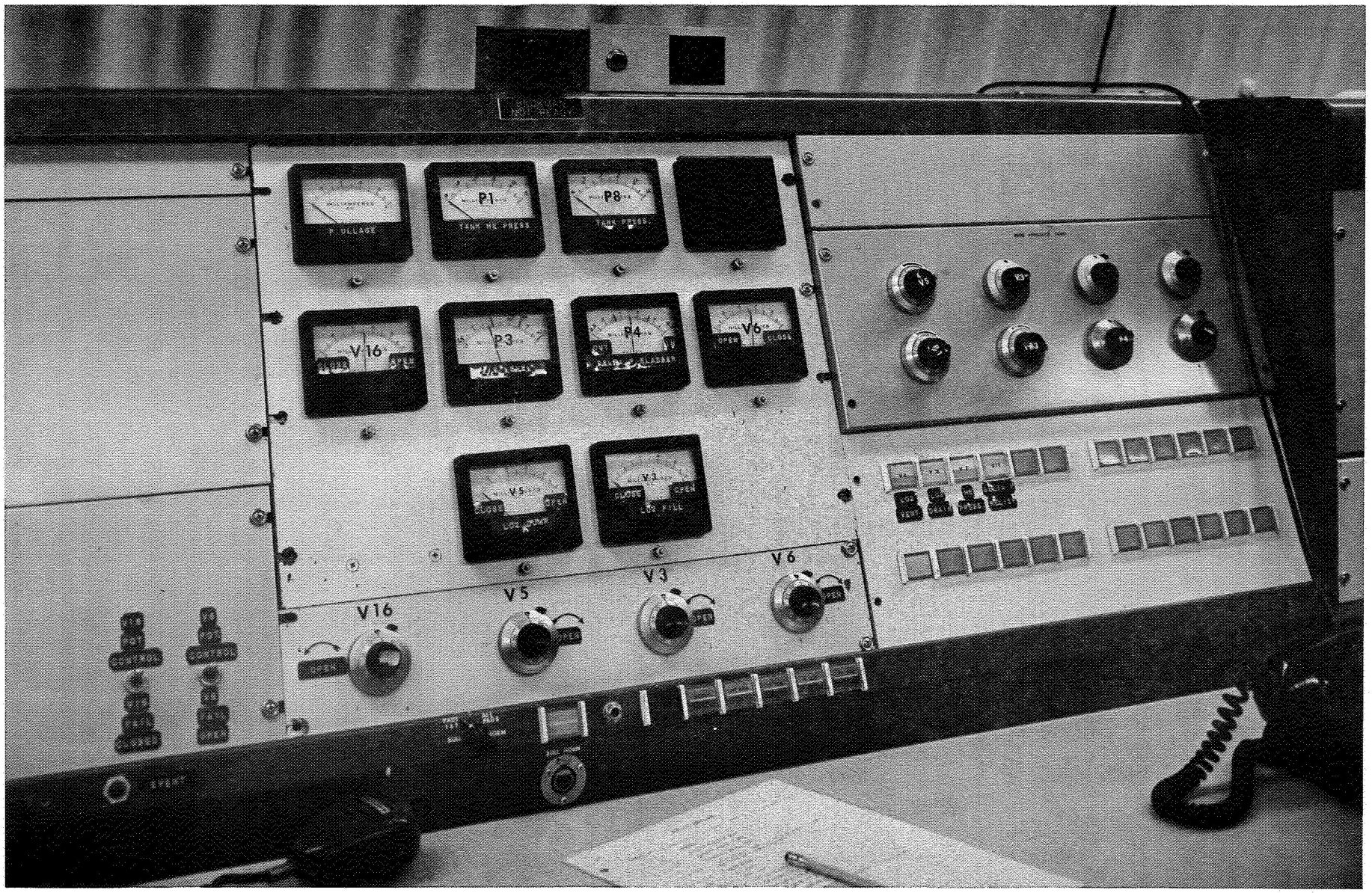

FIGURE 15 CONTROL CONSOLE

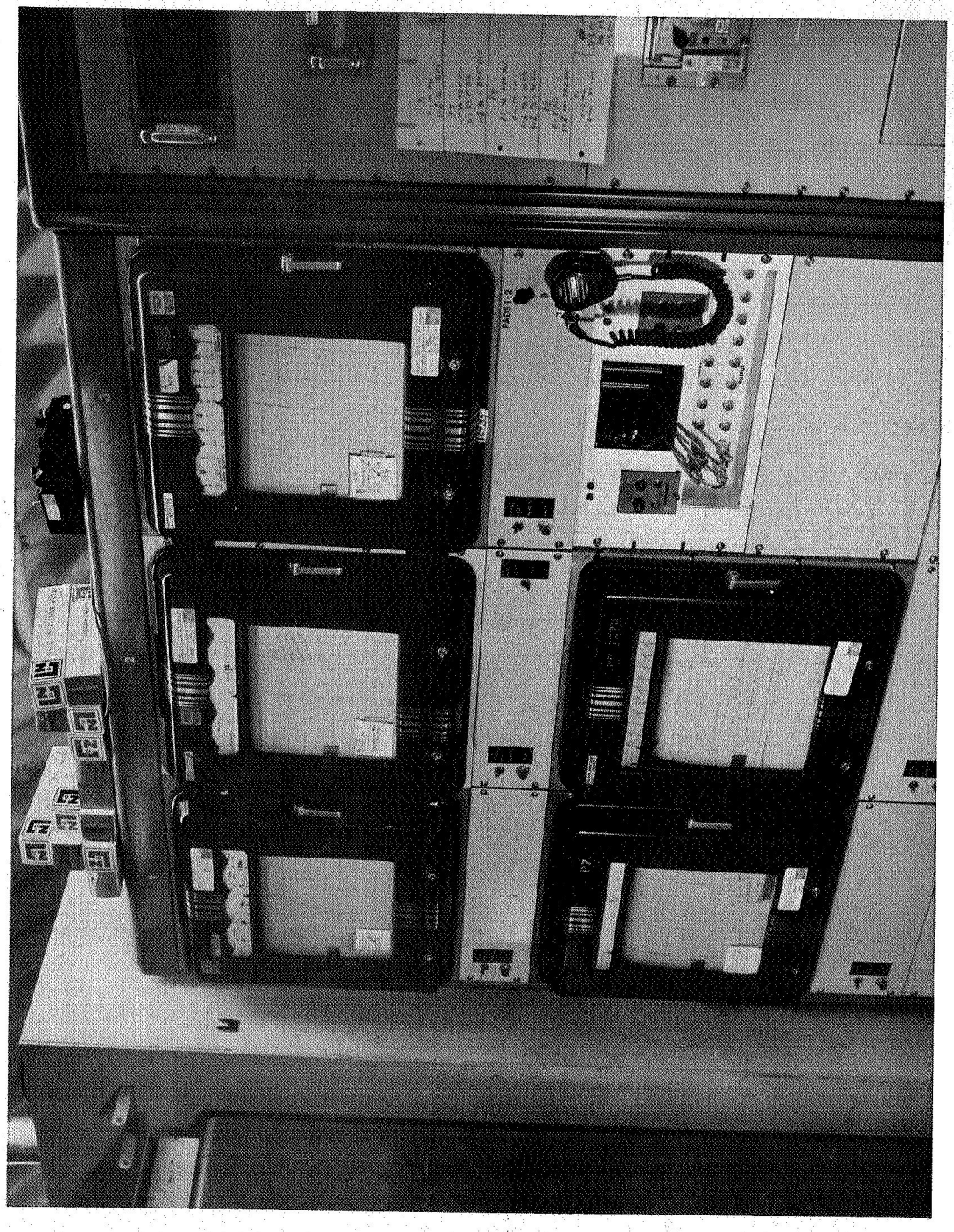

FIGURE 16 STRIP CHART RECORDING UNIT

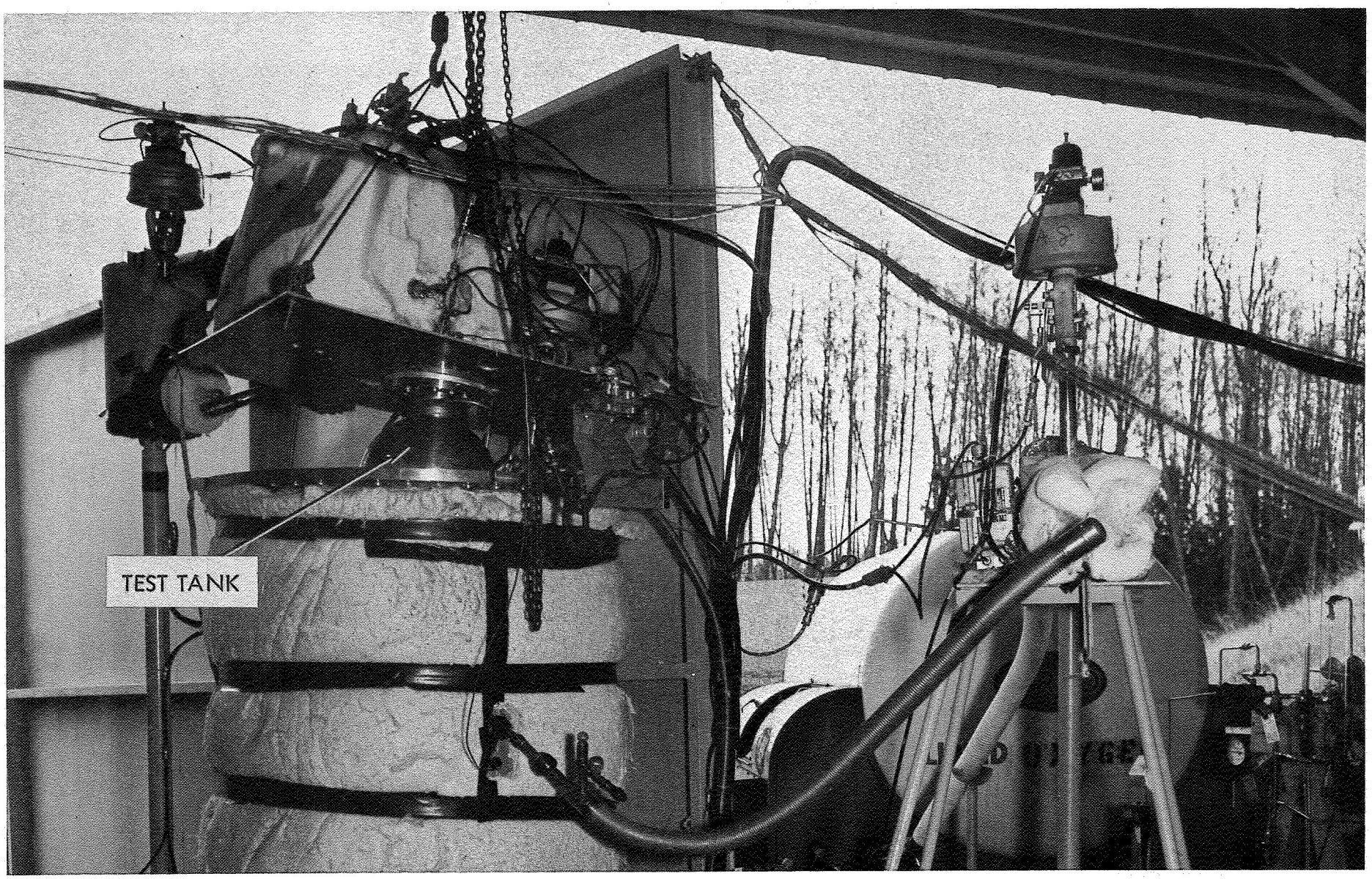

FIGURE 17 EXPULSION TEST SETUP - TASK II

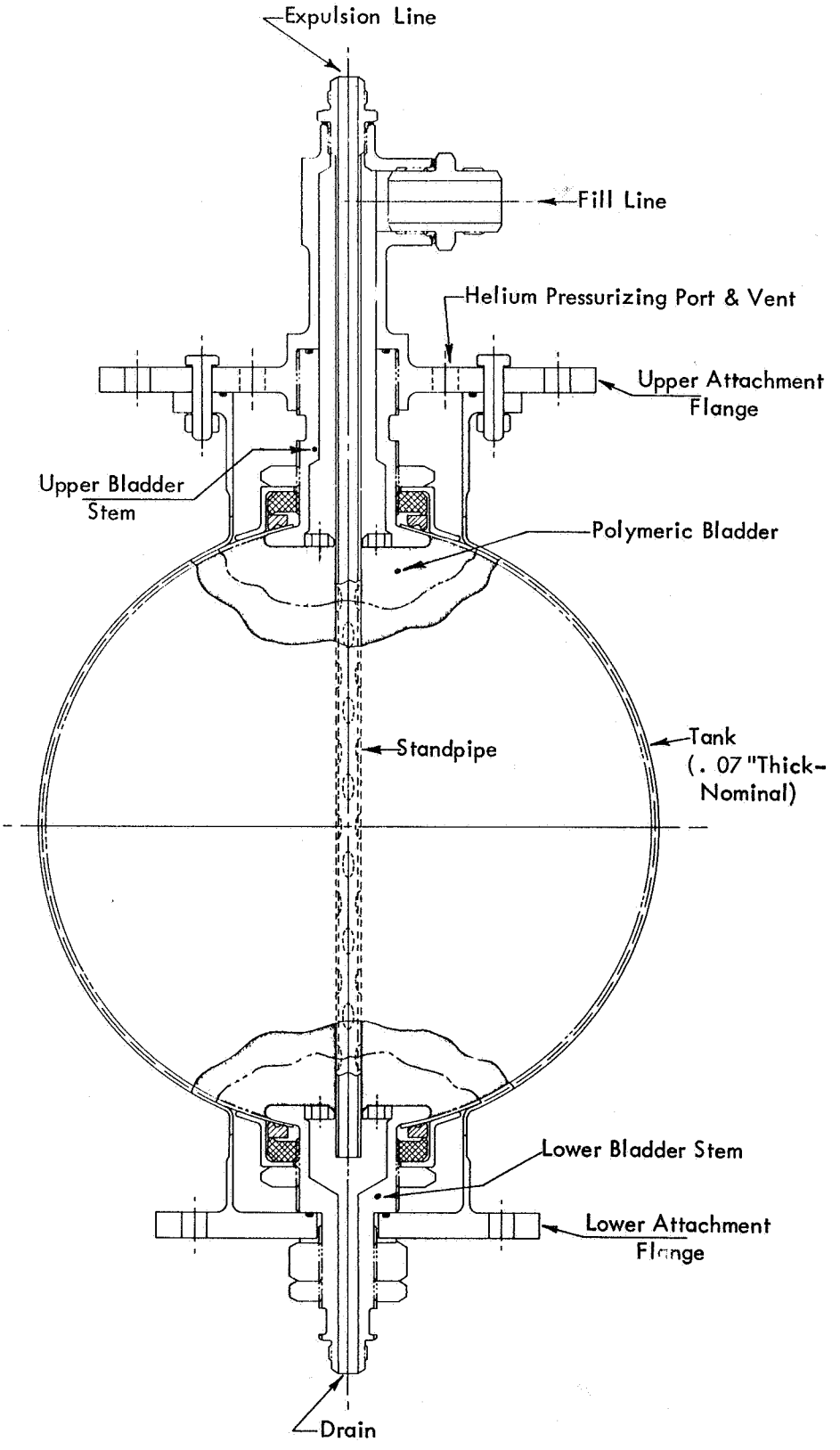

FIGURE 18 TANK ASSEMBLY

FIGURE 19 STEEL TEST TANK WITHOUT FITTINGS

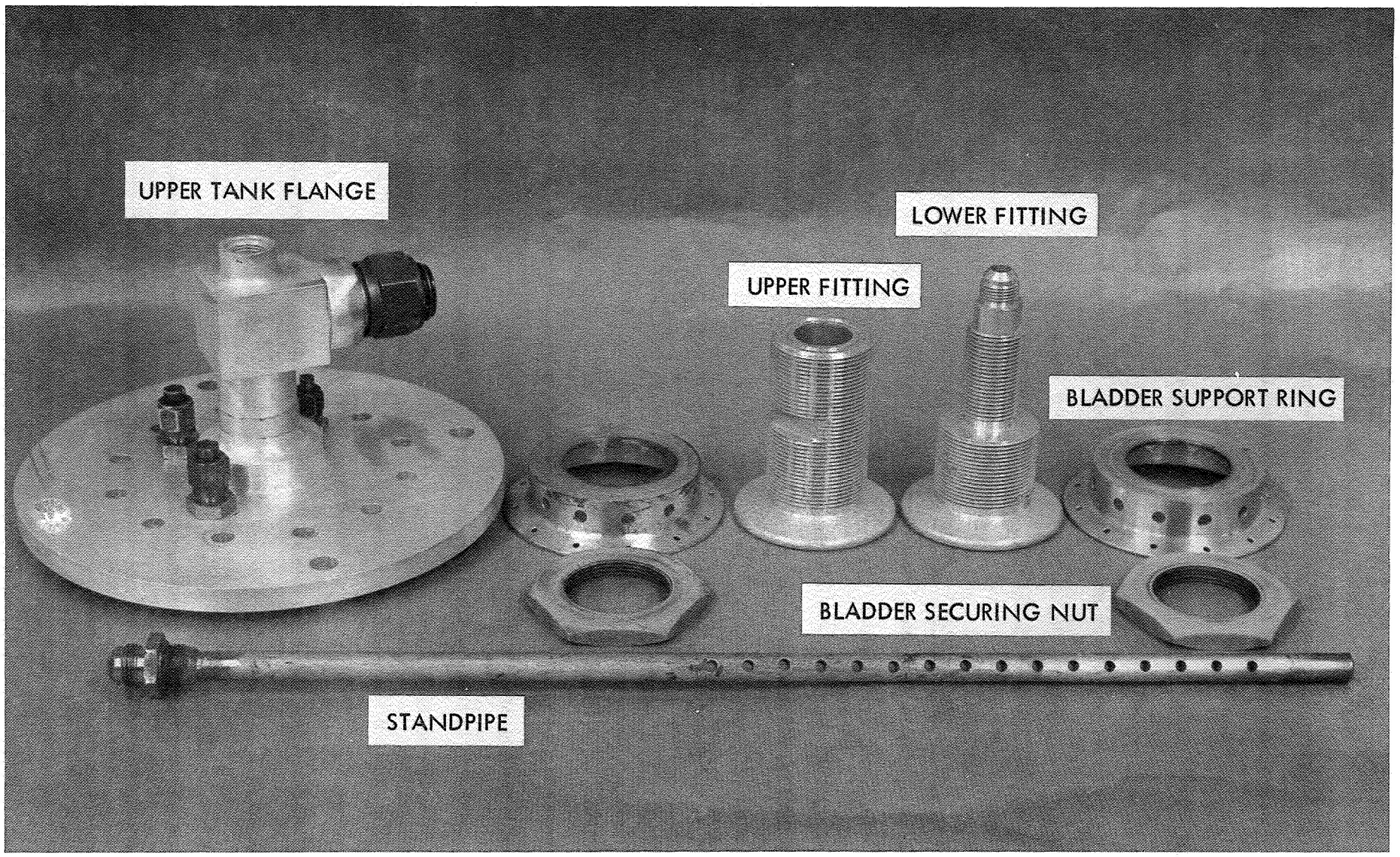

FIGURE 20 BLADDER AND TANK HARDWARE

3.2.5 TEST PROCEDURE

3.2.5.1 Bladder Installation - The bladder was installed in the test tank through the upper flange. Index marks on each of the flanges and fittings permitted installation of the unit without any twists or misalignments which would stress the bladder. After assembly the bladder/tank assembly was leak checked at room temperature by pressurizing the interior of the bladder to 1 psi with helium gas. After a 30 minute stabilization period, each joint and fitting was examined with a helium leak detector to assure a tight seal. After successfully passing this check, the pressure was released, all fittings capped, and the tank sent to the test site for the expulsion testing.

3.2.5.2 Expulsion Cycling - At the start of each test run, the entire system, including the tank/bladder assembly, was purged three times with gaseous nitrogen to remove any traces of air and moisture. Following the purge the tank assembly was checked for leaks using Method A (see Section 3.2.5.3 Leak Checking). After determining the initial bladder and system leakage and recording, the bladder cycling test was started provided the bladder leakage was zero. If a reading other than zero was obtained the bladder fittings were tightened or the proper repairs made in the tank assembly to obtain a zero reading.

The bladders were filled with liquid oxygen at a flow rate of approximately 1 gpm. The fill pressure would be adjusted to obtain the desired flow. The interior and exterior of the bladder was vented to the atmosphere during filling. The fill volume of liquid oxygen was measured by recording the differential pressure between the top and bottom of the tank. This was recorded on a continuous strip chart recorder, giving fill volume versus time. The percent fill is defined as the volume of liquid oxygen in the tank on a given cycle versus the actual capacity of the tank (0.51 ft^3). For expulsion, the vent lines were closed and the annulus between the tank and bladder was pressurized with cold helium gas at a differential pressure across the bladder of 0.5-1.0 psi. The helium gas was supplied from ten helium cylinders joined in parallel and cooled in the heat exchanger prior to entering the tank. The expulsion rate and time were recorded. The percent expulsion tabulated in the test results is the percentage of liquid oxygen in the tank that was expelled on a given cycle.

Instrumentation on the test tank recorded tank temperature, liquid level, pressure inside the tank, pressure differential across the bladder, and expulsion flow rates. Each test bladder was repeatedly cycled until failure. After each 5th cycle (or at the start and end of each test run if less than 5 cycles), the leakage rate of the bladder was checked using Method A below. The cyclic tests were terminated when the bladder leakage rate was in excess of 200 std cc/min or indications of poor performance (inter-ply inflation, etc.) were noted.

3.2.5.3 Leak Checking - Method A - This method of leak checking was used to determine the integrity of the bladder while it was in the expulsion cycling test facility. The tank/bladder assembly was chilled to -297°F by passing liquid oxygen into the bladder and allowing it to vaporize while simultaneously spraying the exterior of the tank with liquid nitrogen. When the temperature of the system reached -280° ±10°F, the interior of the bladder was pressurized with cold helium gas to a pressure differential of 1 psi across the bladder. After a 30 minute stabilization period, flow ratings were taken of the quantity of helium permeating the bladder. The helium flowmeter was located ahead of the heat exchanger as shown in Figure 14 and measured the flow rate at standard conditions while the bladder and assembly were at -280°F.

To account for any possible system leakage, before and after each test the valve to the test tank was closed and the leakage rate of the system was measured. This reading was deducted from the total system reading to obtain a net leakage rate for the bladder.

Method B - This method was used as a post-test determination of bladder leakage. The equipment used for this leak check is shown in Figure 21. It consisted of a bell jar (test chamber), an upstream manometer, a back pressure manometer and an accumulator (burette).

The bladder, with one end capped, was placed in the bell jar in the collapsed position. The other stem was attached to the lid of the bell jar which attached to the system. The interior of the bladder was then pressurized to 28 inches of water with helium gas. After

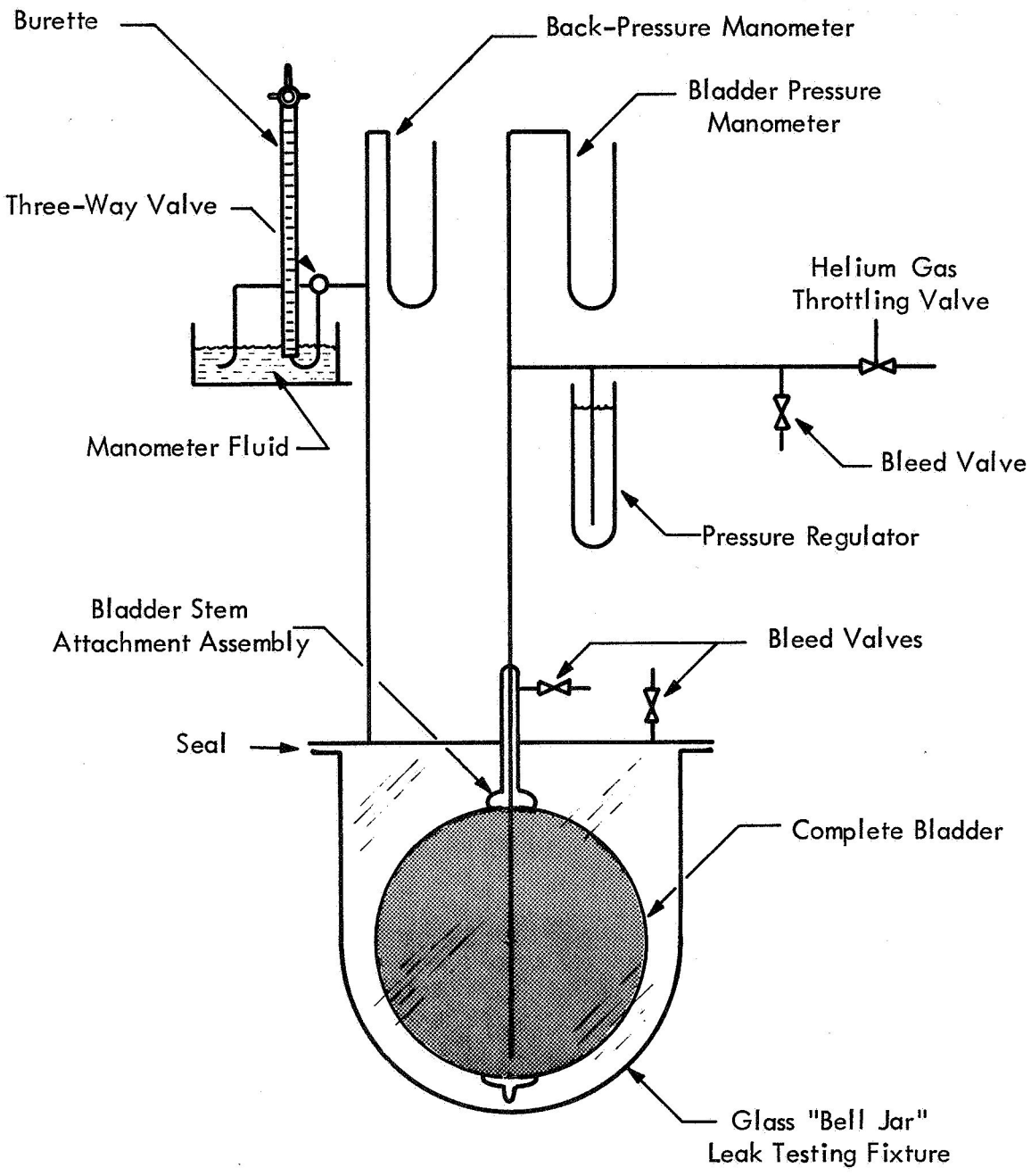

FIGURE 21 SCHEMATIC FOR BLADDER LEAK CHECKING

a 30 minute stabilization period, the three-way valve shown in Figure 21 was turned to direct the helium bubble flow into a burette. The leakage was measured over a known period (5 to 30 minutes depending on the leakage rate of the bladder). All leakage tests were conducted at 70° ±2°F.

This method of leak checking was used in NASA Contracts NAS3-6288 and NAS3-11192 (References 4 and 6 respectively), and represents the one common test between the three programs.

3.2.5.4 Fill and Expulsion Efficiency - The actual fill capacity (fill efficiency) and expulsion efficiency of the tank/bladder assembly was determined in the laboratory using water as the fluid and air as the expelling gas. To measure the fill capacity the vessel was simply filled with water, under a 1 psi differential across the bladder, and the quantity of fluid recorded.

The expulsion efficiency was determined by pressurizing the exterior of the bladder with air using a pressure differential of 1 psi, measuring the volume of expelled fluid and dividing this quantity by the known capacity. The gross expulsion efficiency was obtained by dividing the volume of fluid expelled by the gross ullage volume of the tank. Some fluid is retained in the standpipe and end fittings and cannot be expelled by the bladder. This quantity of fluid is designated "non-recoverable fluid". Therefore the net expulsion efficiency is obtained by dividing the volume of fluid expelled by the net ullage volume of the tank.

The parameters for the test tank and bladders used on this program are as follows:

A.	Gross Ullage Volume of Tank	0.519 ft^3
B.	Volume of Fluid Expelled	0.508 ft^3
C.	Gross Expulsion Efficiency ($100 \times \frac{B}{A}$)	97.9%
D.	Volume of Non-Recoverable Fluid	.0025 ft^3
E.	Net Ullage Volume of Tank (A-D)	.5165 ft^3
F.	Net Expulsion Efficiency ($100 \times \frac{B}{E}$)	98.4%

3.2.5.5 Post-Test Evaluation Procedures - Following the cyclic endurance test of each bladder, they were removed from the test tank and subjected to (1) room temperature leak check, and (2) a ply-by-ply visual inspection to determine the general condition of the bladder and the magnitude and location of any failures.

Leak Check - A room temperature leak check was performed using Method B, Section 3.2.5.3.

Visual Inspection - After performing the leak test, each bladder was completely disassembled to determine the magnitude and location of each failure and to ascertain if there was any pattern to the failures.

The stems were removed from each end by making a small cut across the adhesive in the attachment area and then lifting the stems out. Each ply was then cut along a baseline meridian and removed from the bladder. The gores were numbered consecutively from one edge of the cut and individually examined for tears, punctures, and seam failures. Each failure was recorded so that failures in one ply could be correlated with failures in the other plies.

Since the barrier plies were essentially transparent and the detection of small holes very difficult with standard visual examination, a special inspection technique was used. The ply under inspection was placed between two crossed polarizing plastic plates and back-lighted with a fluorescent tube light box. The birefringence characteristics and the refractive indices of the barrier ply films produced sufficient rotation of the polarized light to show the barrier films as a light background. Any holes or tears, where the polarized light was not rotated, showed up as black areas. For quick viewing, the technique worked well with a single polarizing plastic plate and polarized sunglasses worn by the inspector.

3.2.6 TEST RESULTS

Summarized in Tables VI through XI are the results of the Task II Static Expulsion Tests. A discussion of the performance of each bladder is presented below:

3.2.6.1 Bladder No. 1 (5 ply-12 gore Mylar) - The contract initially specified that all bladders were to be tested in an inward mode of expulsion. However, before any expulsion testing could be accomplished results were made available from a liquid hydrogen bladder program (Reference 4) which indicated that an outward expulsion was preferred over inward expulsion since it minimized inter-ply inflation. The NASA project manager then requested that the outward mode of expulsion be investigated with the initial bladders in this program. Unfortunately at the time, the test tanks had been designed and fabricated for inward expulsion and modifications had to be made. Holes were drilled in the bladder attachment ring to permit liquid oxygen flow to the exterior of the bladder. This was the extent of the modifications that could be made to the tank without a redesign and fabrication of new tank elements.

Bladder No. 1 was tested and it ruptured on the first cycle. This resulted when the tank could not be filled using the standard 1 psi pressure differential across the bladder and the ΔP was increased to approximately 5 psi. As the tank was filling a pressure surge in the fill line ruptured the bladder. Upon investigation it was determined that the venting capacity of the system was inadequate; prohibiting filling of the tank. The venting capacity was increased for the 2nd bladder by tapping an additional hole in the upper flange.

Bladder No. 1 failed in the bridging area at the upper stem as shown in Figure 22.

3.2.6.2 Bladder No. 2 (10-ply 12-gore Mylar) - Several attempts were made, without success, to test bladder No. 2 using outward expulsion. The tank would fill properly on each cycle but the liquid oxygen could not be expelled at a reasonable rate. In fact, all rates were less than 0.1 gpm.

A tight woven Teflon fabric, Style T-138, was used as an abrasion ply on the bladder. It was intended for outward expulsion, that the fabric serve as a colander ply as well as a protective ply, and permit the free flow of LOX; but the material appeared to seal off the flow when the pressure was applied. Further attempts to use Teflon felt strips to aid in the flow were not successful.

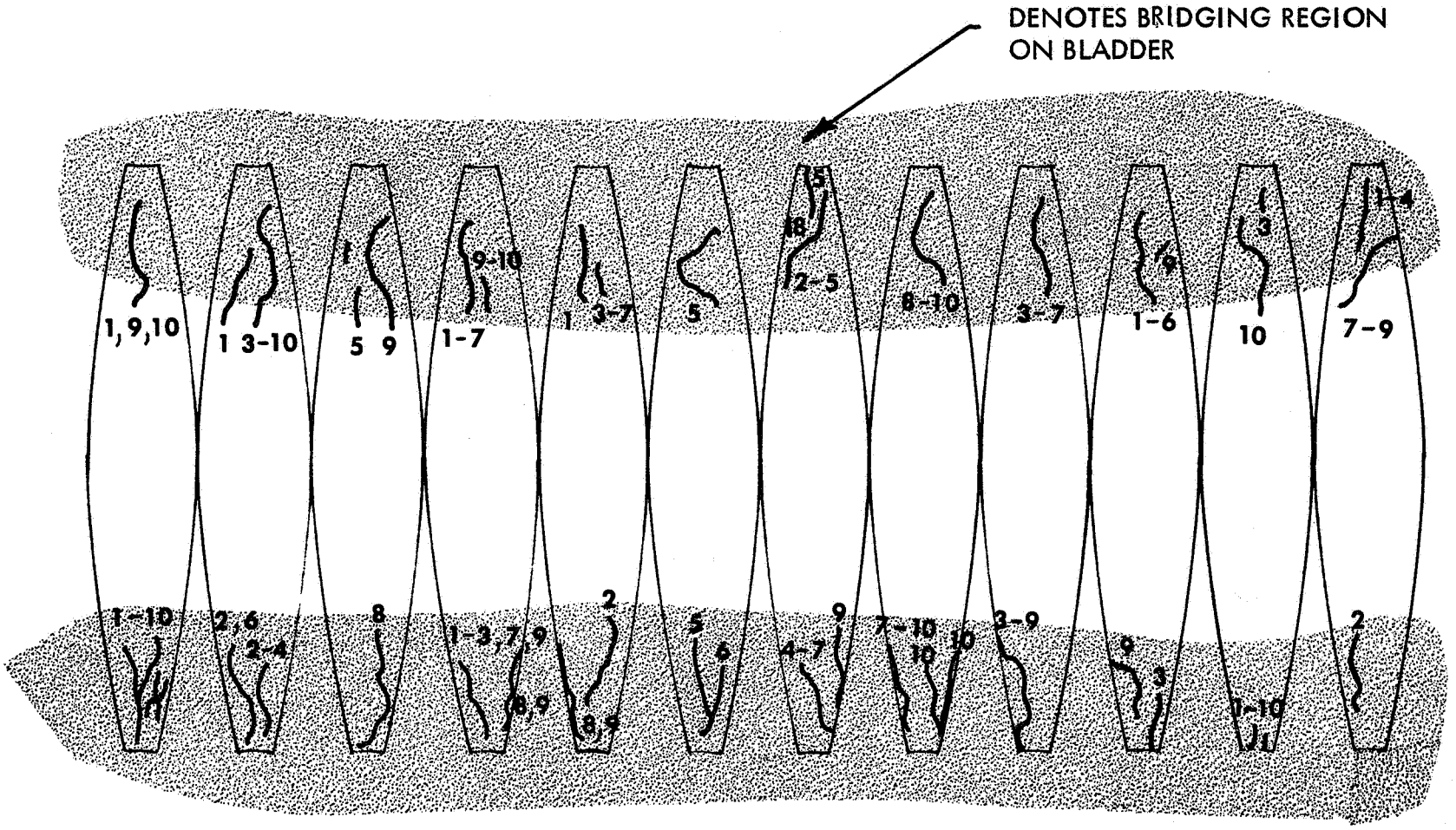

Numbers denote ply on which failure occurred, counting from inside of bladder

FIGURE 22 FAILURE LOCATIONS — BLADDER No. 1

After exhausting possibilities of making the outward expulsion technique perform with the existing tank, the test set-up was revised to permit inward expulsion. At this point bladder No. 2 had undergone 8 partial cycles.

The following information was obtained concerning the outward mode of expulsion:

A. No inter-ply inflation was noted.

B. If a fabric is to be used as a colander it should be of a very loose weave, with large diameter fiber. If possible two individual plies should be used, but ideally the tank should be designed for outward expulsion with an integral metallic colander.

After the system was established for inward expulsion, bladder No. 2 was installed in the system and expulsion cycled to failure. The bladder was subjected to 10 expulsion cycles (20 reversals) at -297°F before failure was detected. Helium permeability checks were made prior to the 1st and after the 2nd, 5th, 7th and 10th cycles. A leakage of 9600 cc/min was detected after the 7th cycle, and after the 10th cycle the rate was in excess of 77,000 standard cc/min. The test was terminated at this point. A summary of the test is shown in Table VI.

Examination of the bladder, showed the room temperature permeability rate (using Method B, Section 3.2.5.3) to be 28,300 cc/min, with failure occurring in the adhesive seams. The barrier films showed no visible or detectable damage. Examining the fabrication records, it was discovered that this bladder was made from the second of two adhesive batches of GT-300 adhesive purchased for the program. That particular batch had only 0.25-0.30 mils of adhesive on 0.5 mil Mylar versus the 0.5 mil of adhesive specified and generally obtained. The bonding characteristics and strength of the adhesive were checked prior to bladder fabrication and they appeared satisfactory even though the adhesive layer was thin. Three bladders (No!s 1, 2 and 7) were made from this particular batch of adhesive but unfortunately bladders 1 and 7 failed very early in their testing due to other reasons, preventing any definite conclusions to be

TABLE VI CYCLIC EXPULSION TEST RESULTS - BLADDER NO. 2

Cycle	Fill Rate, gpm	Expulsion Rate, gpm	Fill, %	Expulsion, %	Leakage Rate - Std. cc/min. -280°F	Leakage Rate - Std. cc/min. R.T.
0	-	-	-	-	0	0
1	.082	2.00*	93	N.A.*		
2	.099		100		0	
3	.055		74.7			
4	-**		-			
5	.043		34		0	
6	.203		69			
7	.156		73			
8	-**	-	-		9,600	
9	.047	1.74	53			
10	.031	-	24			
11	.054	2.28	75		77,000	28,300

*Accurate expulsion rate and volume was not obtained due to equipment malfunction.

**Cycled with cold gas.

drawn. Despite the cause, poor adhesive or poor seam fabrication, the Mylar bladder experienced no damage to the barrier film and with good seams would have withstood several more cycles.

3.2.6.3 Bladder No. 3 (10 ply-12 gore Mylar) - The bladder completed 17 expulsion cycles (-297°F) before the test was terminated due to excessive leakage. Presented in Table VII is the data and information of this test. The failure locations are shown in Figure 23. Failure occurred mostly around the upper and lower stems, with a few additional leaks around the center periphery. Seven leak points were detected from the exterior of the bladder. Tears in the 7th to 9th plies constituted the most significant damage to the bladder.

3.2.6.4 Bladder No. 4 (10 ply-12 gore Kapton) - Bladder No. 4 completed 25 expulsion cycles, the previously set goal of this task. After the 25 cycles the bladder had a leakage rate of 182 cc/min at -297°F and 128 cc/min at room temperature (Table VIII). Examination of the bladder revealed that all leakage occurred around the stem attachment. Each ply of the bladder was removed and checked for pinholes and damaged seams. No damaged areas were detected and the film was in relatively good condition. Precautions were taken in the succeeding bladders to insure a tighter seal in the stem attachment area by adding a little more GT-100 and duPont 46971 adhesive to the region.

3.2.6.5 Bladder No. 5 (10 ply-12 gore Kapton) - Like bladder No. 4, No. 5 successfully withstood 25 expulsion cycles with a final room temperature leakage rate of 7 cc/min (Table IX). The bladder's appearance after test was very good. In fact, the barrier film on both bladder No. 4 and 5 were quite similar after testing, possibly indicating that bladder No. 4 would have had an equivalently low leakage rate after 25 cycles had not leakage occurred in the stem attachment.

After completing the expulsion tests on bladder No. 5 and the tank was warm, it was impossible to extract the bladder from the tank. The gas between the individual bladder plies expanded on warm-up, inflating the bladder almost to full size. Since the bladder

TABLE VII CYCLIC EXPULSION TEST RESULTS - BLADDER NO. 3

Cycle	Fill Rate, gpm	Expulsion Rate, gpm	Fill, %	Expulsion, %	Leakage Rate - Std. cc/min. -280°F	Leakage Rate - Std. cc/min. R.T.
0					0	0
1	.310	.985	70	97		
2						
3						
4						
5	.298	.985	54	99	0	
6	.128	-	46	97		
7	.670	.940	18	99		
8	.278	.980	73	65		
9	.405	.930	79	81		
10	.350	.94	76	93	710	
11	.097	.855	79	83		
12	.555	.90	84	84		
13	.130	.81	36	99		
14	.288	.96	66	99		
15	.389	.99	71	90	935	
16	.084	-	36	-		
17	.206	-	76	-	12,000	2,600

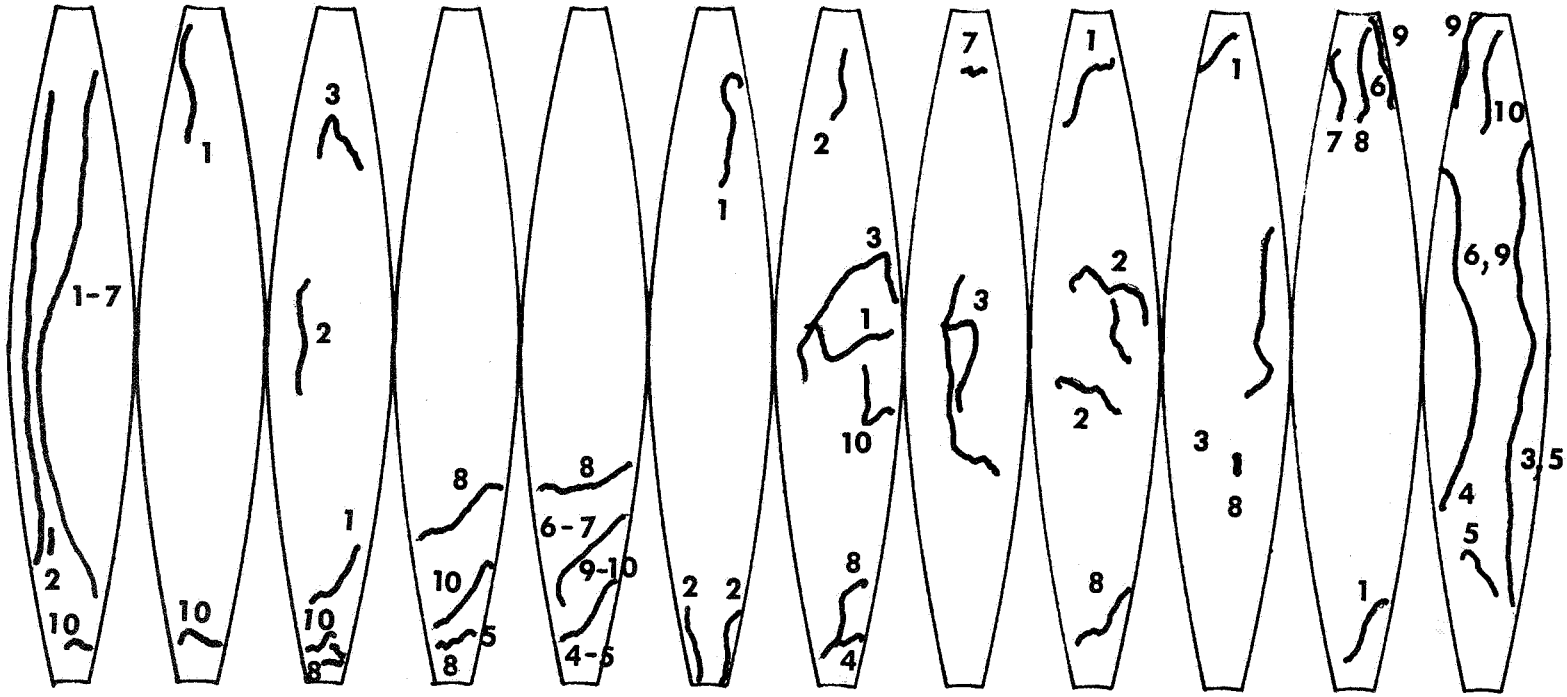

Numbers denote ply on which failure occurred, counting from inside of bladder

FIGURE 23 FAILURE LOCATIONS — BLADDER No. 3

TABLE VIII CYCLIC EXPULSION TEST RESULTS - BLADDER NO. 4

Cycle	Fill Rate, gpm	Expulsion Rate, gpm	Fill, %	Expulsion, %	Leakage Rate - Std. cc/min. -280°F	Leakage Rate - Std. cc/min. R.T.
0					0	
1	.1	1.05	71	100		
2	.31	1.01	73	99		
3	.30	1.02	73	100		
4	.28	1.01	71	99		
5	.52	1.05	66	100	0	
6	.28	.93	65	100		
7	.33	.87	66	99		
8	.42	.92	72	100		
9	.15	1.02	67	100		
10	.31	1.01	71	100	23	
11	.075	1.00	72	99		
12	.28	1.01	71	98		
13	.36	1.07	70	99		
14	.14	1.00	72	98		
15	.35	1.02	35	99	94	
16	.20	.94	70	100		
17	.36	.96	66	100		
18	.44	.95	66	100		
19	.56	.99	67	100		
20	.57	.98	65	99	137	
21	.30	-	-	-		
22	.80	-	-	-		
23	.52	.96	68	99		
24	.61	1.00	68	100		
25	.60	.97	69	99	182	128

TABLE IX CYCLIC EXPULSION TEST RESULTS - BLADDER NO. 5

Cycle	Fill Rate, gpm	Expulsion Rate, gpm	Fill, %	Expulsion, %	Leakage Rate - Std. cc/min. -280°F	Leakage Rate - Std. cc/min. R.T.
0						
1	.118	-	89	-	0	0
2	.370	-	86	-		
3	..258	-	87	-		
4	.479	3.2	87	100		
5	.712	-	89	-	0	
6	.376	1.74	89	75		
7	.974	1.93	86	80		
8	1.46	1.90	80	80		
9	.770	1.97	79	88		
10	.780	1.80	82	56	10	
11	.197	1.71	76	74		
12	1.79	1.75	96	65		
13	.841	1.83	89	65		
14	.917	1.89	86	73		
15	.568	1.95	80	79	18	
16	.336	1.62	78	44		
17	2.74	1.46	95	18		
18	.342	1.60	80	73		
19	.680	1.50	70	55		
20	.590	1.78	80	57	21	
21	.310	-	92	-		
22	.293	1.85	70	80		
23	.612	1.73	80	62		
24	1.25	1.81	93	24		
25	.630	1.73	93	23	23	7

had, for all practical purposes, no leakage, the gas had no way to escape. Liquid nitrogen was used to cool the system down to the point where the bladder could be removed. This was the first evidence of inter-ply inflation. Examination of the bladder showed that a pin-hole leak developed in the first ply and a seam leak in the second ply permitting cryogen to become trapped between the 1st and 2nd - and 2nd and 3rd plies (Figure 24). As the bladder warmed up, the cryogen inflated the bladder. The fill volume and expulsion volume strip charts were examined to see if there was any evidence of inter-ply inflation during test, and the results showed that noticeable inter-ply inflation began to occur after about the 15th cycle.

3.2.6.6 Bladder No. 6 (10 ply-12 gore Kapton) - Bladder No. 6 was the same configuration and construction as bladders No. 4 and 5. This specimen completed 20 cycles at -297°F before the test was terminated due to excessive leakage. The results of this test are shown in Table X.

The leakage of the bladder in the test stand was 216 cc/min at -297°F. In the laboratory, using Method B (Section 3.2.5.3) to check for leakage, a reading of 8 cc/min was obtained. This large difference in readings is accounted for by the fact that at room temperature the thin film plies tend to seal against one another under a 1 psi pressure differential giving a lower leakage rate. At -297°F the bladder film by comparison is much more rigid and cannot readily seal resulting in an unobstructed leak path between plies. Both readings are taken at steady state. Also at the cryogenic temperatures, leakage around the stem attachment area, should any be present, becomes more pronounced due to the thermal contraction of the metal and adhesive. The fittings are initially tightened and leak checked at room temperature.

Examination of bladder No. 6 showed that the leakage occurred in the attachment area and in the adjacent regions (Figure 25). The damage to the Kapton bladder was very slight in the mid-section.

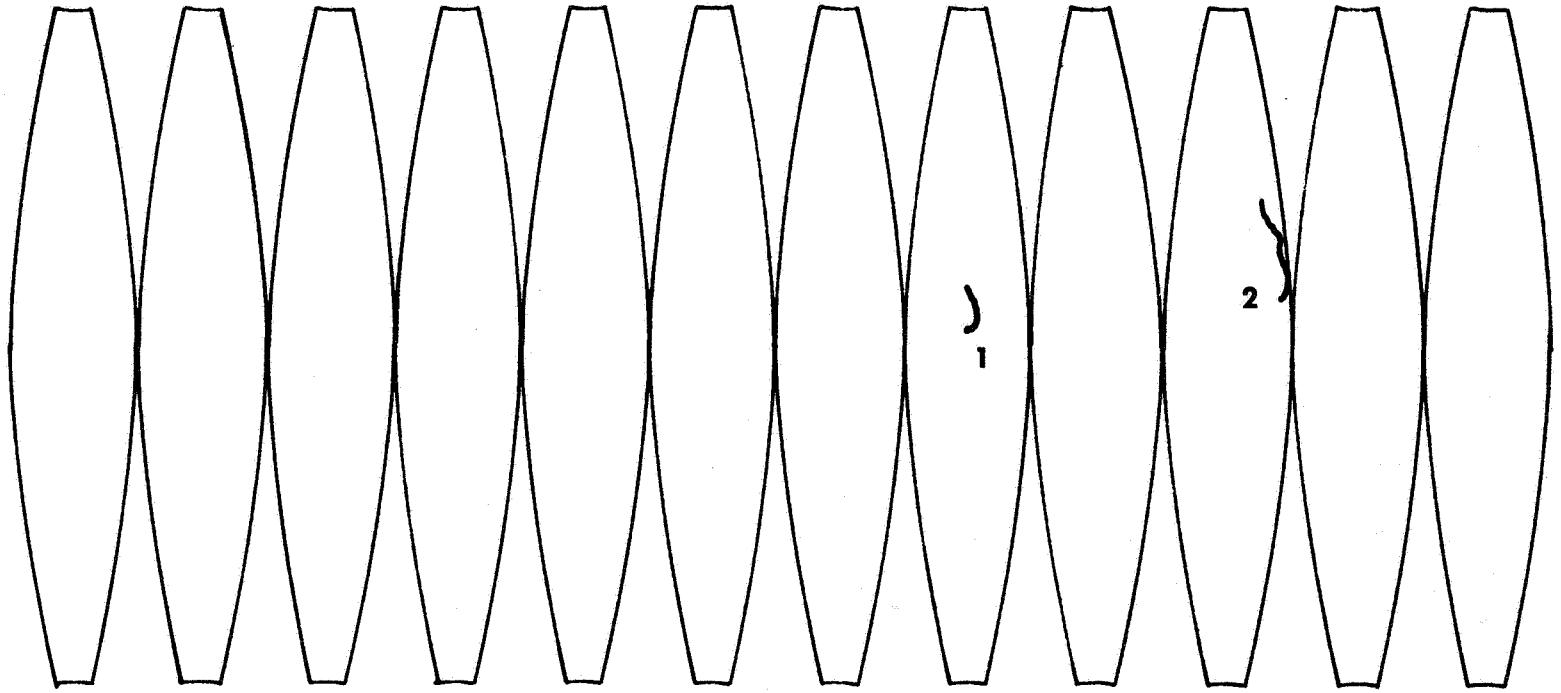

Numbers denote ply on which failure occurred, counting from inside of bladder

FIGURE 24 FAILURE LOCATIONS — BLADDER No. 5

TABLE X CYCLIC EXPULSION TEST RESULTS - BLADDER NO. 6

Cycle	Fill Rate, gpm	Expulsion Rate, gpm	Fill, %	Expulsion, %	Leakage Rate - Std. cc/min. -280°F	Leakage Rate - Std. cc/min. R.T.
0					0	0
1	.085	.565	96	67		
2	.150	.990	93	86		
3	.216	.840	95	83		
4	.260	.940	96	79		
5	.157	.895	64	71		
6	.254	.705	100	73		
7	.674	.840	100	80		
8	1.08	.890	100	81		
9	1.41	.990	100	83		
10	1.36	1.01	98	80	40	
11	.39	.94	98	87		
12	.87	.970	96	82		
13	1.06	.99	98	82		
14	.667	.96	98	78		
15	.722	1.02	98	77	51	
16	.39	.72	88	71		
17	1.00	.90	90	64		
18	.60	1.0	98	54		
19	1.08	1.1	98	53		
20	1.09	1.03	98	67	216	8

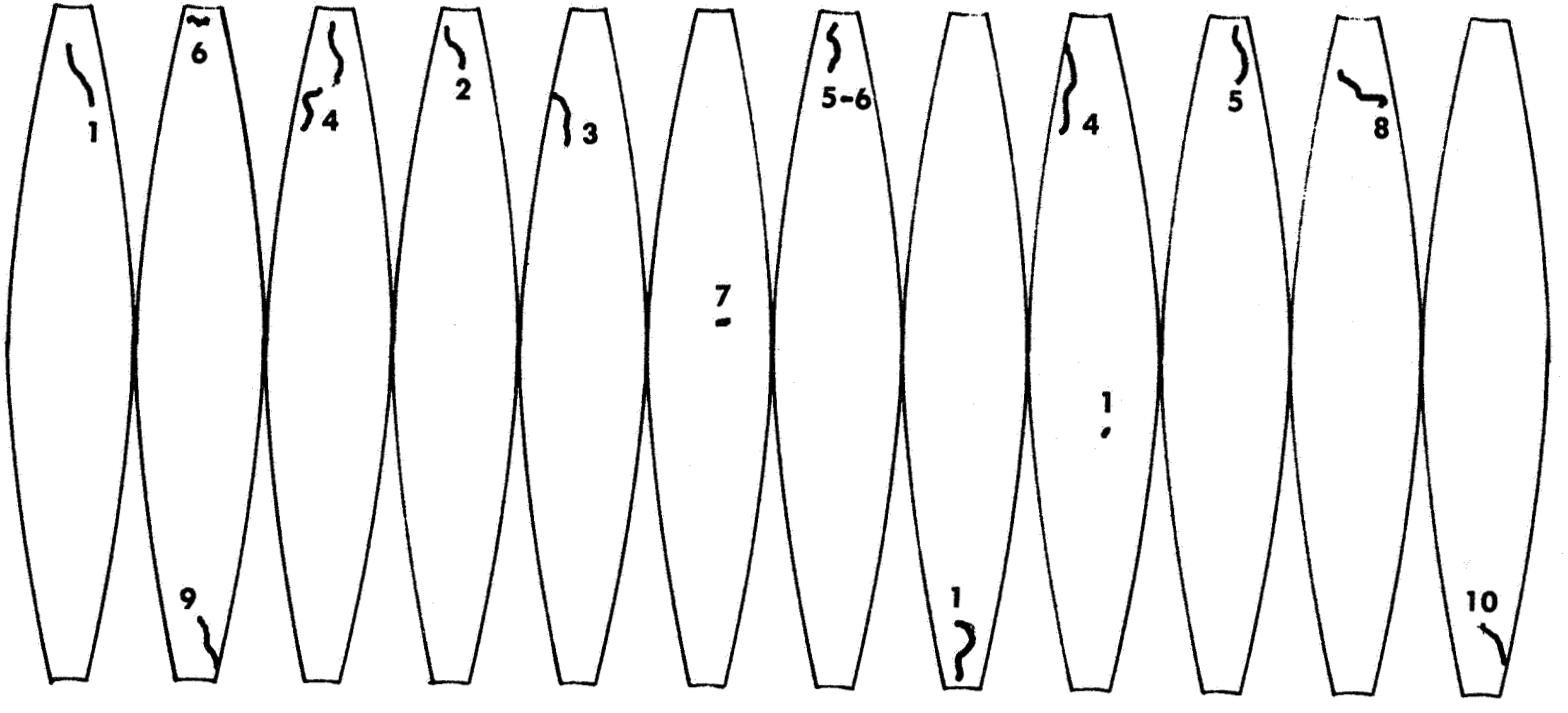

Numbers denote ply on which failure occurred, counting from inside of bladder

FIGURE 25 FAILURE LOCATIONS — BLADDER No. 6

3.2.6.7 Bladder No. 7 (10 ply-12 gore Mylar) - Bladder No. 7 failed on the first cycle. Damage was in the shoulder areas of the bladder, adjacent to each pole piece. The film in these areas split randomly in the longitudinal direction (Figure 26). That is, the tears did not coincide from ply-to-ply. All evidence indicates that the bladder failed on the expulsion cycle. Due to the random nature of the tears, the damage was not a result of over pressurization. More likely the 1/4-mil film plies became individually bridged in random areas and could not withstand the pressure differential of 0.5-1.0 psi. This type of failure was not experienced with any of the other 10-ply bladders.

3.2.6.8 Bladder No. 8 (5 ply-12 gore Kapton) - Bladder No. 8 failed similarly to No. 7 on the first cycle, in the bridging area adjacent to both pole pieces. Again, the failures were random between plies and consisted of large tears (approximately 1" long) running in the longitudinal direction. Bladder No. 8 was only a 5-ply bladder, while No. 7 contained 10 plies plus a substrate ply.

The failure locations are illustrated in Figure 27.

3.2.6.9 Bladder No. 9 (5 ply-12 gore Mylar) - Bladder No. 9 failed on the first expulsion cycle as did the previous 5 ply-12 gore bladder; however the failure locations differed. In this case the failures were randomly distributed around the circumference (Figure 28) or center portion of the bladder. The tears propagated in all directions; not following any particular pattern. In bladders 7 and 8 the tears were all longitudinal. The failure location on this bladder somewhat reinforces the conclusion drawn with bladder No. 7, in that if an overpressurization had occurred the center portion of the bladder would be the least likely area to be damaged. More likely the plies of the bladder are acting as individual layers resulting in sequential failure of the layers during the expulsion cycle. The same effect may be occurring with the 10-ply bladders except the chance of one ply carrying the initial loads independently is less probable but possible as in the case of bladder No. 7. Bladders No. 7 and 9 were made from the same continuous section of Mylar film and the film may have had inherent flaws which were not detected, but this does not account for the failure of bladder No. 8, which was made with Kapton film.

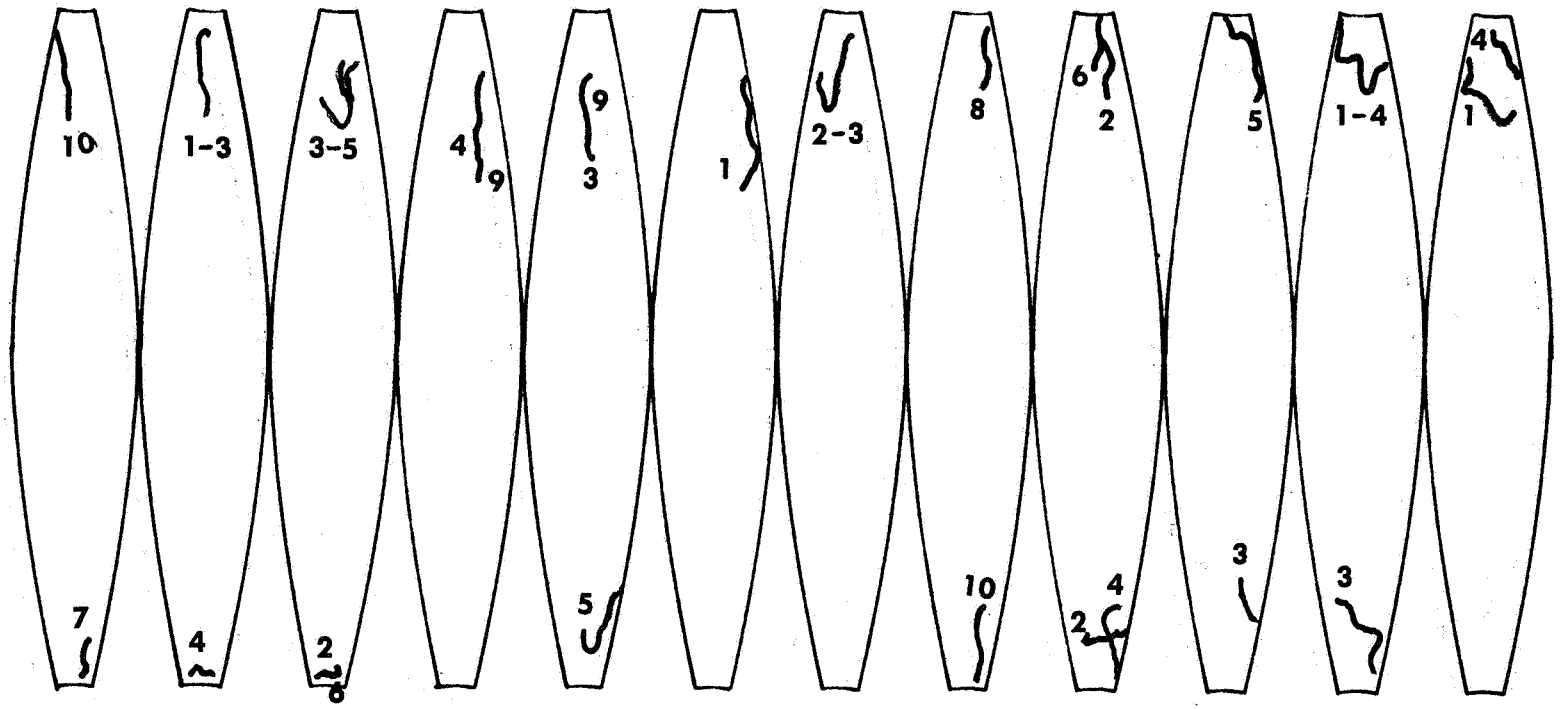

Numbers denote ply on which failure occurred, counting from inside of bladder

FIGURE 26 FAILURE LOCATIONS — BLADDER No. 7

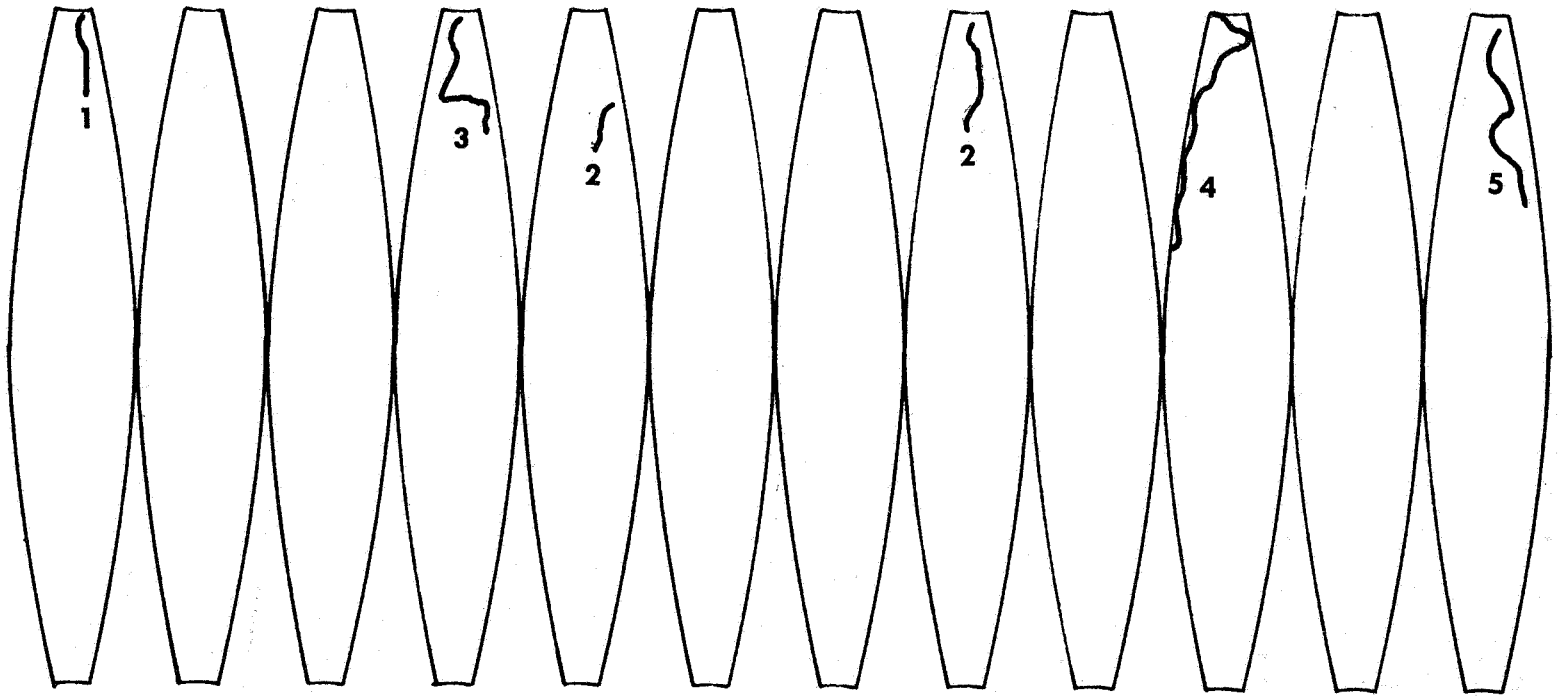

Numbers denote ply on which failure occurred, counting from inside of bladder

FIGURE 27 FAILURE LOCATIONS — BLADDER No. 8

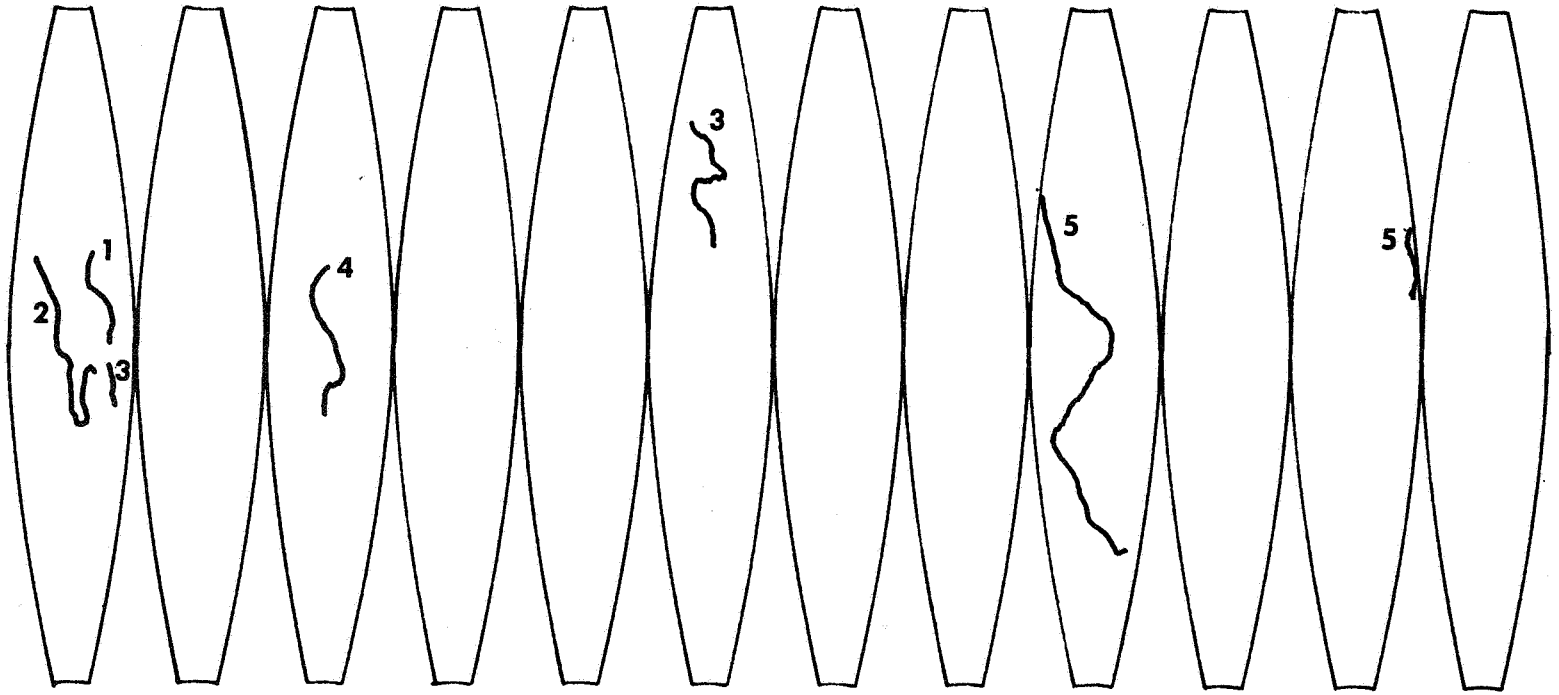

Numbers denote ply on which failure occurred, counting from inside of bladder

FIGURE 28 FAILURE LOCATIONS — BLADDER No. 9

3.2.6.10 Bladder No. 10 (5 ply-6 gore Mylar) - Bladder No. 10 failed after the 5th cycle with a final leakage rate of 310 cc/min (Table XI). The failure consisted of nine small failures, seven of which were in the bridging area (Figure 29). Except for the torn areas, the visual condition of the barrier film was excellent, with only slight wrinkling.

No sign of interply inflation was noted with this bladder. The increased permeability of the thermoformed film may have been a detriment if the bladder had been subjected to the cryogen for an extended period of time, such as 24 hours.

Although the bladder went four more cycles than either of the other 5-ply Mylar bladders, no conclusions can be drawn from one specimen concerning the merit of 6-gore versus 12-gore construction.

3.3 TASK III - DYNAMIC EXCITATION OF POLYMERIC BLADDERS

The objectives of this task were to dynamically excite tank/bladder assemblies to study the structural integrity and chemical compatibility of the polymeric bladders in a liquid oxygen environment. The environmental modes of excitation evaluated were slosh, vibration, impact (both blunt and penetration) and burst.

The dynamic testing was performed to evaluate the capability of a polymeric bladder to withstand shocks and movements representative of flight conditions and also to establish the severity of impact required to cause spontaneous ignition. Dynamic environments to which a propellant tank will be subjected in service include acceleration and vibrations within the launch vehicle, orbit insertion, maneuver oscillations, and unexpected (or emergency) transient maneuvers.

The magnitudes of the dynamic loadings selected for the bladder tests which are representative of most space missions include slosh frequencies of 0-10 cps, vibration frequencies of 10-160 cps, accelerations up to 4 times the acceleration due to gravity and blunt impacts of up to 216 ft-lbs of energy. The ballistic penetration and burst tests represent dynamic type loadings which are generally over and above a system design requirement.

TABLE XI - CYCLIC EXPULSION TEST RESULTS - BLADDER NO. 10

Cycle	Fill Rate, gpm	Expulsion Rate, gpm	Fill, %	Expulsion, %	Leakage Rate - Std. cc/min. -280°F	Leakage Rate - Std. cc/min. R.T.
0					0	
1	.11	.98	73	80		
2	.40	.78	79	73		
3	.43	-	-	-		
4	-	-	-	-		
5	.25	1.01	62	71	310	

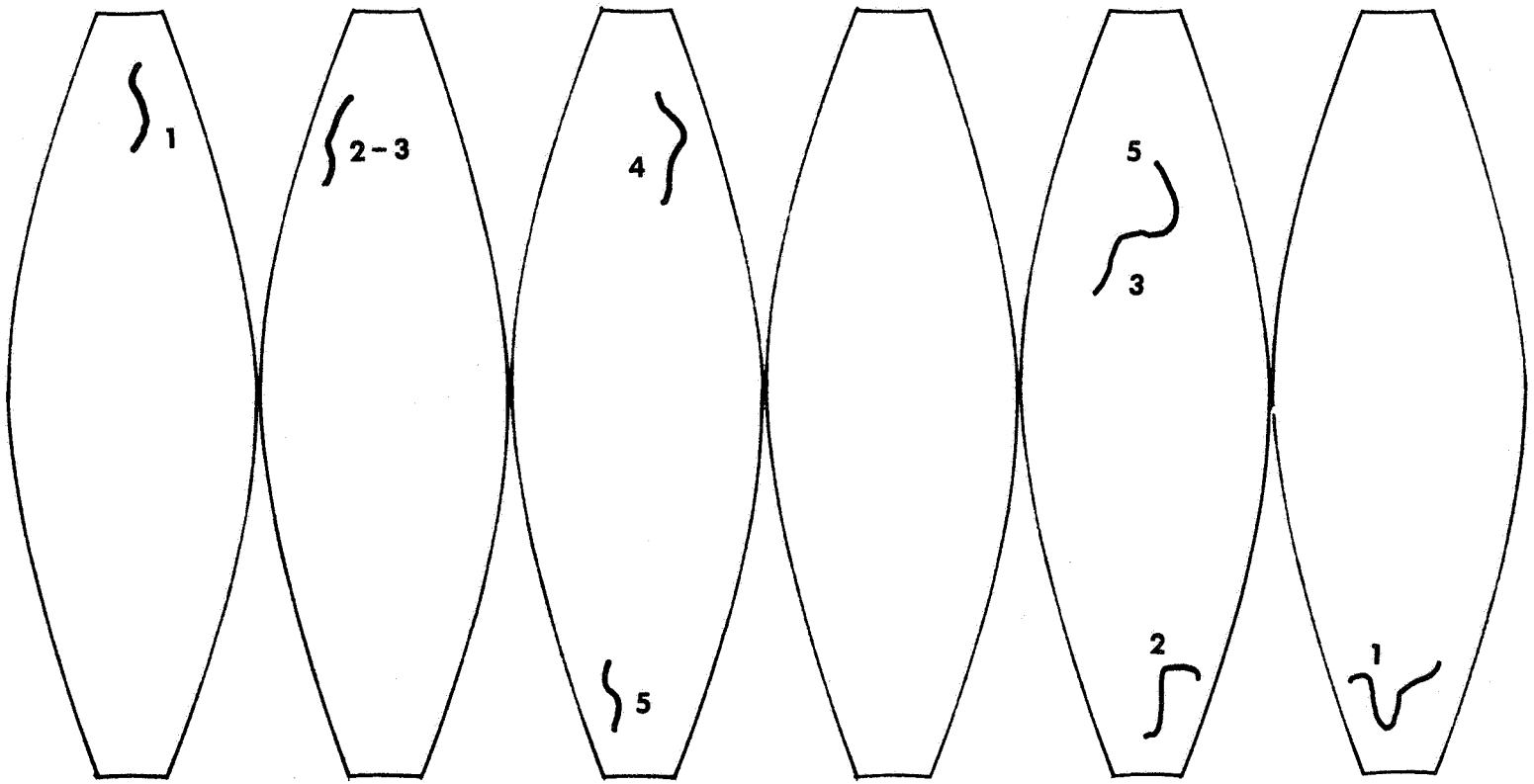

Numbers denote ply on which failure occurred, counting from inside of bladder

FIGURE 29 FAILURE LOCATIONS — BLADDER No. 10

3.3.1 SLOSH TEST

3.3.1.1 Test Specimens - Two expulsion bladders, one Mylar (No. 11) and one Kapton (No. 12), were tested in a slosh mode of excitation. The specimen configurations and construction techniques are presented in Table XII and Section 3.2.3, respectively. The bladders were evaluated in the stainless steel test tanks (Section 3.2.4) used in Task II.

3.3.1.2 Test Equipment - The slosh tests were conducted on electromechanical vibrators designed and fabricated by The Boeing Company. An amplidyne motor-generator set was used in conjunction with the vibrators to obtain the low frequency required for the slosh test. A schematic of the test set-up is shown in Figure 30 and the list of equipment tabulated in Tables XIII and XIV. One vibrator was used for sloshing in the antisymmetric mode (laterally) and a second for the symmetric (vertical) slosh mode. This equipment is shown in Figures 31 to 36.

In the test set-up flexible lines were used for the LOX fill line, the LOX drain line, in two sections of the bladder by-pass line, and the two vent lines. All lines were vacuum jacketed.

The stainless steel tank was insulated with a rigid polyurethane foam to reduce the heat leak (Figure 36).

3.3.1.3 Test Procedure - The test consisted of a low level sine sweep from 0.5 to 10 cps at approximately a 1-inch double amplitude, followed by a 10 minute hold at the natural slosh frequency. Each bladder was tested in the 0%, 50%, and 100% fill condition on both the symmetric (longitudinal) and antisymmetric (lateral) axis of the tank. In the empty condition the tank assembly was cycled three times through the frequency range since a slosh frequency is not obtainable.

The fundamental slosh frequencies were theoretically calculated using the methods presented by McCarty and Budiansky in References 9 and 10.

TABLE XII EXPULSION BLADDER CONFIGURATIONS - TASK III

BLADDER NUMBER	BARRIER FILM PLIES				NUMBER OF ABRASION PLIES	NUMBER OF ▷ SUBSTRATE PLIES
	Material	Thickness (mils)	No. of Plies	Gores per ply		
11	Mylar	0.25	10	12	2	1
12	Kapton	0.50	10	12	2	1
13	Mylar	0.25	10	12	2	1
14	Kapton	0.50	10	12	2	1
15	Mylar	0.25	10	12	2	1
16	Kapton	0.50	10	12	2	1
17	Mylar	0.25	10	12	2	1
18	Kapton	0.50	10	12	2	1

▷ Located between 5th and 6th barrier film plies.

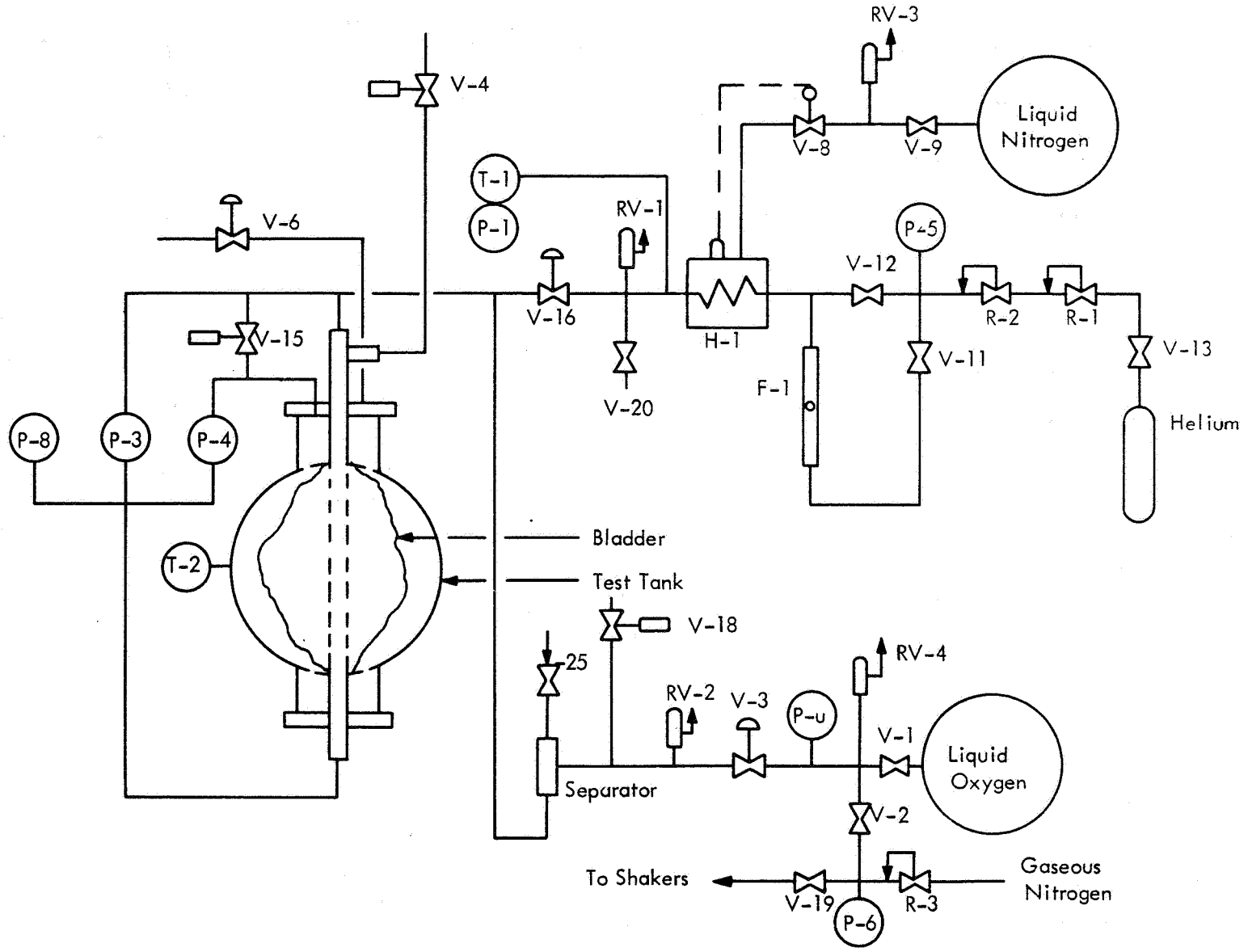

FIGURE 30 TEST SCHEMATIC FOR VIBRATION AND SLOSH EVALUATIONS

TABLE XIII - EQUIPMENT LIST - TASK III

SYMBOL	DESCRIPTION	RANGE	ACCURACY	INDICATOR
P_1	GHe Pressurization Pressure	0-15 psig	± 5%	Strip Chart & Panel Meter
P_3	Δ P Liquid Level	-1.5 to +2.5 psid	± 5%	Strip Chart & Panel Meter
P_4	Δ P Across Bladder	± 2.5 psid	± 5%	Strip Chart & Panel Meter
P_5	R_2 Output Pressure Gage	0-50 in. of H_2O	± 10%	Manometer
P_6	R_3 Output Pressure Gage	0-30 psig	± 10%	Gage
P_8	Test Tank Pressure	0-15 psig	± 5%	Strip Chart & Panel Meter
T_1	GHe Temperature	140 to 520°R	± 5°R	Strip Chart
F_1	Manostat Rotameter	4 - 232 scc/M He	± 10%	Rotameter
P_u	LO_2 Fill Line Pressure	0-15 psig	± 5%	Panel Meter
T_2	Test Tank Temperature	140-520°R	± 5°R	Strip Chart

TABLE XIV EQUIPMENT LIST - TASK III

SYMBOL	DESCRIPTION	SIZE	TYPE	SERVICE	REMARKS
-	Test Tank Assembly	12" dia.	Sph.	LO_2	
-	Dewar	600 gal.	-	"	
-	Dewar	600 gal.	-	LN_2	
-	Bottle Manifold	10 cyl.	-	GHe	
H-1	Heat Exchanger	1"dia.x120'	Cu. Tube	LN_2-GHe	
R-1	Pressure Regulator, High Pressure	0-3000 psi	Dome Loaded	GHe	
R-2	Pressure Regulator, Low Pressure	0-25 psi	Diaphragm	GHe	Grove
R-3	Pressure Regulator, Purge	0-150 psig	Diaphragm	GN_2	Conoflow
R-4	Pressure Regulator, High Capacity				
RV-1	Heat Exchanger Relief Valve	1/2"	Poppet	GHe	Circle Seal, 35 psig
RV-2	Test Tank Relief Valve	1/2"	Poppet	LO_2	Circle Seal, 10 psig
RV-3	LN_2 Line Relief Valve	1/2"	Poppet	LN_2	Circle Seal, 35 psig
RV-4	LO_2 Line Relief Valve	1/2"	Poppet	LO_2	Circle Seal, 35 psig
F-1	Rotameter	4-232 scc/M	Sph. Float	GHe	Manostat No. 36-541-04
F-2	Orifice Meter	.1 to 10 gpm			
V-1	LO_2 Shut-Off Valve	3/4"	Globe	LO_2	Powell, On Dewar
V-2	GN_2 Shut-Off Valve	1/2"	Ball	GN_2	Jamesbury
V-3	LO_2 Control Valve	3/4"	Globe		Annin, $C_v = 1.5$
V-4	LO_2 Vent Valve	1-1/2"	Ball	LO_2	Jamesbury
V-6	He Space Vent Valve	3/4"	Globe	GHe	Annin, $C_v = 1$
V-8	LN_2 Control Valve	1/2"	Poppet	LN_2	Leslie MCR
V-9	LN_2 Shut-Off Valve	1/2"	Globe	LN_2	Powell, On Dewar
V-11	Flowmeter Shut-Off Valve	1/2"	Needle	GHe	Hoke
V-12	Flowmeter By-Pass Valve	1/2"	Ball	GHe	Jamesbury
V-13	GHe Shut-Off Valve	1/2"	Ball	GHe	Jamesbury
V-15	Bladder By-Pass Valve	1/2"	Ball	GO_2	Jamesbury
V-16	GHe Control Valve	3/4"	Globe	GHe	Annin, $C_v = 0.6$
V-18	LO_2 Drain Valve	1/2"	Ball	LO_2	Jamesbury

TABLE XIV - EQUIPMENT LIST - TASK III (Continued)

SYMBOL	DESCRIPTION	SIZE	TYPE	SERVICE	REMARKS
V-19	Shaker Purge Shut-off Valve	1/2"	Ball	GN_2	Jamesbury
V-24	Purge Gas Vent Valve	1/2"	Ball	GHe	Jamesbury
V-21	GN_2 Shut-off Valve	3/4"	Ball	GN_2	Jamesbury
V-22	Cylinder Pressurization Control Valve				
V-23	Cylinder Vent Valve	1/4"	Poppet	GN_2	Asco
V-20	GHe Bleed Valve	1/4"	Needle	GHe	Hoke
CV-2	GHe Check Valve	1/4"	Poppet	GHe	Circle Seal

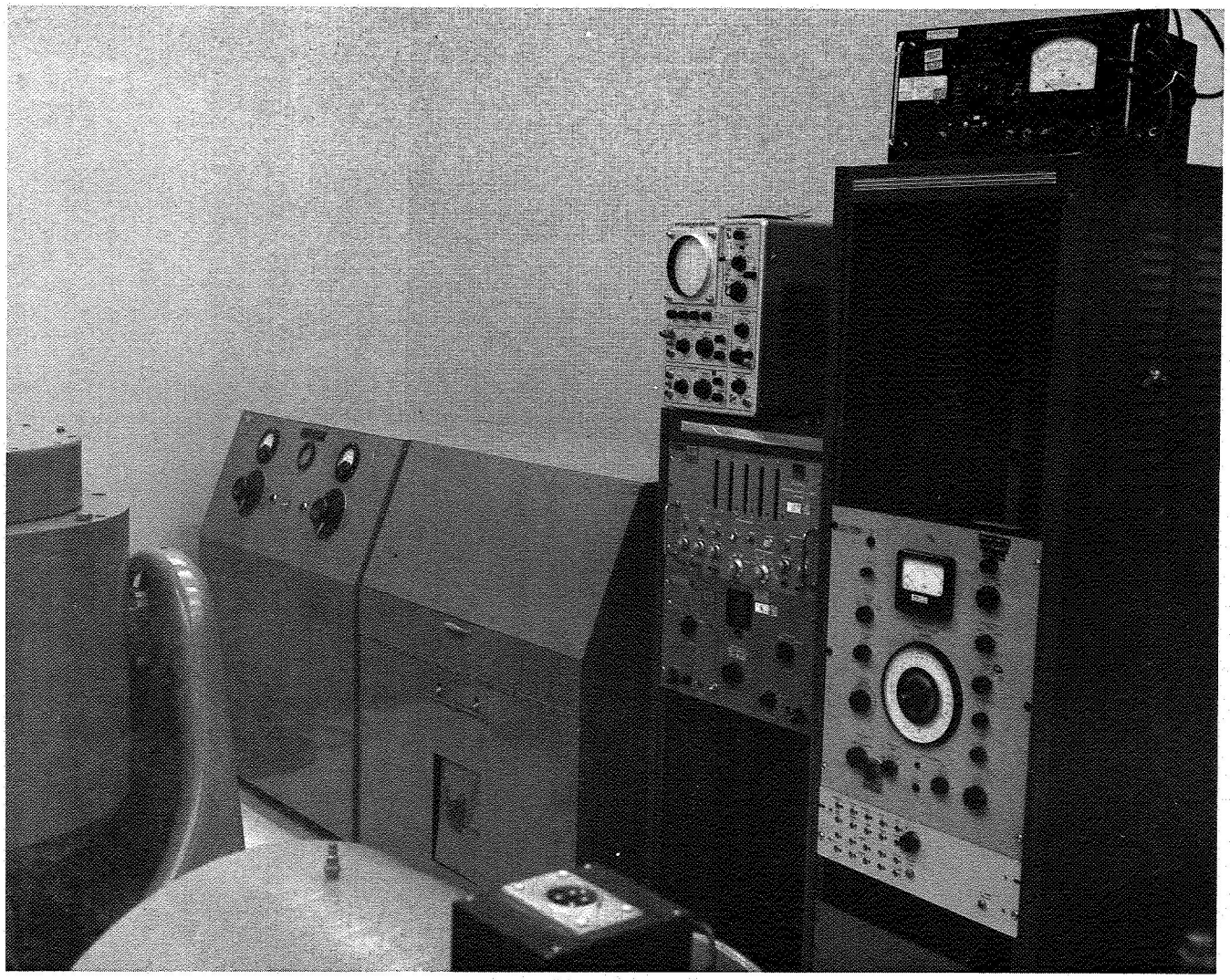

FIGURE 31 VERTICAL VIBRATION CONTROL UNITS

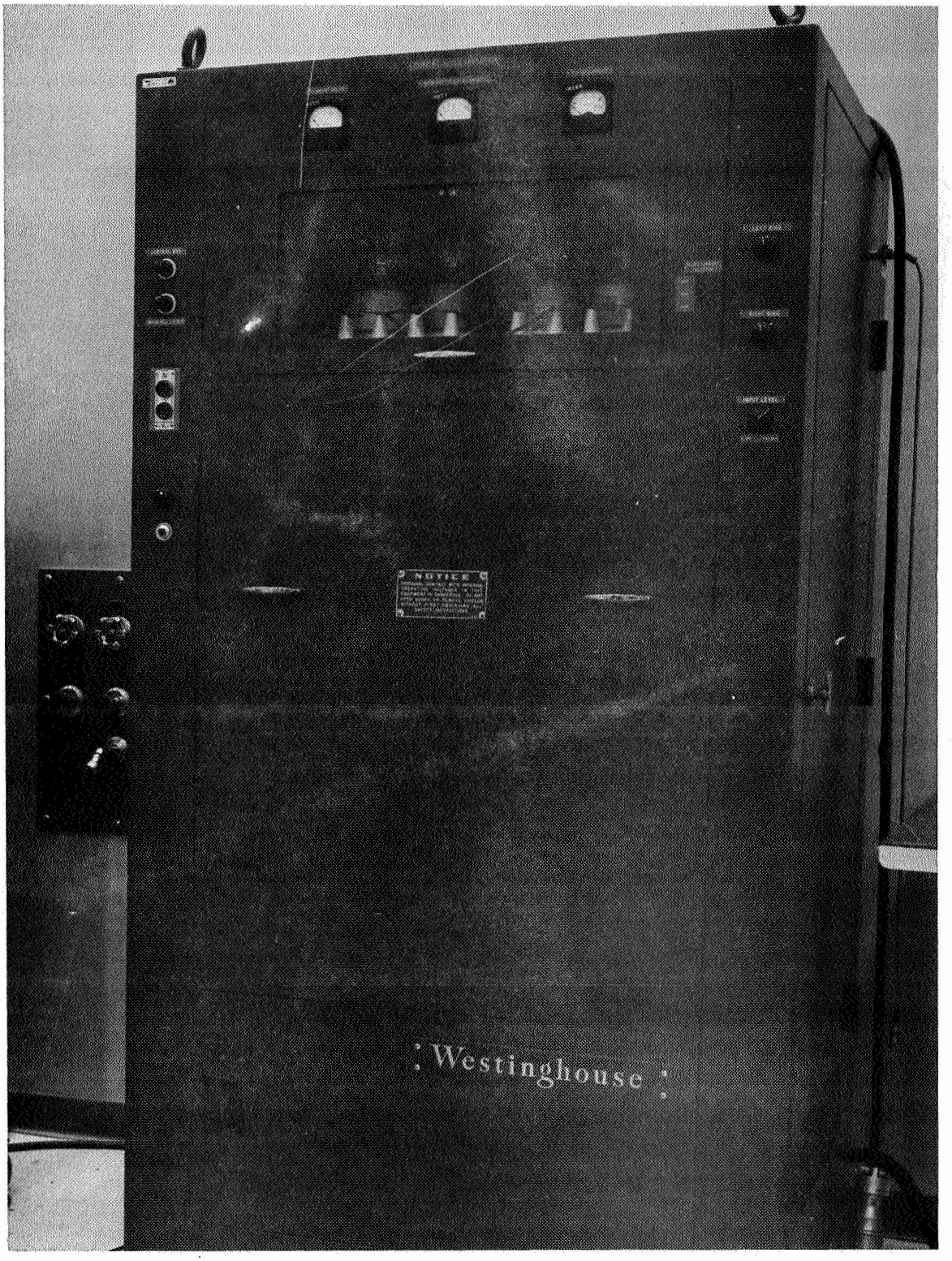

FIGURE 32 HORIZONTAL VIBRATION CONTROL UNIT

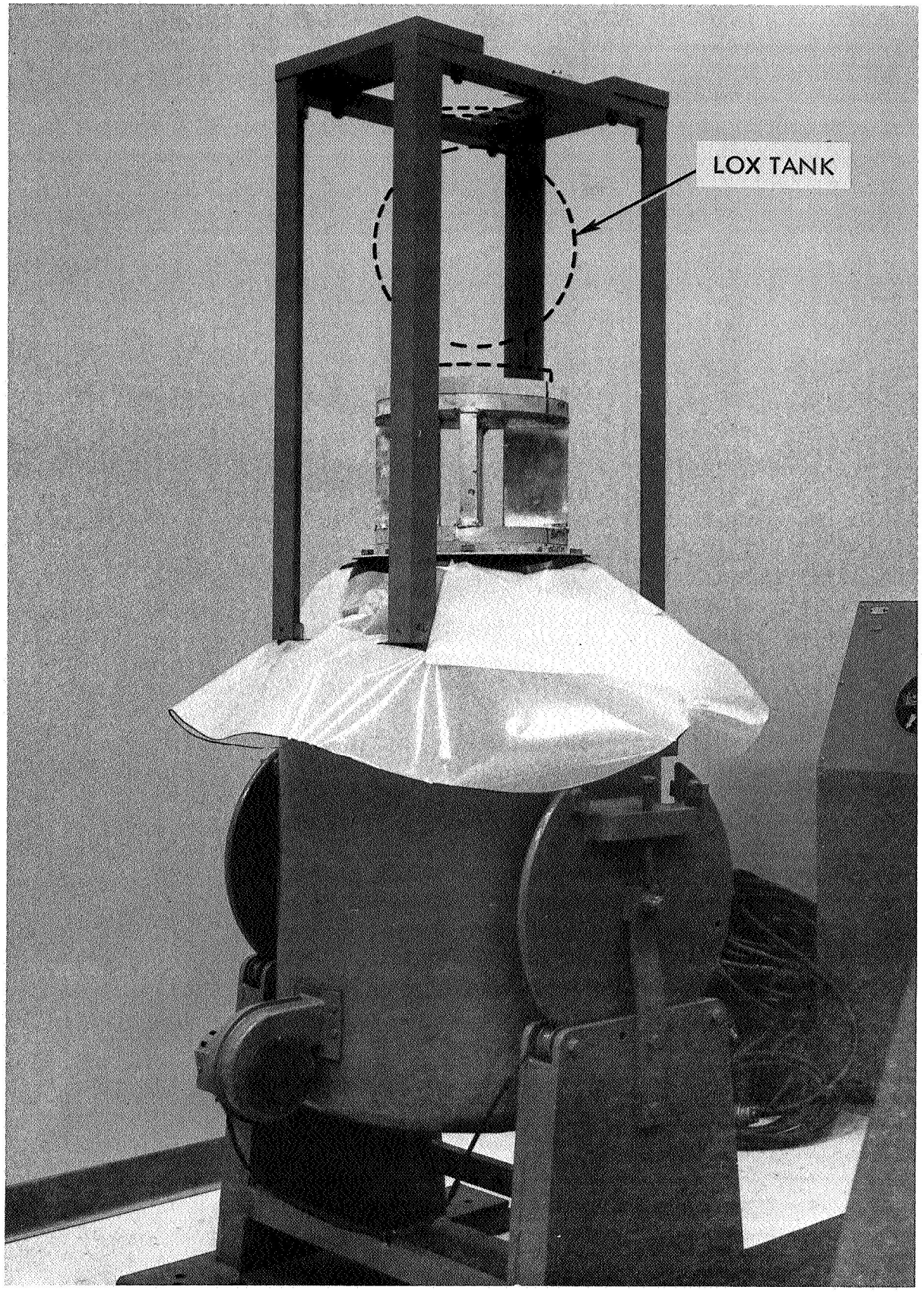

FIGURE 33 VERTICAL VIBRATION FIXTURE

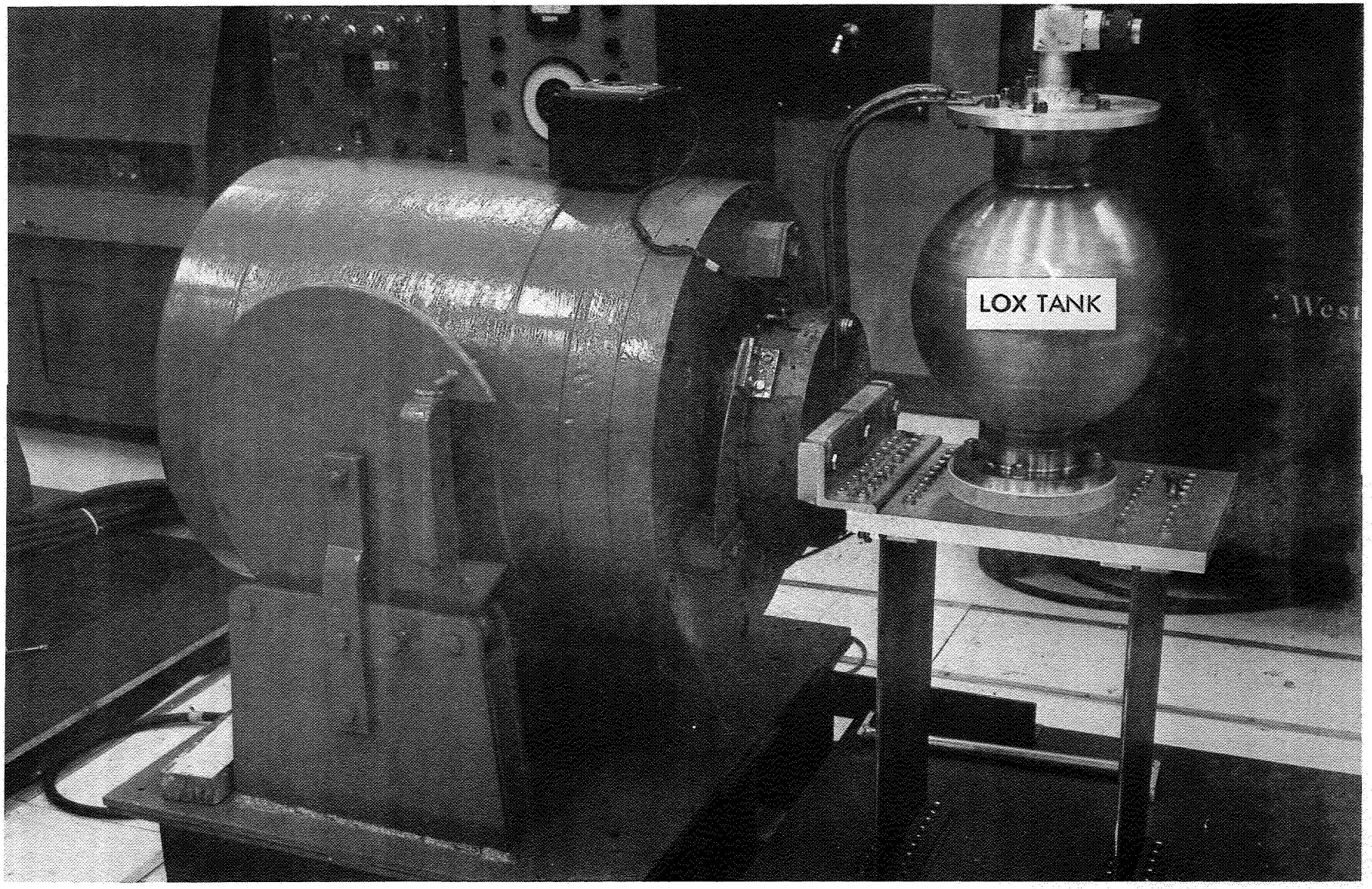

FIGURE 34 HORIZONTAL VIBRATION FIXTURE

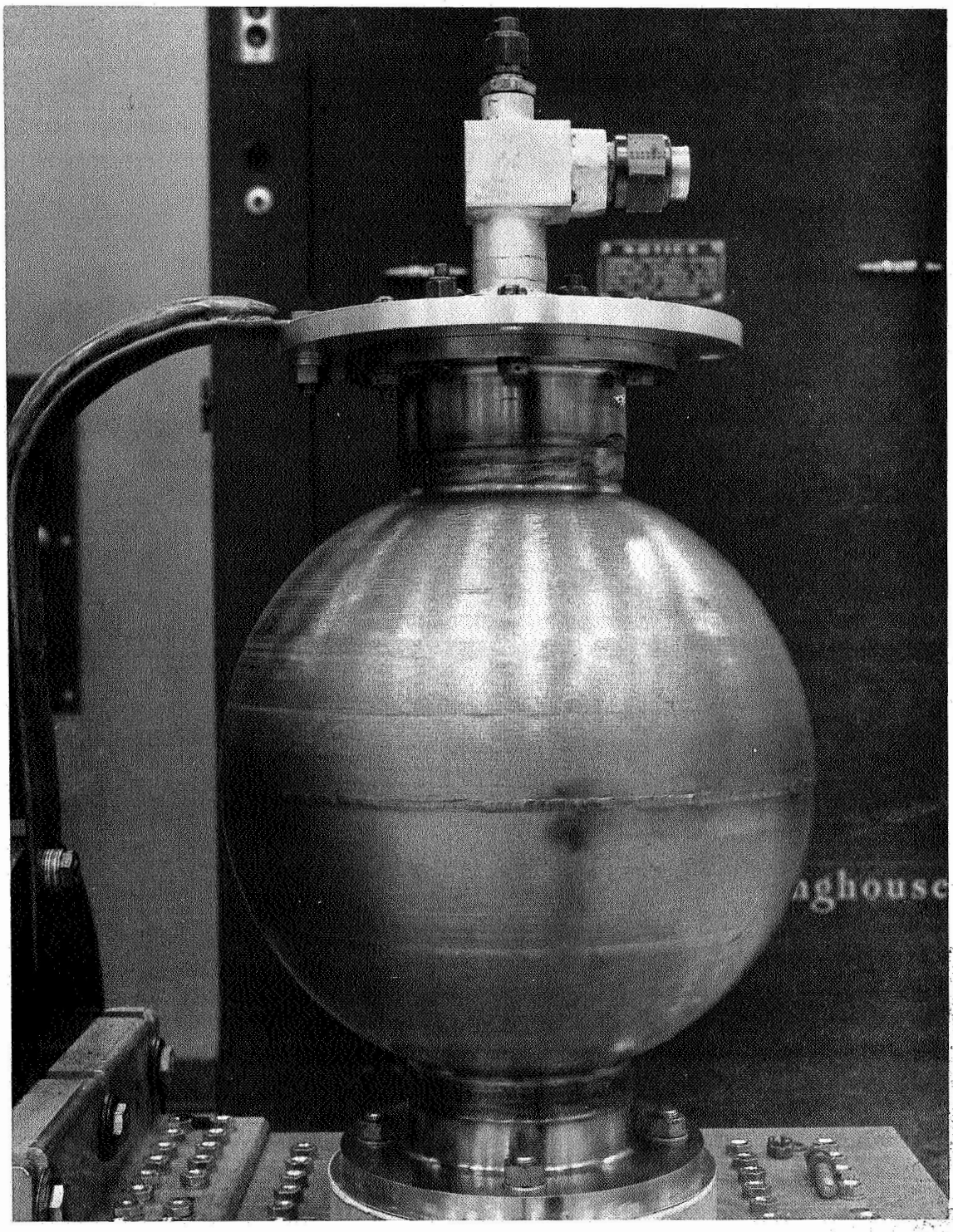

FIGURE 35 TANK MOUNTED FOR HORIZONTAL VIBRATION

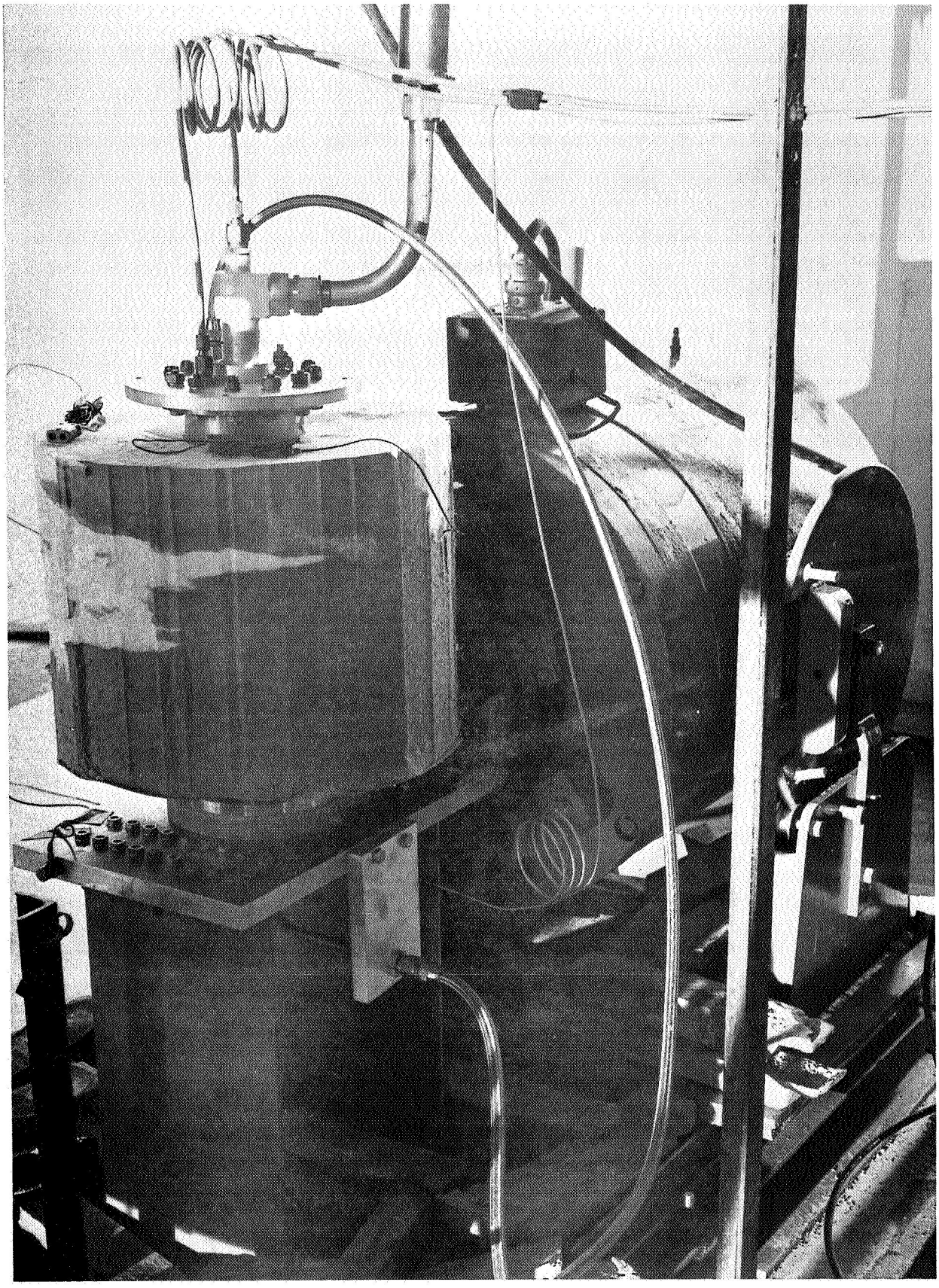

FIGURE 36 HORIZONTAL VIBRATION FIXTURE IN TEST FACILITY

The antisymmetrical and symmetrical slosh modes were calculated by the following two methods, with the calculations being restricted to the first mode only.

Antisymmetrical Mode

The antisymmetrical mode is excited by displacements along the lateral axis of the tank. This mode has been well studied and the methods used to calculate the slosh frequencies has been verified by a considerable amount of experimental data (Reference 9 and 10). Reference 9 verifies the methods of calculations of Reference 10 with experimental data. Both references give non-dimensionalized frequency parameters for the natural slosh frequencies. The calculation made here is the application of these parameters to the tank in question, i.e., a spherical tank of radius six inches. It is assumed that the bladder, with 50% or more liquid in the tank, has negligible effect upon the slosh frequencies. This assumption can be made for the following two reasons:

1. The mass of the liquid is much greater than the mass of the bladder.
2. The bladder will conform to the shape of the outer tank for the pressure will be equal on both sides of the bladder.

Reference 9 denotes the frequency parameter as λ_1 and Reference 10 as $(\lambda_1)^{1/2}$, even though they are the same parameter. To lessen the confusion, λ_1 of Reference 9 was called A_1 and $(\lambda_1)^{1/2}$ of Reference 10 called B_1. Values for A_1 and B_1 are tabulated in Table XV, for various tank fill levels. They were scaled from Figure 6 of Reference 9 and Figure 9 of Reference 10. The one exception is the value of B_1 for the half-full condition, which was given in Table 2 of Reference 10. As can be seen from Table XV there is some variance in the last two digits of A_1 and B_1. This is the error introduced by scaling the graphs in References 9 and 10.

To minimize this error, an average of A_1 and B_1 was taken and denoted as C_1 in Table I: To calculate the slosh frequencies, the equation $C_1=W_1 (R/g)^{1/2}$, of Reference 9 was used. Rearranging, $W_1=C_1/ (R/g)^{1/2}$ or $F_1= 1/2\pi \times C_1/(R/g)^{1/2}$, where F_1 is the slosh frequency, R is the radius of the sphere and g is the acceleration due to gravity. After the constants have been calculated, the equation reduces

TABLE XV

NONDIMENSIONALIZED FREQUENCY PARAMETERS
FOR ANTISYMMETRICAL MODE

Fill Height (%)	B_1	A_1	C_1	Slosh Frequency (HZ)
0	1.0	1.0	1.0	1.28
20	1.052	1.040	1.046	1.34
40	1.169	1.186	1.177	1.50
50	1.251*	1.204	1.251*	1.60
60	1.351	1.333	1.342	1.72
70	1.494	1.466	1.481	1.89
80	1.636	1.626	1.631	2.08
90	2.052	2.016	2.034	2.60
95	2.389	2.400	2.394	3.06

*Not an average. Value given in Table 2 of Reference 9

TABLE XVI

NONDIMENSIONALIZED FREQUENCY PARAMETERS
FOR SYMMETRICAL MODE

Fill Height (%)	D_1	$\sqrt{D_1}$	Slosh Frequency (HZ)
10	7.49	2.736	2.47
20	7.49	2.736	2.47
30	7.49	2.736	2.47
40	7.68	2.772	2.50
50	7.88	2.807	2.53
60	8.35	2.890	2.61
70	9.28	3.039	2.74
80	10.94	3.306	2.98
85	12.00	3.470	3.13
90	14.00	3.750	3.39

to $F_1 = 1.278 \times C_1$. The calculations for F_1 are tabulated in Table XV and are plotted versus percent fill height in Figure 37.

Symmetrical Mode

The symmetrical mode is excited by displacements along the longitudinal axis of the tank.

Reference II was used to calculate the natural slosh frequency of the symmetrical mode. This reference gives non-dimensionalized frequency parameters for the natural slosh frequencies. These parameters were applied in a manner similar to that used in the antisymmetrical mode. The parameters designated herein as D_1, were scaled from Figure 7 of Reference II and are tabulated in Table XVI. The equation $D_1 = W_1^2 \times d/g$ of Reference II, was used to calculate the natural slosh frequencies. In this equation, W_1 is the slosh frequency (in radians), d is the diameter of the tank and g is the acceleration due to gravity. Rearranging the equation we obtain $F_1 = 1/2\pi \times (D_1)^{1/2} \times (g/d)^{1/2}$; where F_1 is the slosh frequency. After the constants have been calculated the equation reduces $F_1 = 0.903 (D_1)^{1/2}$. The calculations for F_1 are tabulated in Table 16 and are plotted versus percent fill height in Figure 37.

After completing each slosh test the integrity of the bladder was checked in the test stand by passing gaseous helium into the tank/bladder assembly and measuring air flow rate with a rotameter (F_1 in Figure 30). The helium was injected into the interior cavity of the bladder at a pressure of 1 psi. The leakage tests were conducted after the assembly was warm and all traces of liquid oxygen were gone. The test temperature was recorded and the measured flow rates converted to standard conditions (77°F). After the tank assembly had been removed from test stand, the bladder was removed, visibly inspected and then subjected to a laboratory leak check per Method B, Section 3.2.5.3.

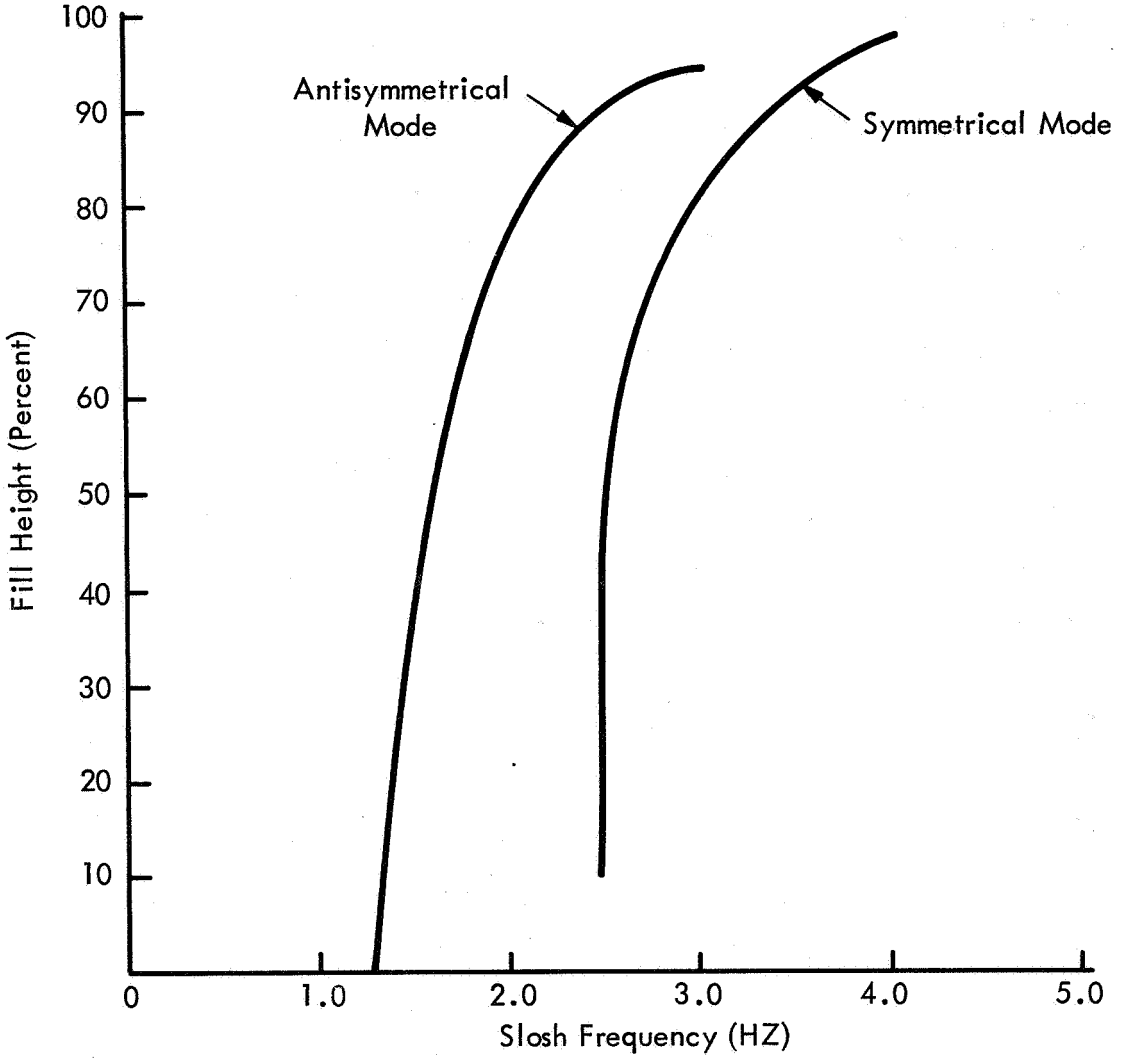

FIGURE 37 RESONANCE FREQUENCY CURVES - SLOSH MODE

3.3.1.4 Test Results - The results of the slosh tests are presented in Table XVII. Both the Mylar (No. 11) and the Kapton (No. 12) bladders successfully passed all phases of the slosh test. No leakage, structure damage or liquid oxygen incompatibility was noted with either material.

A typical amplitude and frequency curve from the individual slosh tests is shown in Figure 38.

3.3.2 VIBRATION

3.3.2.1 Test Specimens - Bladders No. 11 through 14 (Table XII) were subjected to vibration tests. Initially only bladders No. 13 and 14 were scheduled to be tested in this mode of excitation, but unfortunately both bladders failed in the empty condition on the first vibration test (see Results, Section 3.3.2.4). Subsequently, bladders No. 11 and 12, which were still intact after their slosh tests (Section 3.3.1), were installed and tested in the symmetric vibration mode.

The configurations for each bladder are tabulated in Table XII and the fabrication procedures stated in Section 3.2.3.

3.3.2.2 Test Equipment - The vibration tests were conducted on the same equipment utilized for the slosh evaluations and is shown in Figures 30 to 36.

The bladders were installed and tested in the stainless steel test tanks used in Task II (Section 3.2.4).

3.3.2.3 Test Procedures - The tank assembly was subjected to a vibration loading using a repetitive sinusoidal sweep of 10 to 160 cycles per second at a sweep rate of two octaves per minute. The amplitude input levels were held to 4 g's during each sine sweep, with each run having a duration of 10 minutes. The aforementioned test was repeated for each bladder in the 0, 50 and 100% fill condition on both the vertical and horizontal axes.

TABLE XVII - SLOSH AND VIBRATION TESTS

No.	Bladder	Test Mode	LOX Fill Condition %	He Leakage cc/min	Remarks
11	10-ply Mylar	Slosh - H*	0	0	No leakage - bladder intact
			50	0	" "
			100	0	" "
		Slosh - V**	0	0	No leakage - bladder intact
			50	0	" "
			100	0	" "
		Vibration - V	0	0	No leakage - bladder intact
			50	3	Very slight leakage
			100	12	Very slight leakage
12	10-ply Kapton	Slosh - H	0	0	No leakage - bladder intact
			50	0	" "
			100	0	" "
		Slosh - V	0	0	No leakage - bladder intact
			50	0	" "
			100	0	" "
		Vibration - V	0	0	No leakage - bladder intact
			50	0	" "
			100	0	" "
13	10-ply Mylar	Vibration - H	0	300	Bladder failure - stem area. Inter-ply inflation - testing discontinued.
		Vibration - H	50-100	-	Testing discontinued.
14	10-ply Kapton	Vibration - H	-	225	Bladder failure - stem area. Inter-ply inflation - testing discontinued.
		Vibration - H	50-100	-	Testing discontinued.

*Horizontal Axis **Vertical Axis

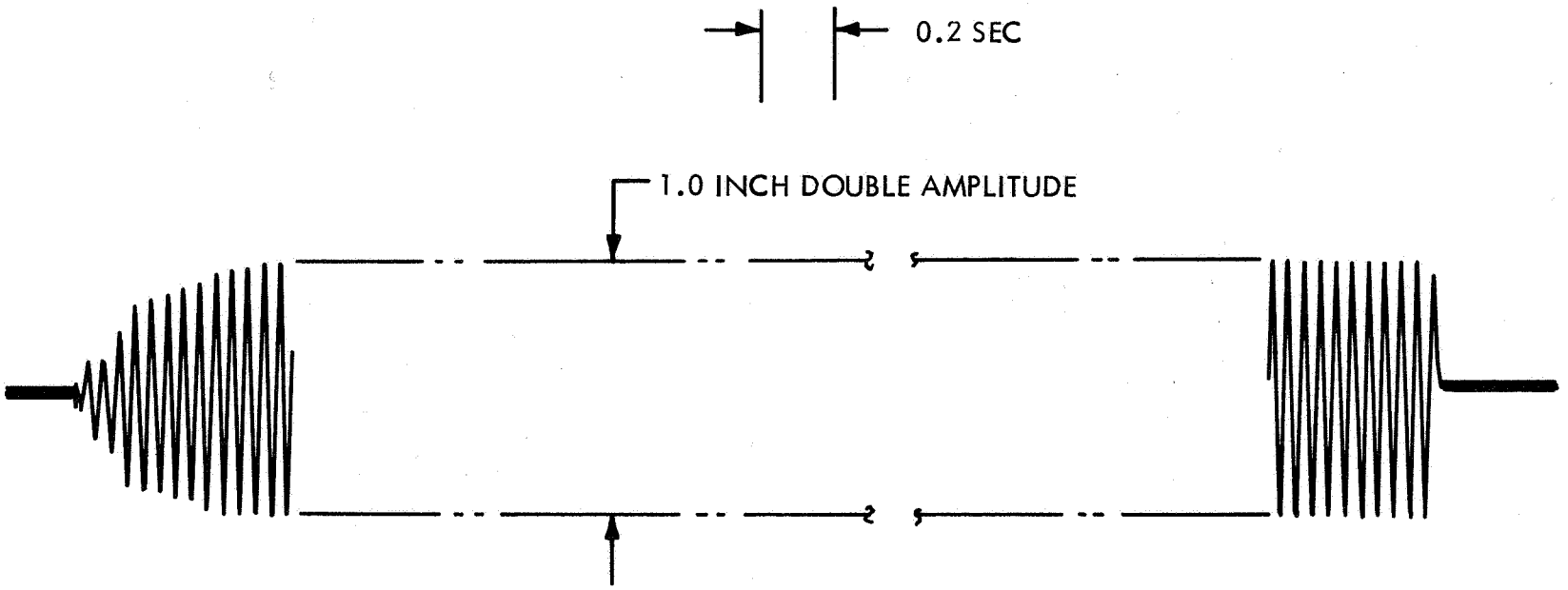

FIGURE 38 TYPICAL FREQUENCY CURVE – SLOSH TEST

As with the slosh tests, during the vibration tests both sides of the bladder were vented to the atmosphere to give the bladder maximum freedom of movement and thereby subjecting it to the maximum vibration loads under the given set of conditions.

The LOX level, tank temperature and pressure readings were recorded as stated in Section 3.2.5.

3.3.2.4 Test Results - The results of the vibration tests are tabulated in Table XVII. As is evident in the table, bladders No. 13 and 14 failed in the empty condition during vibration in the antisymmetric axis. They were vibrated in the empty condition (oxygen gas only) through the designated frequency range. After the dynamic excitation the permeability of bladders 13 and 14 was 300 and 224 cc/minute respectively. These rates constituted major failures, so the bladders were removed and examined. Both failures were just outside the stem attachment area (Figure 39), where, due to the convergence of the adhesive seams, the flexibility of the bladder is minimal. In the Kapton bladder the failures were limited to this area; however in the case of the Mylar bladder a few tears were in the Mylar film plies and randomly spaced. It is quite possible, but not conclusive, that the tears propagated from the cracks in the film adhesive at the base of the stem.

Attempts to fill bladders No. 13 and 14 for subsequent tests (50 and 100% fill conditions) were unsuccessful due to liquid and gaseous oxygen leaking between the bladder plies causing inter-ply inflation. These bladders were discarded and bladders No. 11 and 12 were substituted to continue the vibration tests. Bladders No. 11 and 12 had already successfully completed the slosh test and had no detectable damage. They were each evaluated in the symmetrical axis under 0, 50 and 100% fill conditions (Table XVII). The Mylar bladder (No. 11) had final leakage rate of 12 cc/min and the Kapton bladder (No. 12) had leakage in the laboratory of essentially zero ($\leq$ 1 cc/min).

No sign of LOX incompatibility was noted in any of the four bladders subjected to the vibration tests. Vibration in the symmetrical axis of the tank does not appear to be

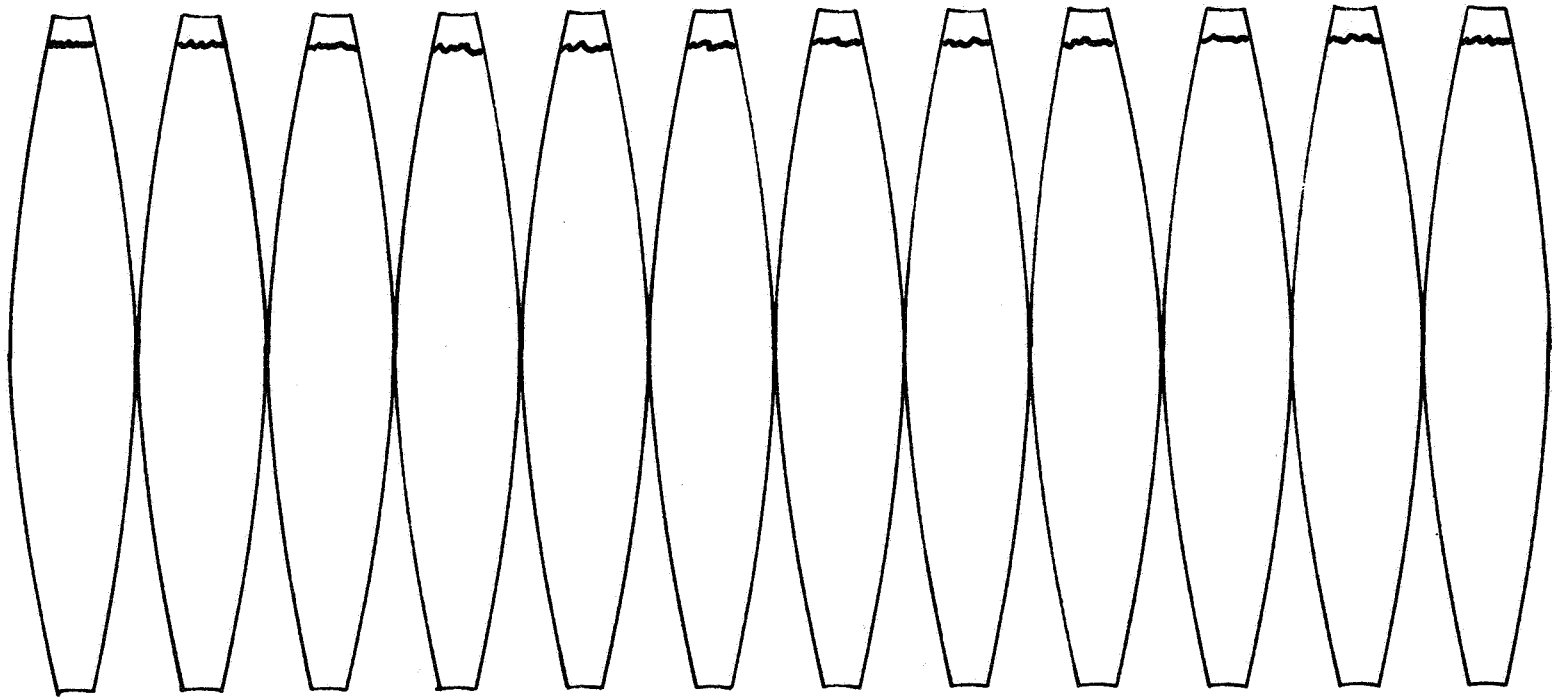

Failures occurred in all plies at the same location on both bladders

FIGURE 39 FAILURE LOCATIONS — BLADDER No. 11 and 12

detrimental to the structural integrity of the bladder; however, the bladder is sensitive to vibrations in the antisymmetrical axis. The latter deficiency can be remedied by modifying the design in the stem attachment area to provide added support to the under surface of the bladder.

3.3.3 IMPACT TESTS

The following is a description of the blunt impact and ballistic penetration test performed on two polymeric expulsion bladders in the presence of liquid oxygen.

3.3.3.1 Test Specimens - Expulsion bladders No. 15 and 16 (Table XII) were evaluated in this portion of the program. Each was fabricated according to the procedures specified in Section 3.2.3.

3.3.3.2 Test Equipment -

Flow Diagram - The test schematic shown in Figure 40 was used for the impact tests. The only function of the system was to fill the test tank with liquid oxygen and maintain a known liquid level. Therefore, the instrumentation consisted of liquid level gauges, P_3 and P_4, pressure gauges, P_1 and P_8 to monitor the Δ P across the bladder, and a thermocouple, T_2, to monitor temperature. The tank was insulated in all areas except at the impact zones.

Blunt Impact - The equipment shown in Figure 41 was used to provide the impact force to the exterior of the test tank. It consists of a pivoted free-swinging 5-foot long arm with a calibrated weighed head attached to the free end. The head weights were 7.2, 14.4 and 21.6 lbs (including the weight of the arm) to provide impact forces of 72, 144 and 216 ft-lbs respectively. The striker pin which formed a portion of the head was a standard test pin used in the ABMA LOX compatibility tests (References 2 and 3). The pin is made of 17-4PH steel and has a diameter of 0.500 inch.

Ballistic Impact Test - Ballistic impact tests were conducted using a 30-06 caliber rifle setup at a distance of 25 feet from the tank and operated remotely from the control house. The ammunition was standard military ball ammunition with a 152 grain copper jacketed

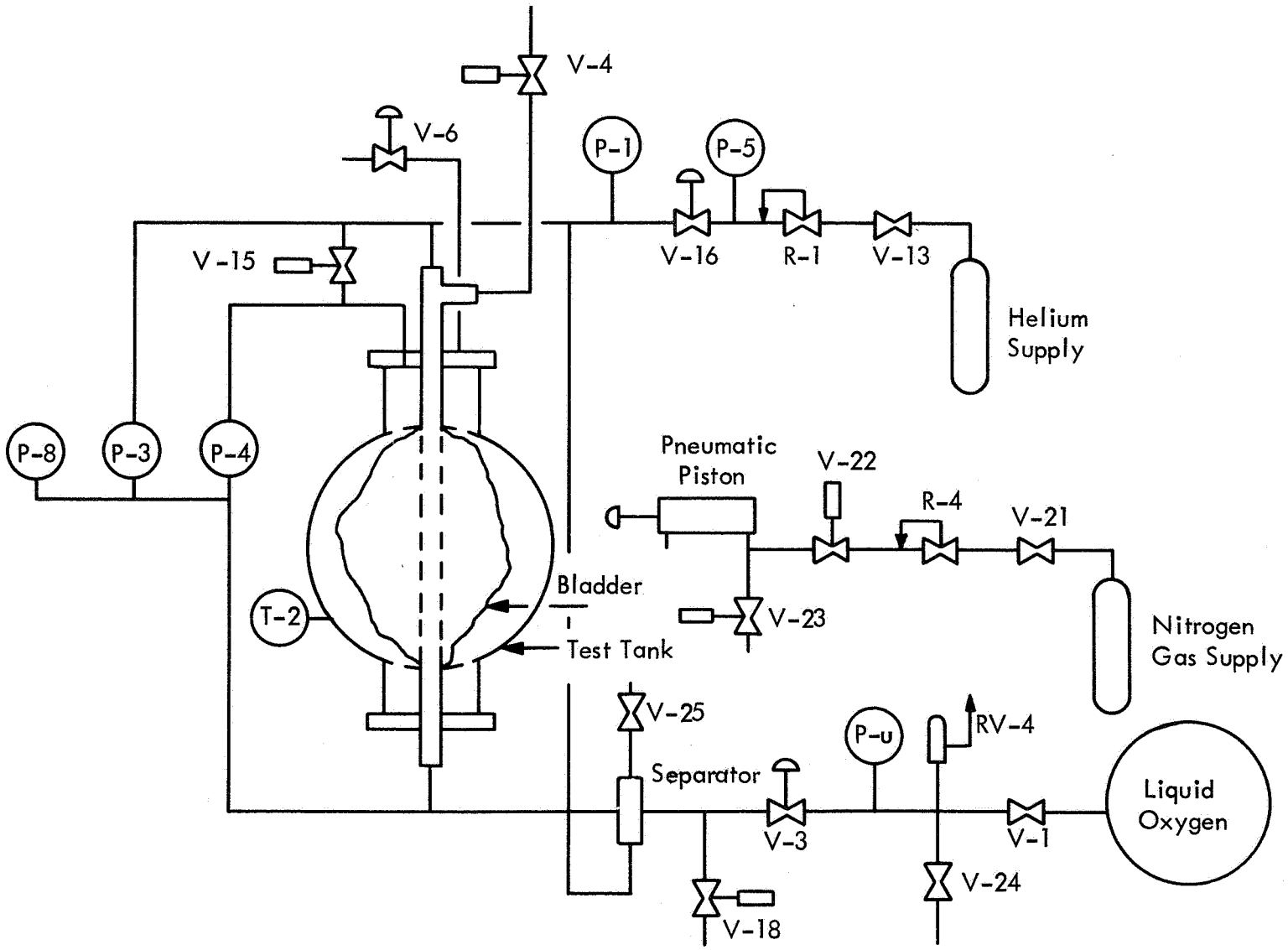

FIGURE 40 TEST SCHEMATIC FOR IMPACT AND BURST EVALUATIONS

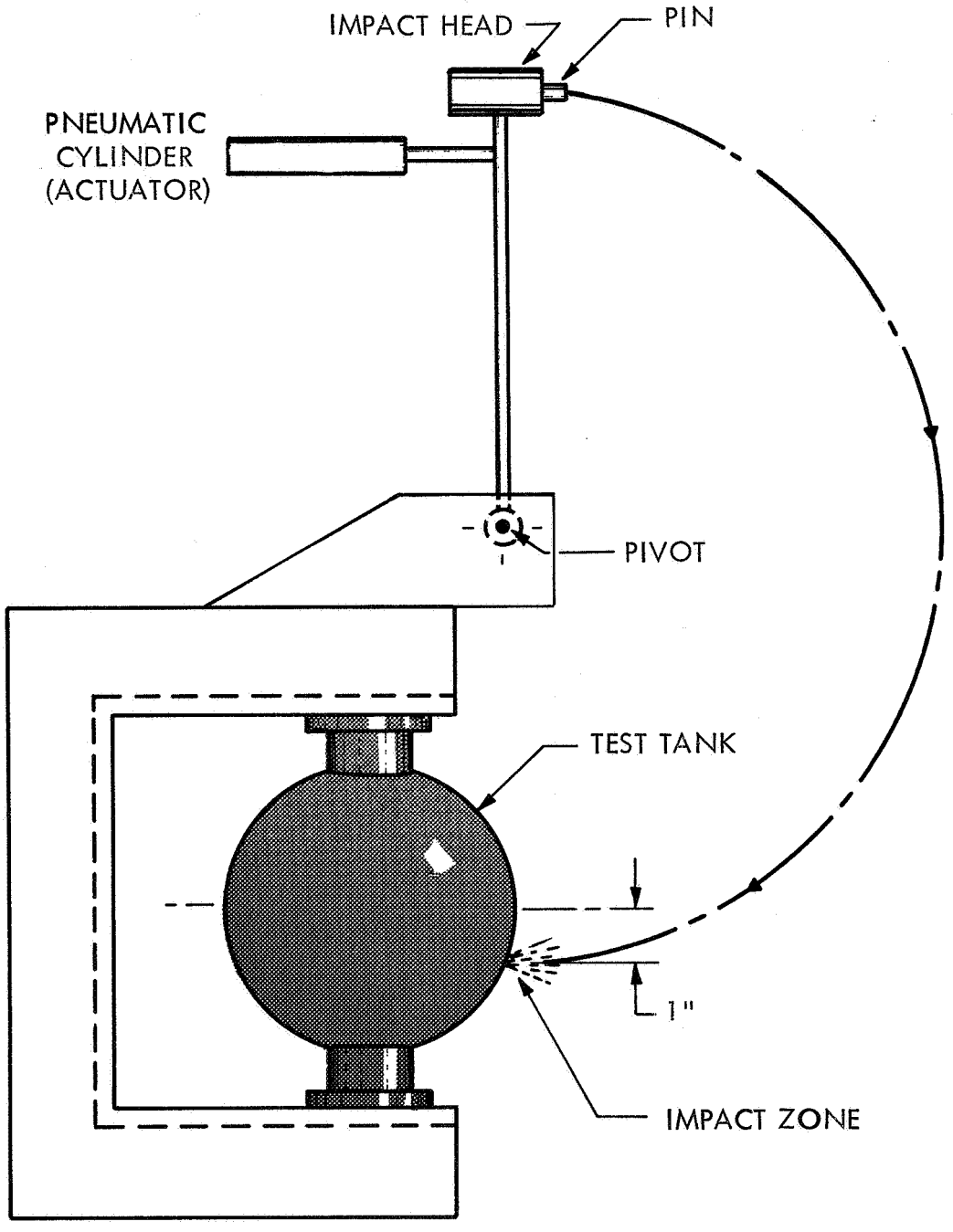

FIGURE 41 IMPACT DEVICE

lead slug produced by Fabrique Nationals D'Armes DeGruerr, Herstal, Belgium. The projectile has an average muzzle velocity of 2800 ft/sec.

3.3.3.3 Test Procedure - Each bladder was subjected to three blunt impacts at 72, 144 and 216 ft-lbs, respectively and one ballistic penetration. Seventy-two ft-lbs was selected as the initial impact level since it is the minimum level of impact energy that a material must withstand without charring or ignition in a liquid oxygen environment to be classified "acceptable" under the ABMA LOX impact test. The next two energy levels of impact were arbitrarily selected at two and three times this base level.

The tank assembly was rigidly installed in the system shown in Section 3.3.3.2 and filled to the 50% level with LOX. This liquid level was maintained by the periodic addition of oxygen and after the level had stabilized, the exterior of the tank was impacted with 72 ft-lbs of energy. The energy was supplied by dropped a 7.2 lb weight 10 feet (see Section 3.3.3.2). The tank was vented to the atmosphere during the impact tests.

The impact zone was located one inch below the centerline of the tank, in the liquid level portion. In this region the bladder is in intimate contact with the tank wall. The exterior of the tank, in the impact zone, was continuously purged with nitrogen gas to prevent any extraneous reactions from occurring.

For the second impact test the tank was rotated approximately 30° in the stand to provide a new impact zone. The weight on the impact head was increased to 14.4 lbs (an impact energy of 144 ft-lbs), a new striker pin installed, and the test repeated. Similarly, a third blunt impact was performed using a 21.6 lb weight (216 ft-lbs).

For the ballistic impact tests, the test tank assembly was penetrated with a conventional 30-06 caliber round (copper jacketed lead) fired from a distance of 25 feet. A copper jacketed projectile was used in lieu of a steel jacket slug to prevent extraneous reactions due to sparking.

In the case of the Mylar bladder (No. 15) the projectile penetrated the tank approximately one inch above the center weld (Figure 49) and in the Kapton bladder (No. 16), the shell hit the center weld (Figure 54). In both cases the tanks were 50% full with liquid oxygen and vented to the atmosphere at the time of impact.

Motion picture coverage was made of both the blunt and ballistic impact tests.

3.3.3.4 Test Results -

Blunt Impact - Blunt impacts to the exterior of the propellant tank at levels up to three times the ABMA acceptance level caused no reactions or material ignition of either the Mylar or Kapton bladders. The impact areas on each tank are shown in Figures 42 to 48. The deformation of the test tank containing the Mylar bladder was 0.016, 0.31 and 0.48 respectively for impacts of 72, 144 and 216 ft-lbs. The second tank assembly (containing the Kapton bladder) experienced deformations of 0.10, 0.35, and 0.45 under an equivalent series of impacts. No leakage was detected in either the tanks or the bladders after the impacts and, with the exception of the deformed impact areas, the structural integrity of the tanks remained intact. In both tests a rapid boil-off of cryogen was experienced after each impact from the addition of energy to the system.

From the blunt impact tests, it is evident that even under severe impact loads to the propellant tank the polymeric bladders do not experience sufficient energy to cause spontaneous bladder ignition.

Ballistic Impact - In the evaluation of the Mylar bladder, the projectile entered the tank approximately one inch above the centerline of the tank as shown in Figure 49, puncturing a hole 0.35 inch in diameter. The projectile continued through the tank, nicked the standpipe and penetrated the back wall approximately one inch above center. The exit hole, 0.50-0.85 inch in diameter, is shown in Figures 50 and 51.

FIGURE 42 MYLAR TANK AFTER BLUNT IMPACT — 72 FT-LBS.

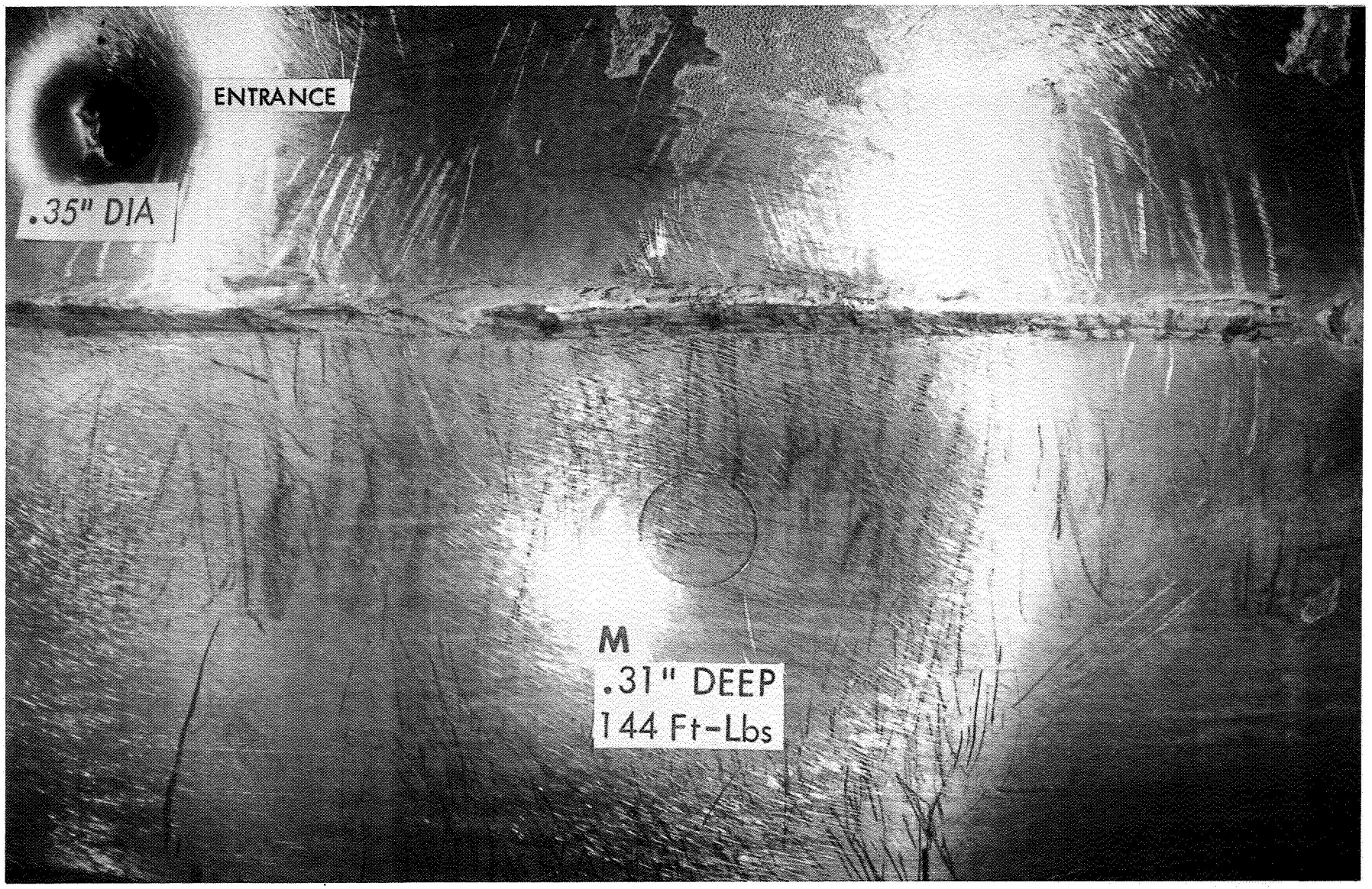

FIGURE 43 MYLAR TANK AFTER BLUNT IMPACT — 144 FT-LBS.

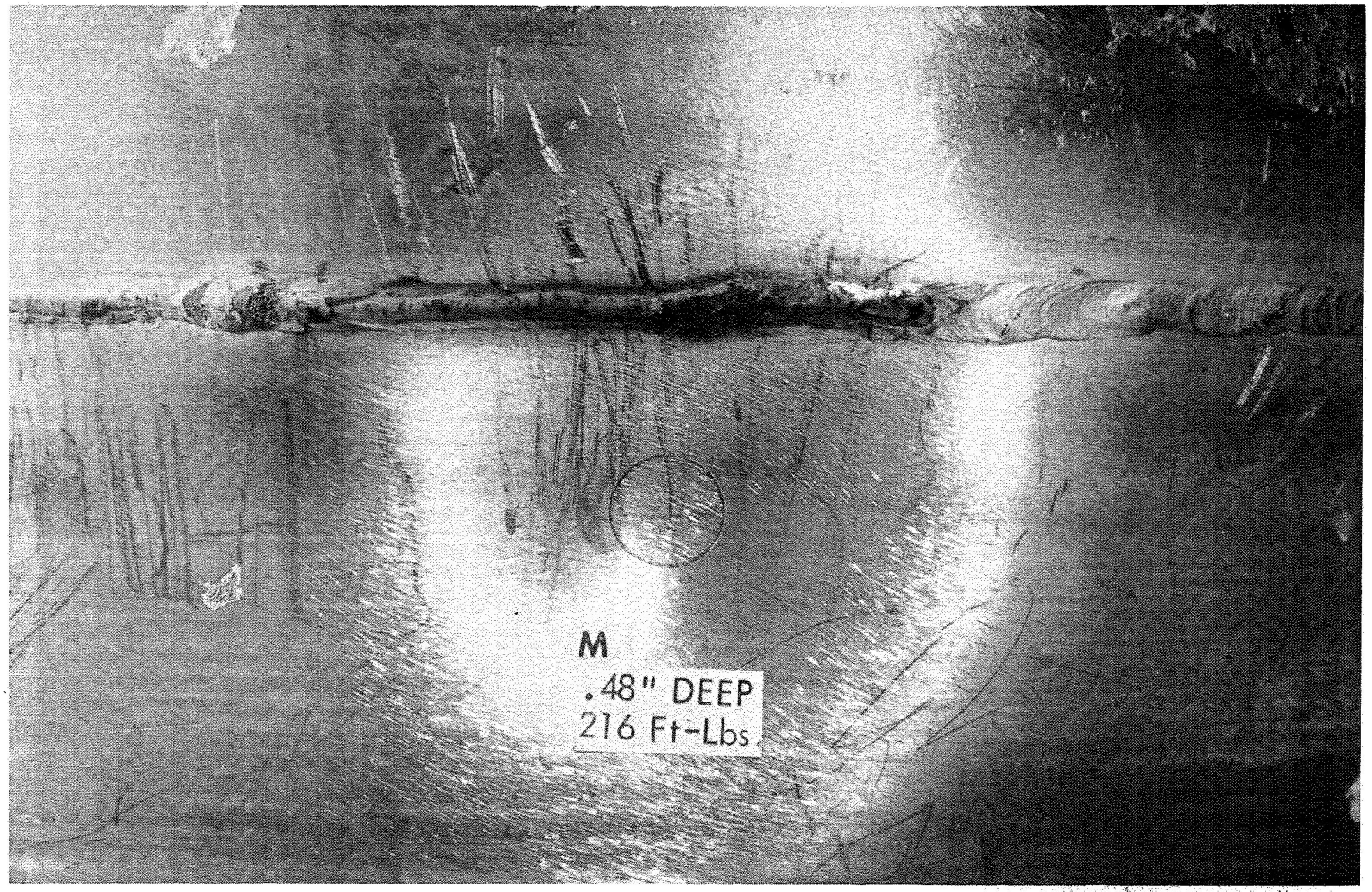

FIGURE 44 MYLAR TANK AFTER BLUNT IMPACT — 216 FT-LBS.

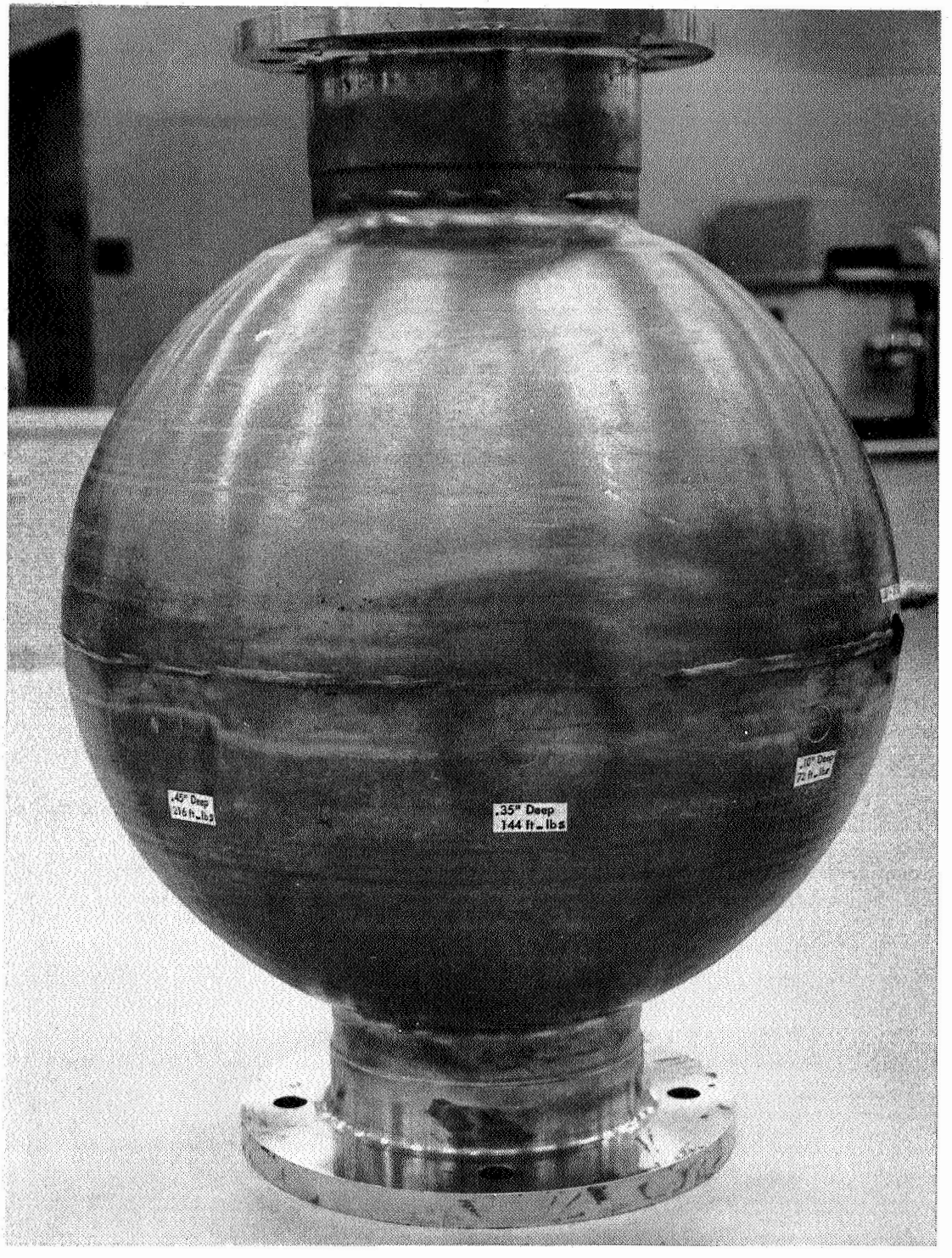

FIGURE 45 KAPTON TANK IMPACT AND PENETRATION

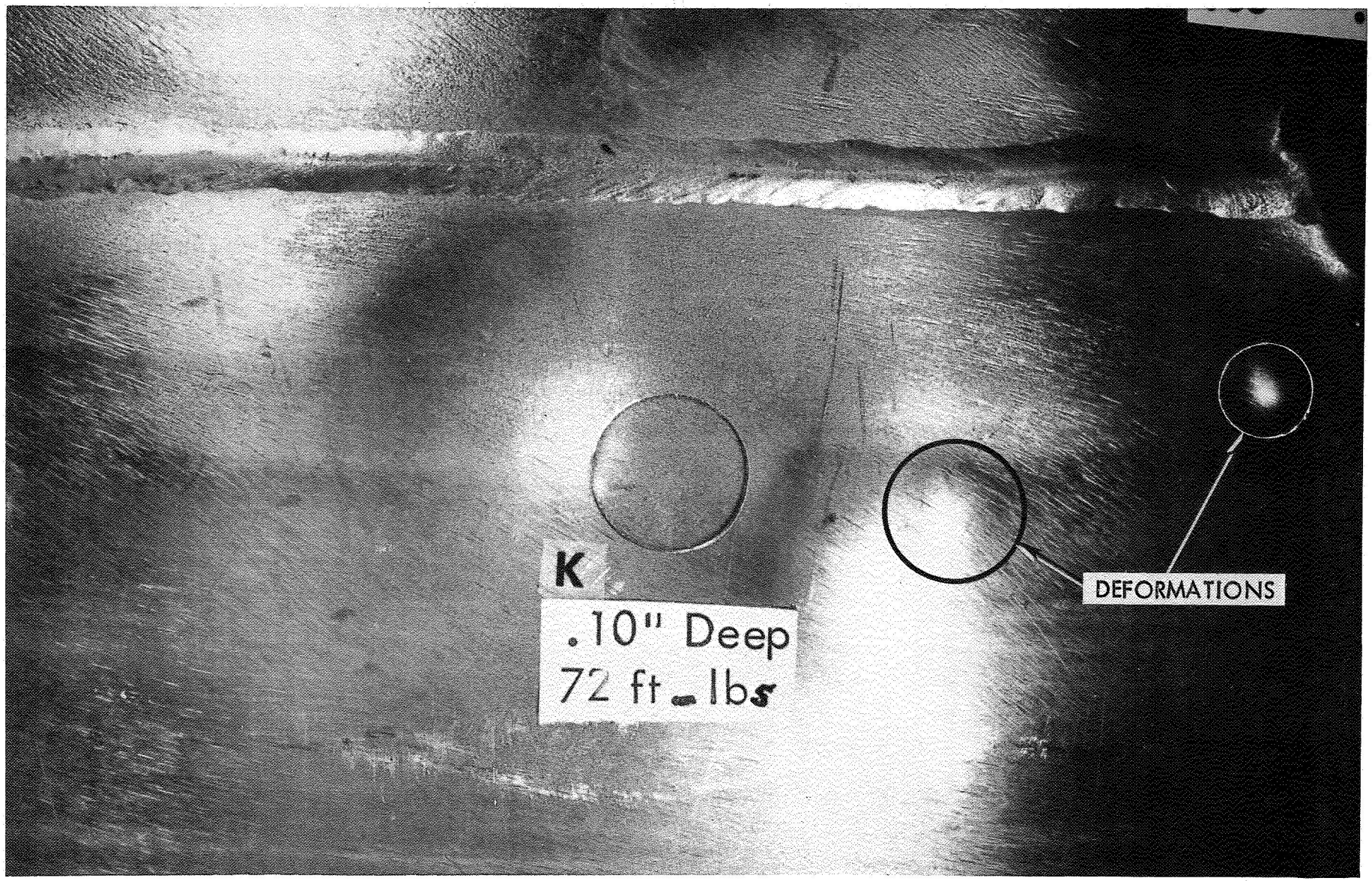

FIGURE 46 KAPTON TANK AFTER BLUNT IMPACT — 72 FT-LBS.

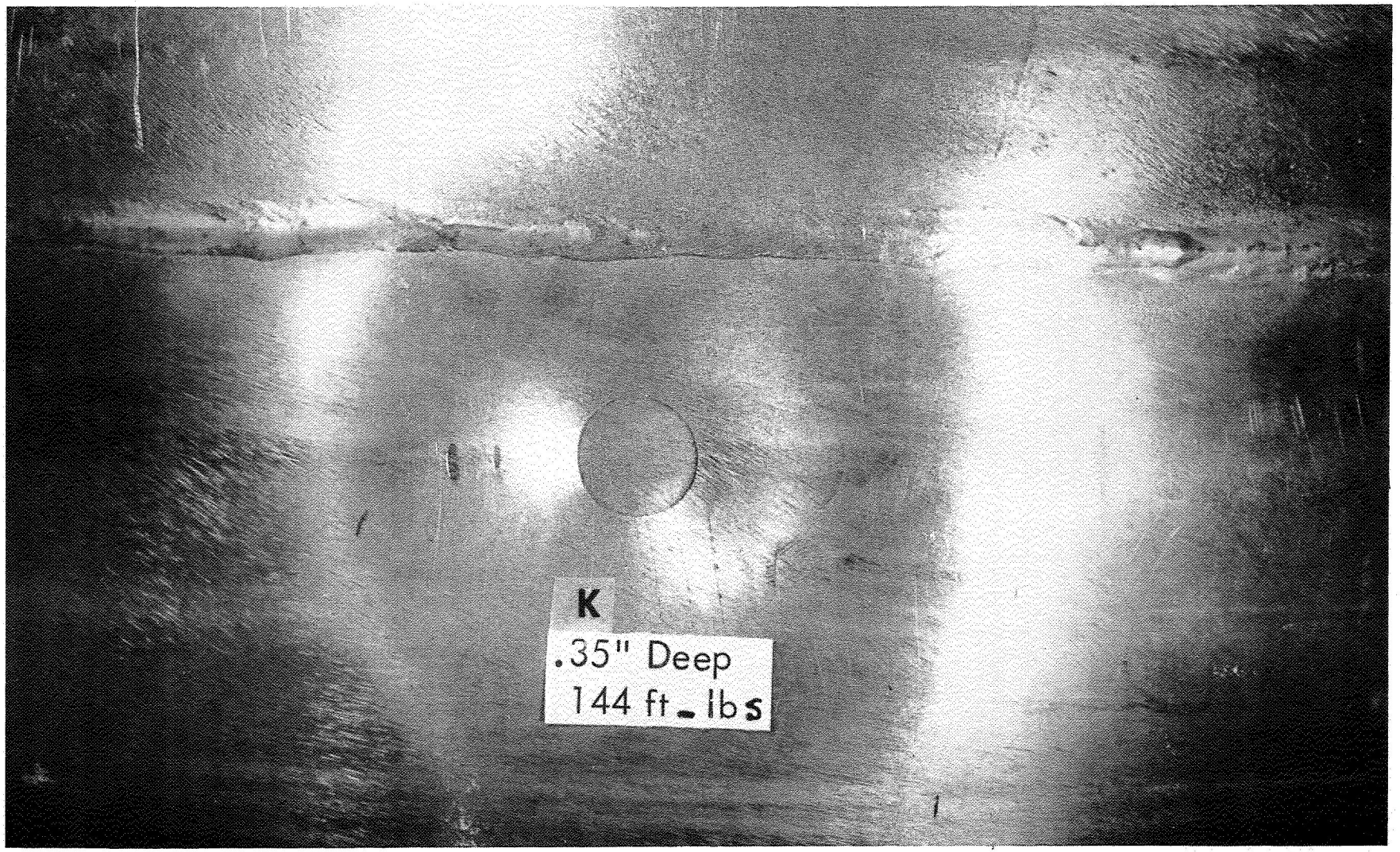

FIGURE 47 KAPTON TANK AFTER BLUNT IMPACT — 144 FT-LBS.

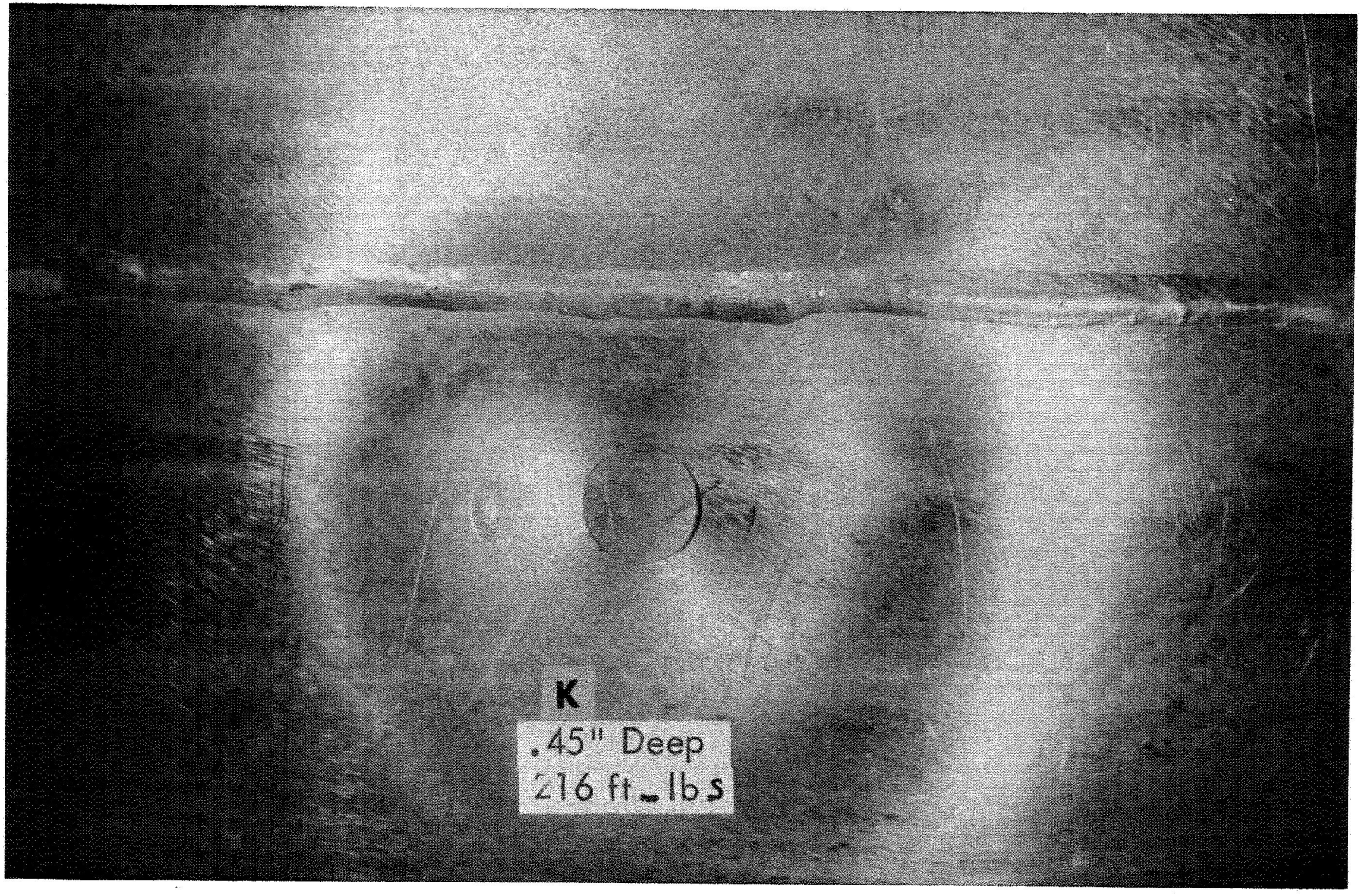

FIGURE 48 KAPTON TANK AFTER BLUNT IMPACT — 216 FT-LBS.

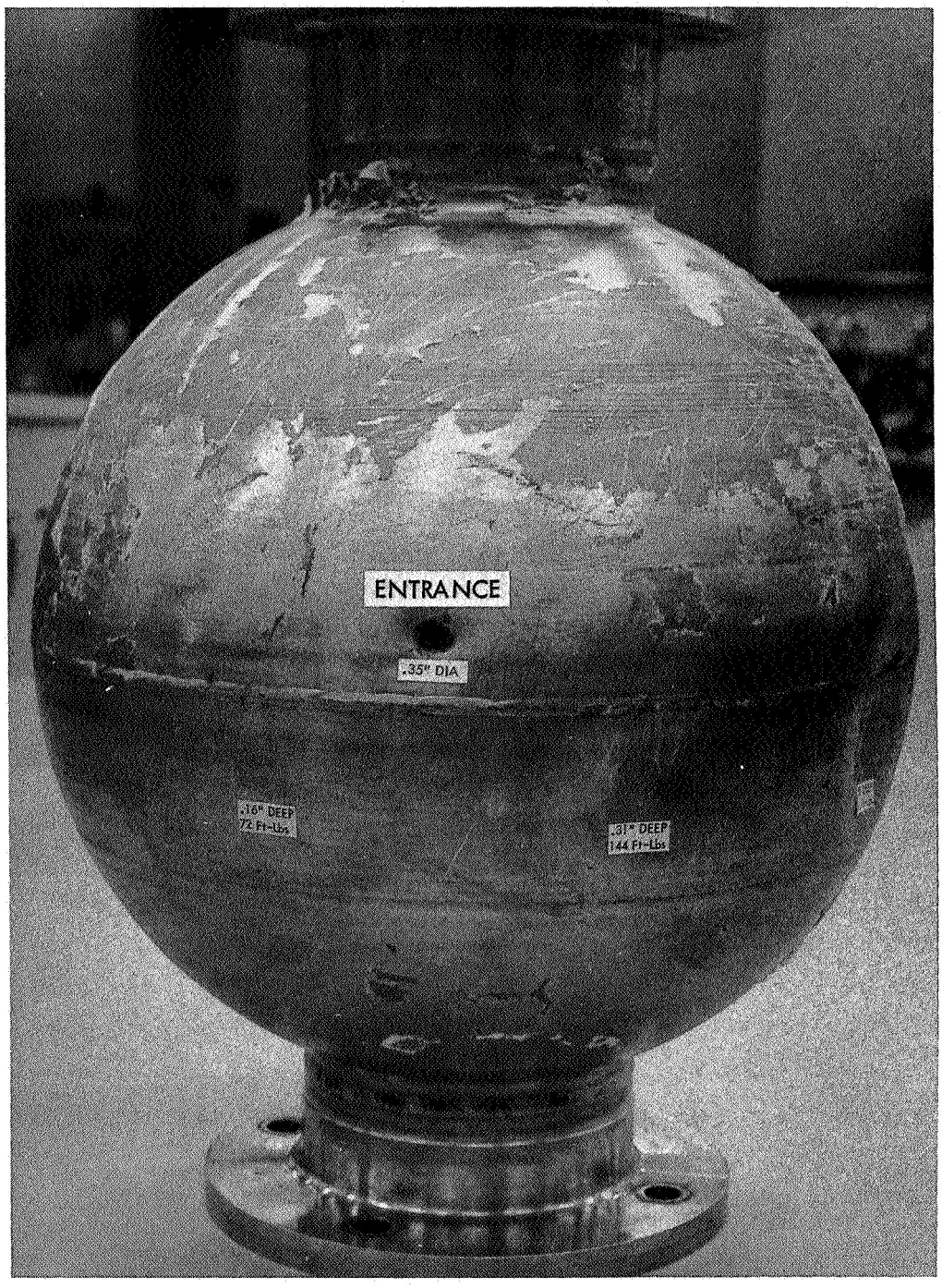

FIGURE 49 MYLAR TANK AFTER BALLISTIC PENETRATION — ENTRANCE

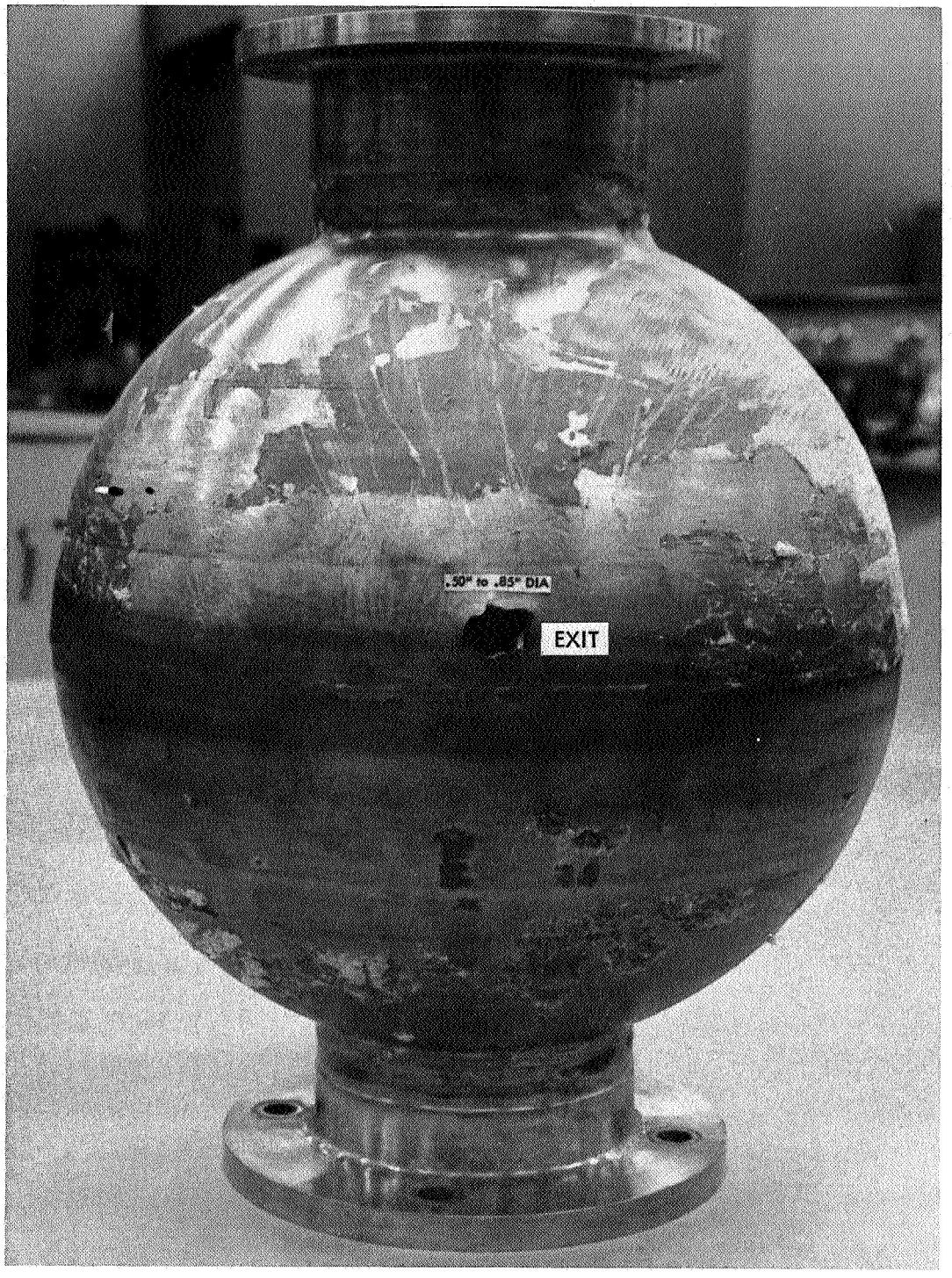

FIGURE 50 MYLAR TANK AFTER BALLISTIC PENETRATION — EXIT

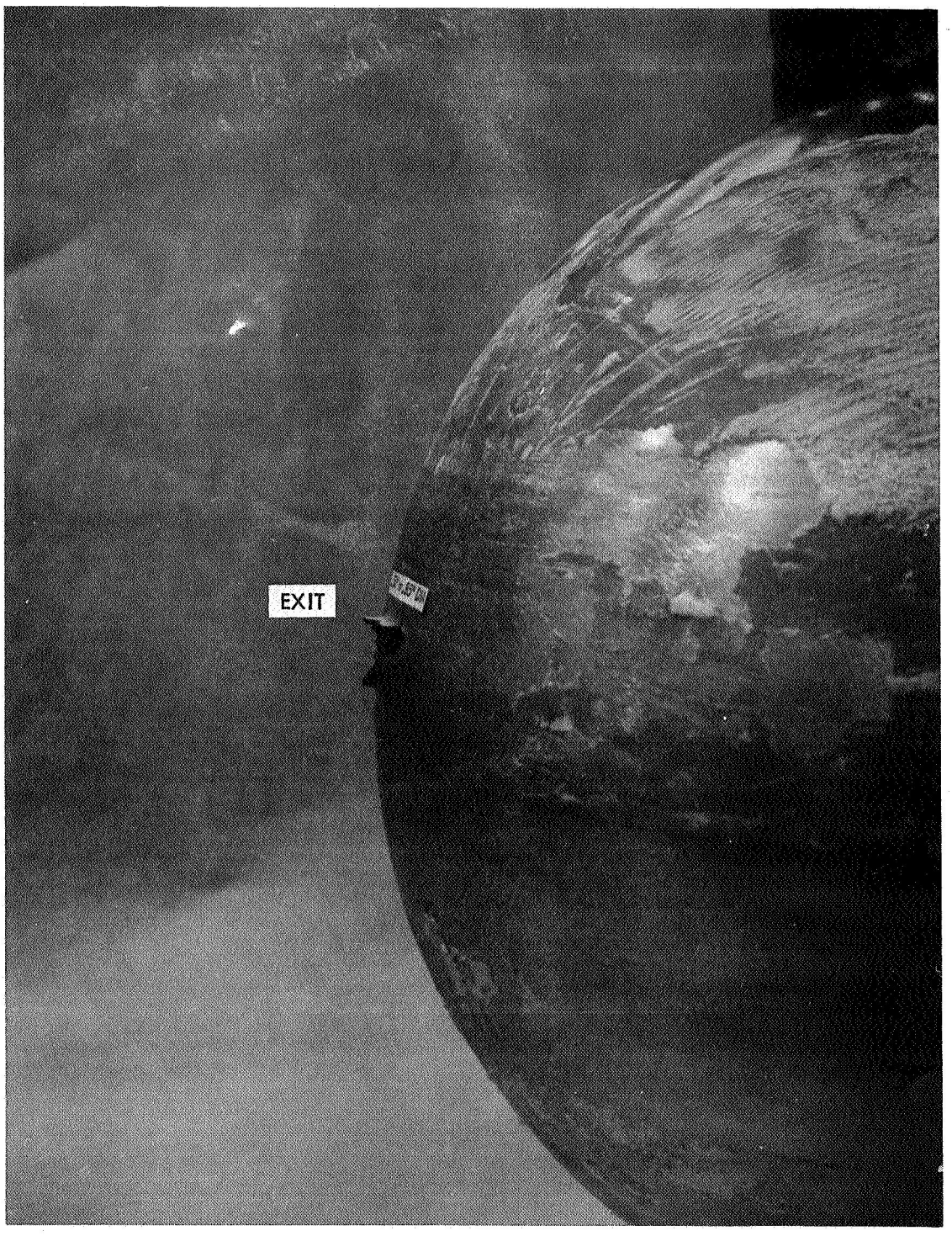

FIGURE 51 MYLAR TANK AFTER BALLISTIC PENETRATION — EXIT

The Mylar bladder showed no evidence of charring where the projectile entered, as shown in Figure 52. However, at the exit hole (Figure 53) surface charring was evident on both the Mylar film and Teflon fabric but neither material showed any sign of actual burning. Charring was also noticed on the interior of the test tank at the location of the exit hole. The charring on the tank radiated from the exit hole and covered approximately 60% of the rear surface. No sign of reaction was noted on either the exterior or interior of the tank at the entrance hole or on the tank exterior at the exit hole.

The copper jacketed lead projectile broke-up as it penetrated the tank as is evident by the cuts and trapped particle in the bladder (Figure 52). Additional particles were removed from the bottom of the tank. No signs of liquid oxygen incompatibility were detected at any of these small damaged areas.

The charred area on the rear inside surface of the tank was substantially greater than that evident on the bladder and radiated from the impact area. Since the bladder remained relatively intact, with very little loss of material, the only other sources of ignition material are from the projectile or the tank itself. Certain alloys of both copper and lead are LOX impact sensitive (Reference 2) according to the ABMA test requirements. Whether or not the materials in the projectile are impact sensitive was not established but it is a good possibility that they are under the high impact loads experienced in these tests. Even fine stainless steel particles from the tank are impact sensitive if finely divided (Reference 2).

In the second ballistic impact test, bladder No. 16 (Kapton) was evaluated. The projectile entered the tank at the center weld as shown in Figure 54, penetrating both walls of the tank. The entrance hole was 0.35 inch in diameter and the exit hole was 0.38-0.67 inch in diameter (Figure 55). The projectile hit the standpipe bending it slightly, breaking up the slug. Three severe deformations were found on the back side of the tank resulting from high impacts on the interior surface. Two of the deformations

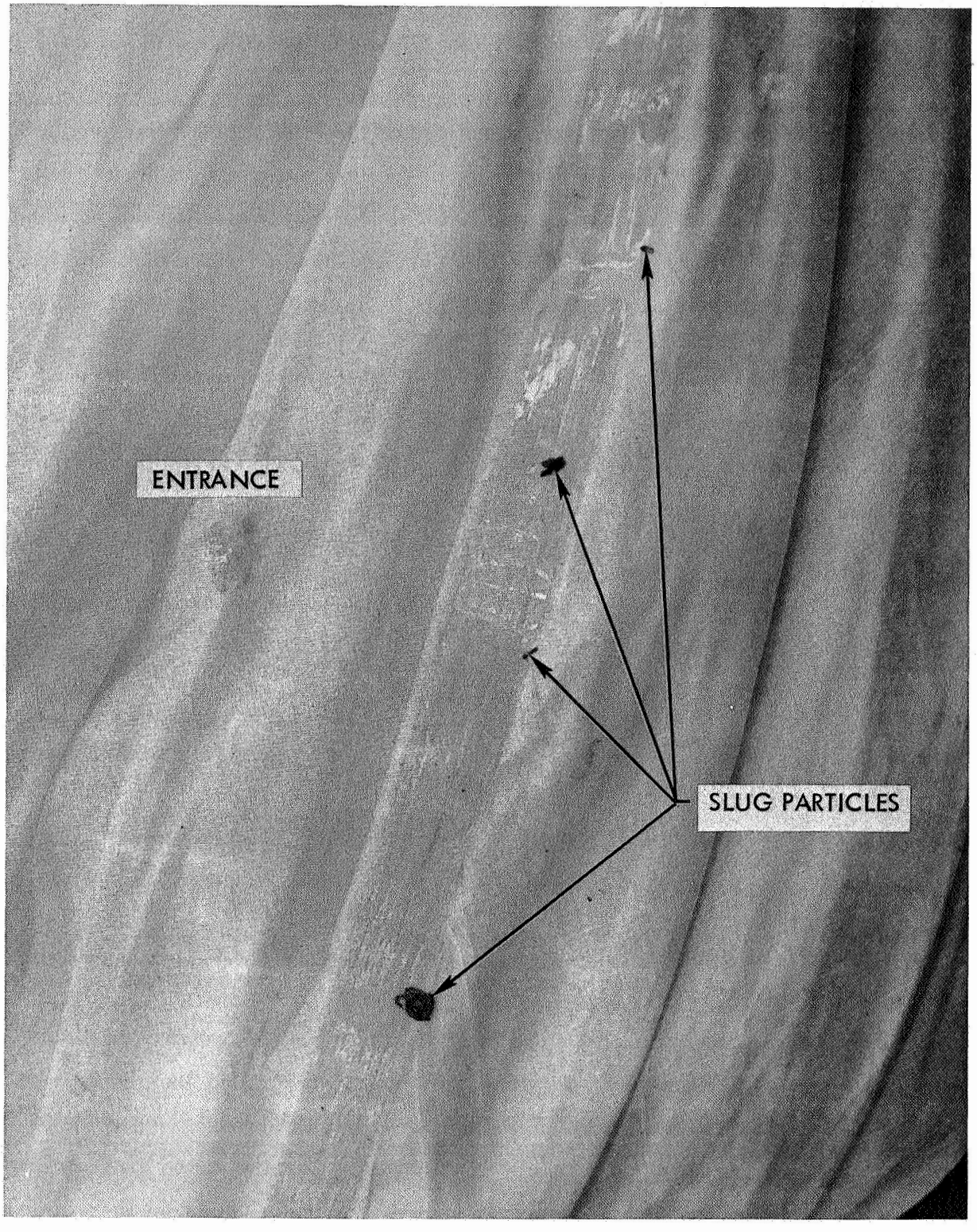

FIGURE 52 MYLAR BLADDER AFTER BALLISTIC PENETRATION

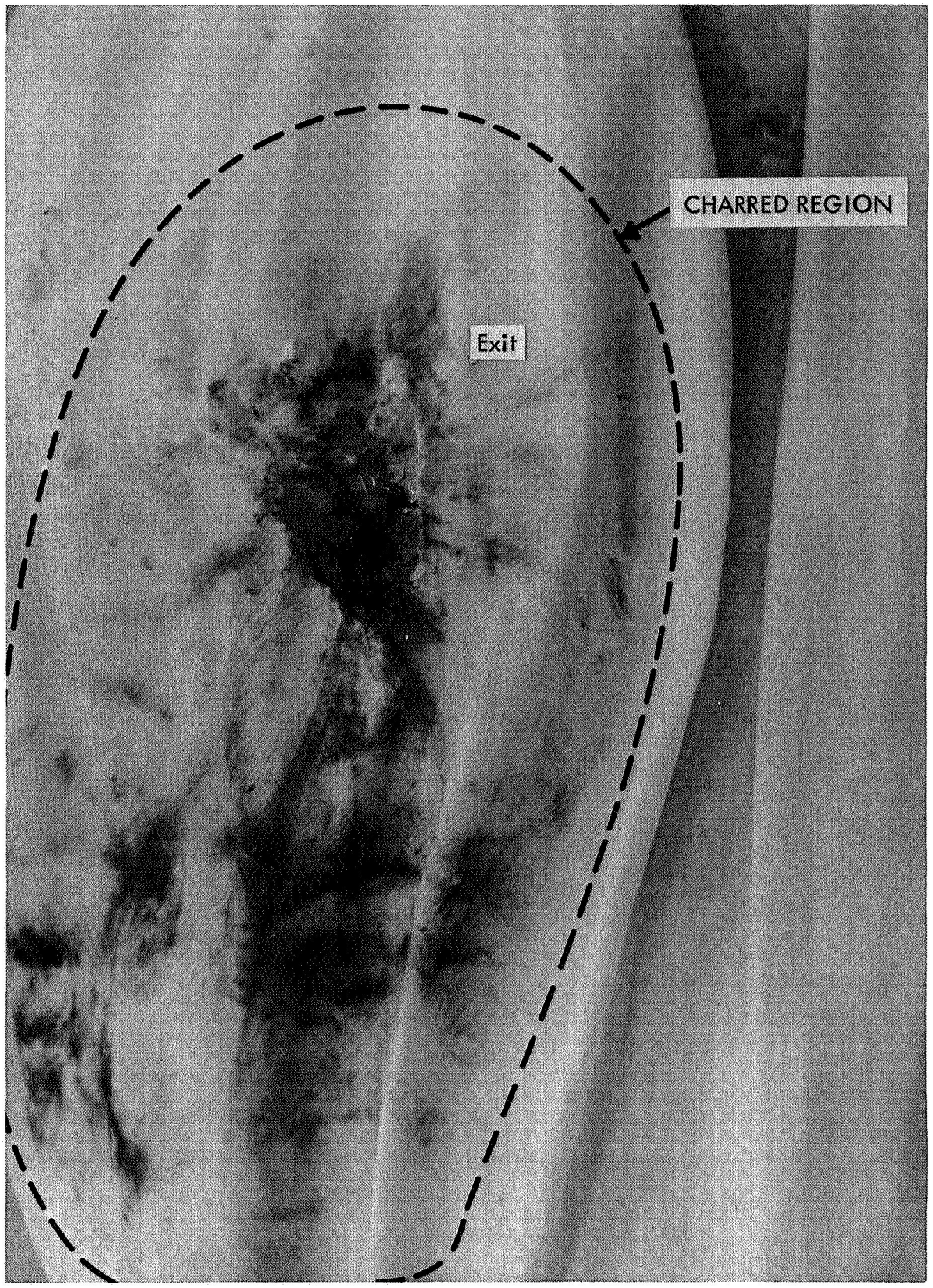

FIGURE 53 MYLAR BLADDER AFTER BALLISTIC PENETRATION

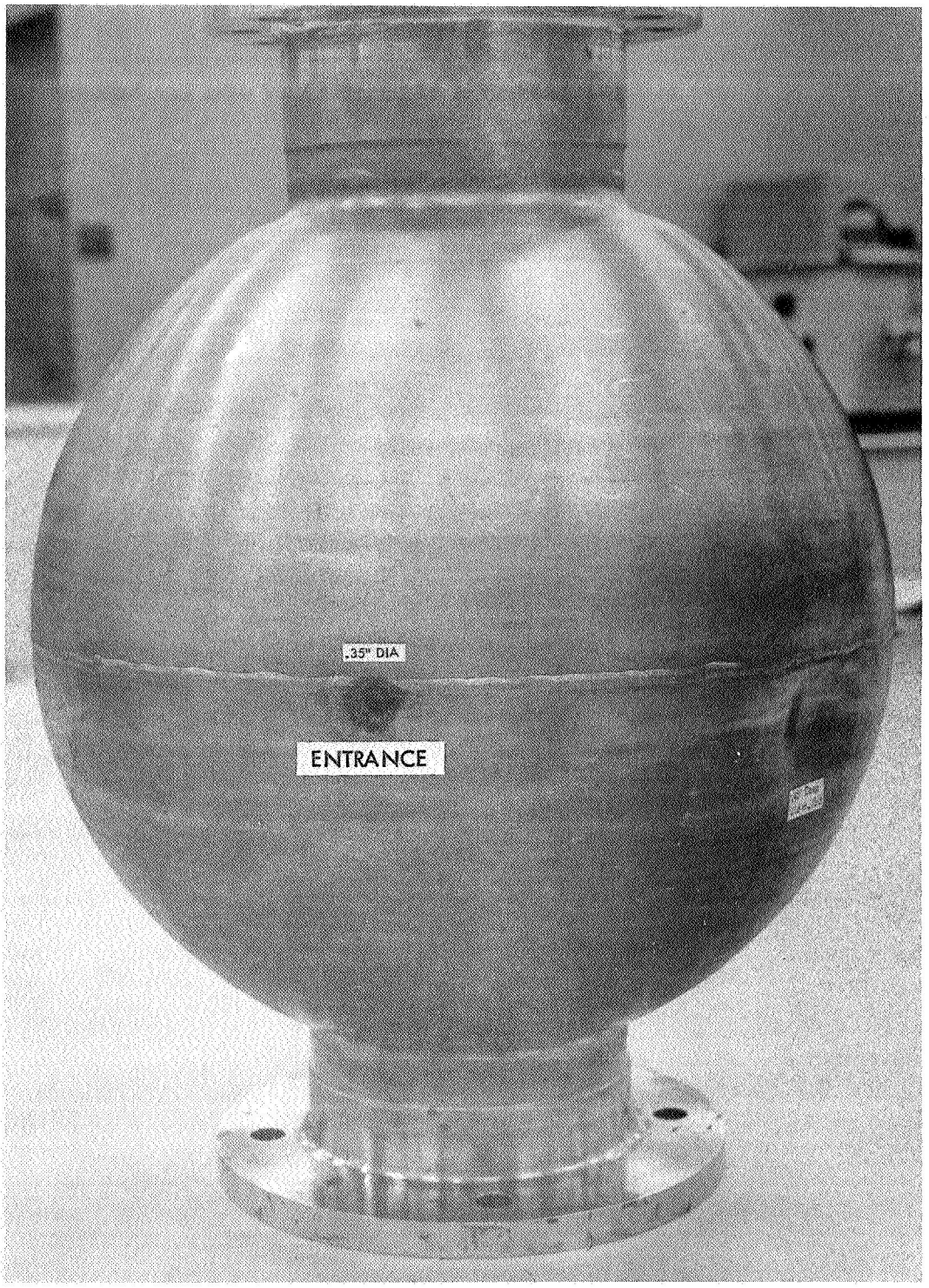

FIGURE 54 KAPTON TANK AFTER BALLISTIC PENETRATION — ENTRANCE

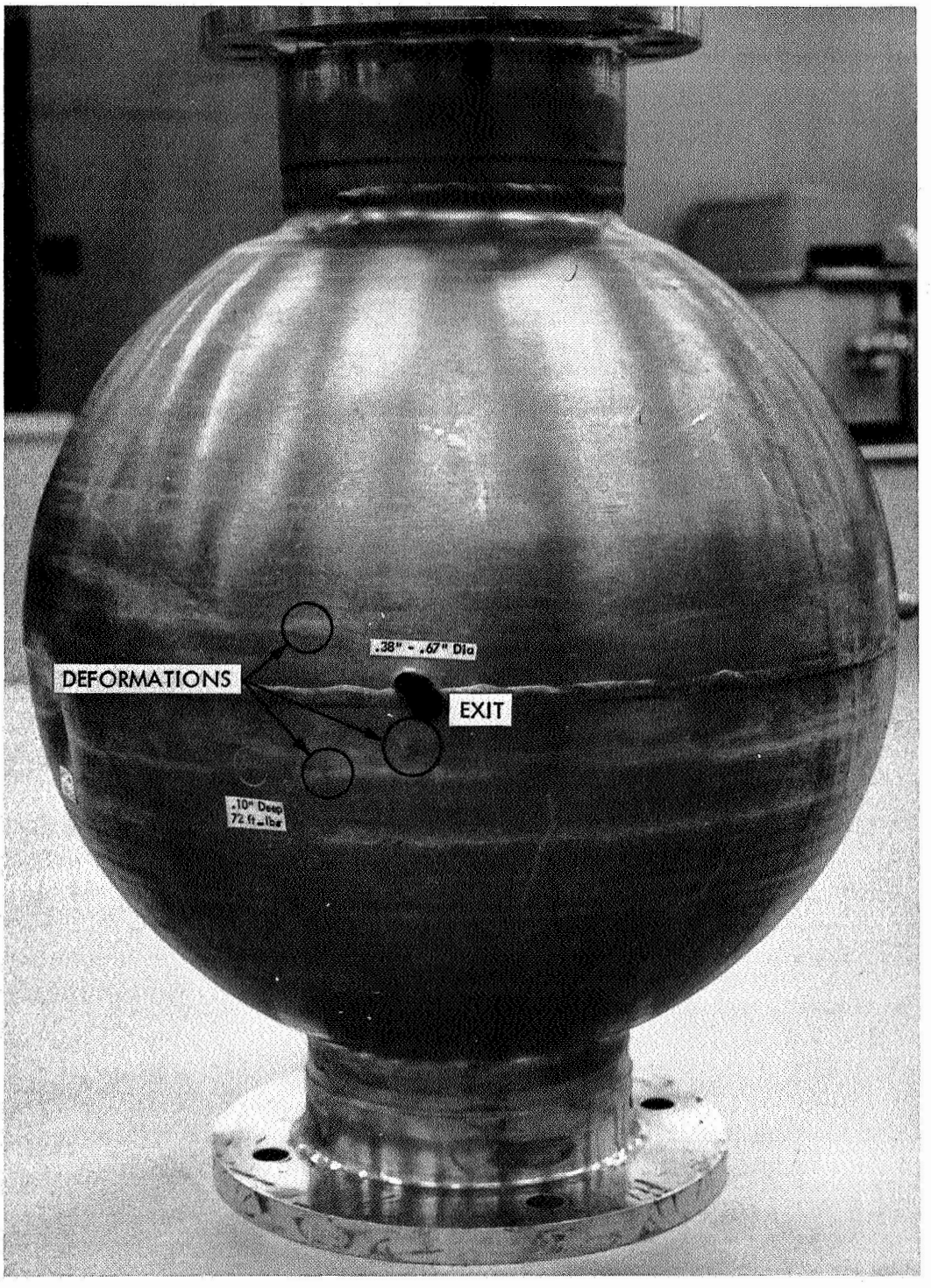

FIGURE 55 KAPTON TANK AFTER BALLISTIC PENETRATION — EXIT

were about 0.20 inch diameter and 0.02 inch high. The third was approximately 0.1 inch in diameter and 0.012 inch high. The three deformations were located within a three inch radius from the exit hole and are marked in Figure 55, but are not clearly visible. Two of the deformations are evident in Figure 46.

About 3 seconds after the projectile penetrated the tank, smoke and sparks began evolving from the exit hole and continued to burn with increasing intensity for approximately 2 minutes. No flames were noted on the exterior of the tank until the fill line burned through, Figure 56.

Inspection of the tank assembly showed that the entire bladder burned with exception of the small piece shown in Figure 56. The flames charred both bladder stems, destroyed the fill and vent lines, severed the standpipe, and gutted the separator. The tank components after test are shown in Figures 56 and 57. It could not be determined conclusively which materials (the bladder or fine metallic particles) initiated the fire but the Kapton bladder sustained the blaze which then passed to the fill line and the separator.

3.3.4 BURST TEST

3.3.4.1 Test Specimens - Bladders No. 17 and 18 were evaluated in the burst study. Their configuration is shown in Table XII and fabrication process given in Section 3.2.3.

3.3.4.2 Test Equipment - A schematic of the test setup is shown in Figure 40. The tanks were instrumented to measure the pressure inside the bladder, differential pressure across the bladder, tank temperature, and liquid level.

The tank, shown in Figure 58, was identical to the stainless steel tanks (Section 3.2.4) used throughout Task II and the previous portion of Task III with the following two exceptions:

(1) The tank shell was made from 3003 aluminum alloy instead of stainless steel.

(2) A gauge section (nominal thickness = 0.0125") was etched in the tank wall to control the burst pressure (Figure 59) and to assure severance of the tank. The tanks were designed for a room temperature burst pressure of 65 psi.

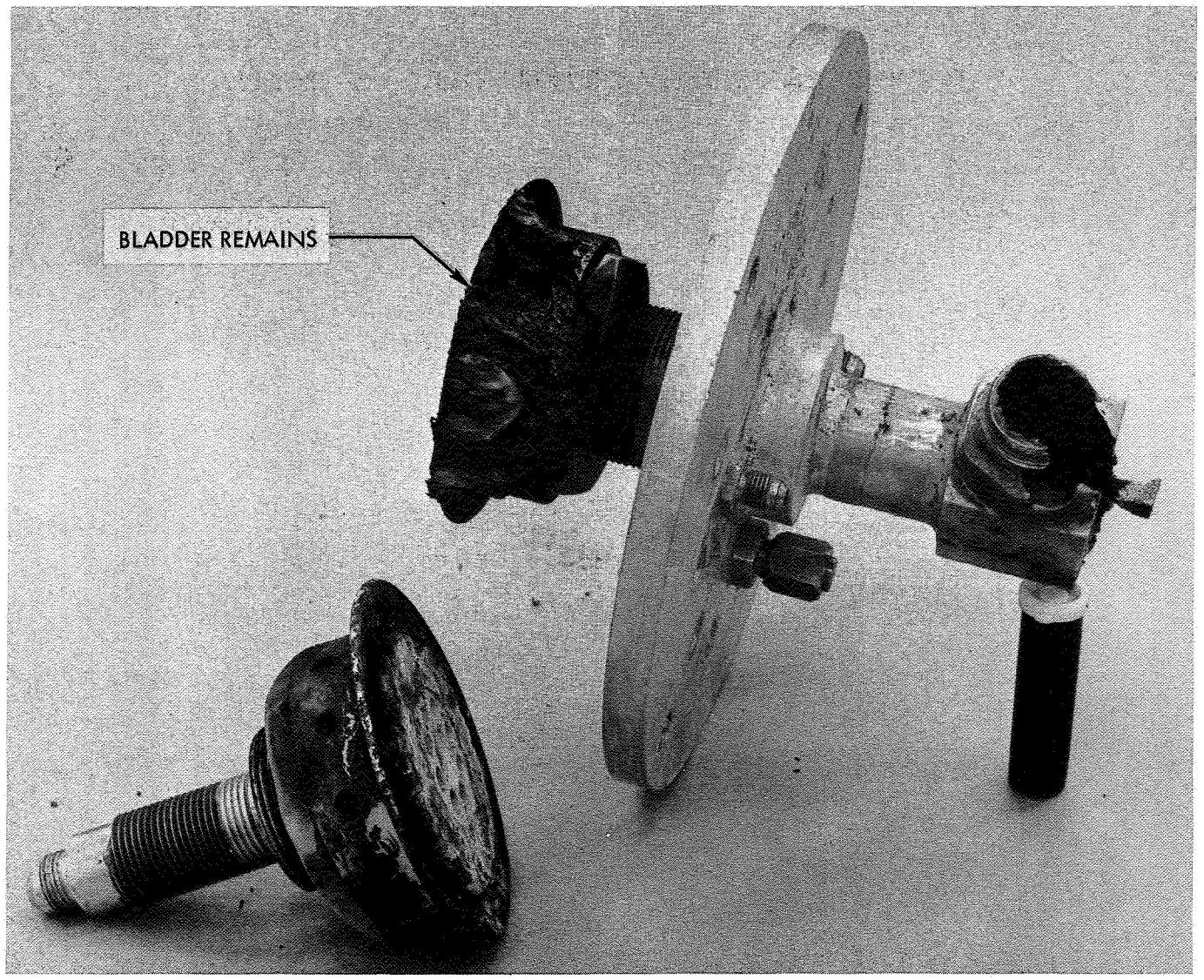

FIGURE 56 KAPTON BLADDER ATTACHMENT HARDWARE BLADDER FITTINGS

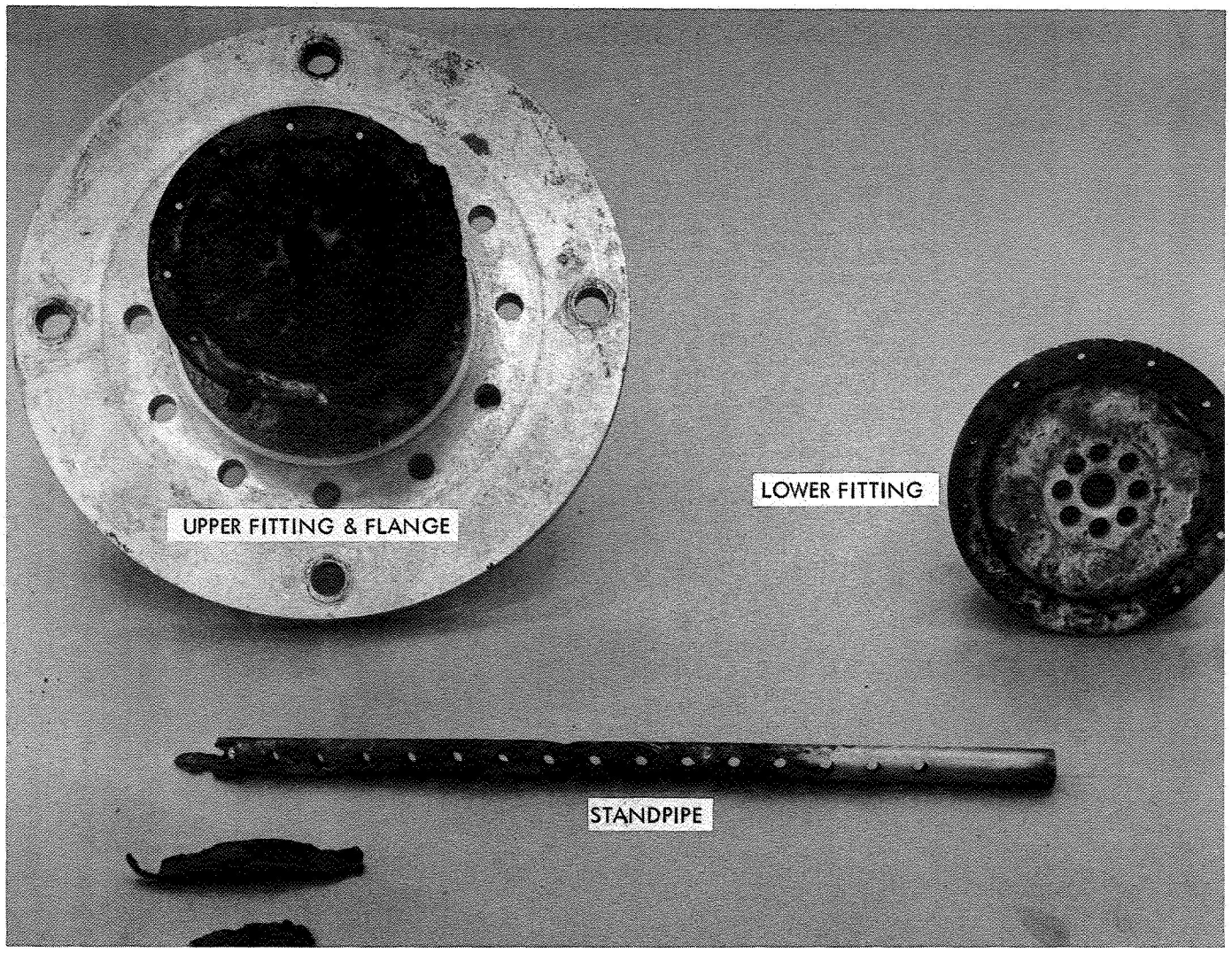

FIGURE 57 KAPTON BLADDER ATTACHMENT HARDWARE

FIGURE 58 ALUMINUM TEST TANK WITHOUT FITTINGS

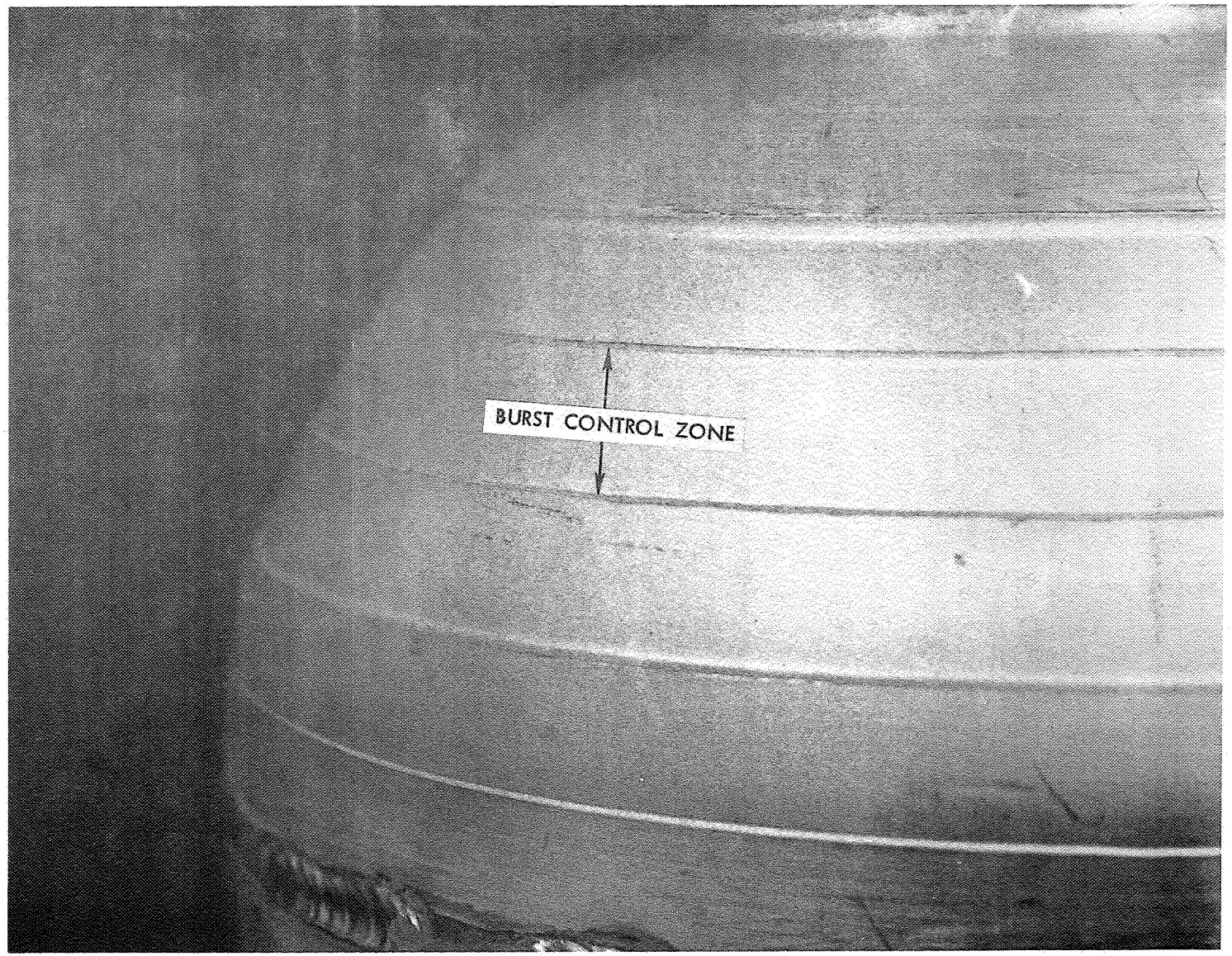

FIGURE 59 ALUMINUM TEST TANK — BURST CONTROL ZONE

The upper flange, the standpipe, and bladder fittings were the same ones used with the stainless steel tanks.

The aluminum tanks had no insulation.

3.3.4.3 Test Procedure - Each tank was installed in the test facility and filled with liquid oxygen to the 50% level. Frost forming on the exterior of the tank provided sufficient insulation. When the liquid level stabilized, the system was closed and the tank pressurized to failure with helium gas, at a rate of 10 psi per second. Movie coverage was made of each test.

3.3.4.4 Test Results - The first tank, containing the Mylar bladder, burst at a pressure of 123 psi (-297°F) and the second tank, with the Kapton bladder, failed at 126 psi (-297°F). Figures 60 to 68 show each tank/bladder assembly after test.

No sign of liquid oxygen incompatibility (no charring or ignition) was noted on either bladder or tank. Both bladders experienced extensive damage (Figures 61 and 65) as one would expect. The damage was concentrated in the burst area with a considerable amount of crack propagation and tearing radiating from the area.

The bladders remained firmly attached to the stems. There was no evidence that the bladder was extruded in the small gap between the tank wall and the bladder stem indicating the design tolerances in this area provided adequate support. The barrier films were not "blown" in this region from over pressurization, although there was random film damage from crack propagation extending to the stems.

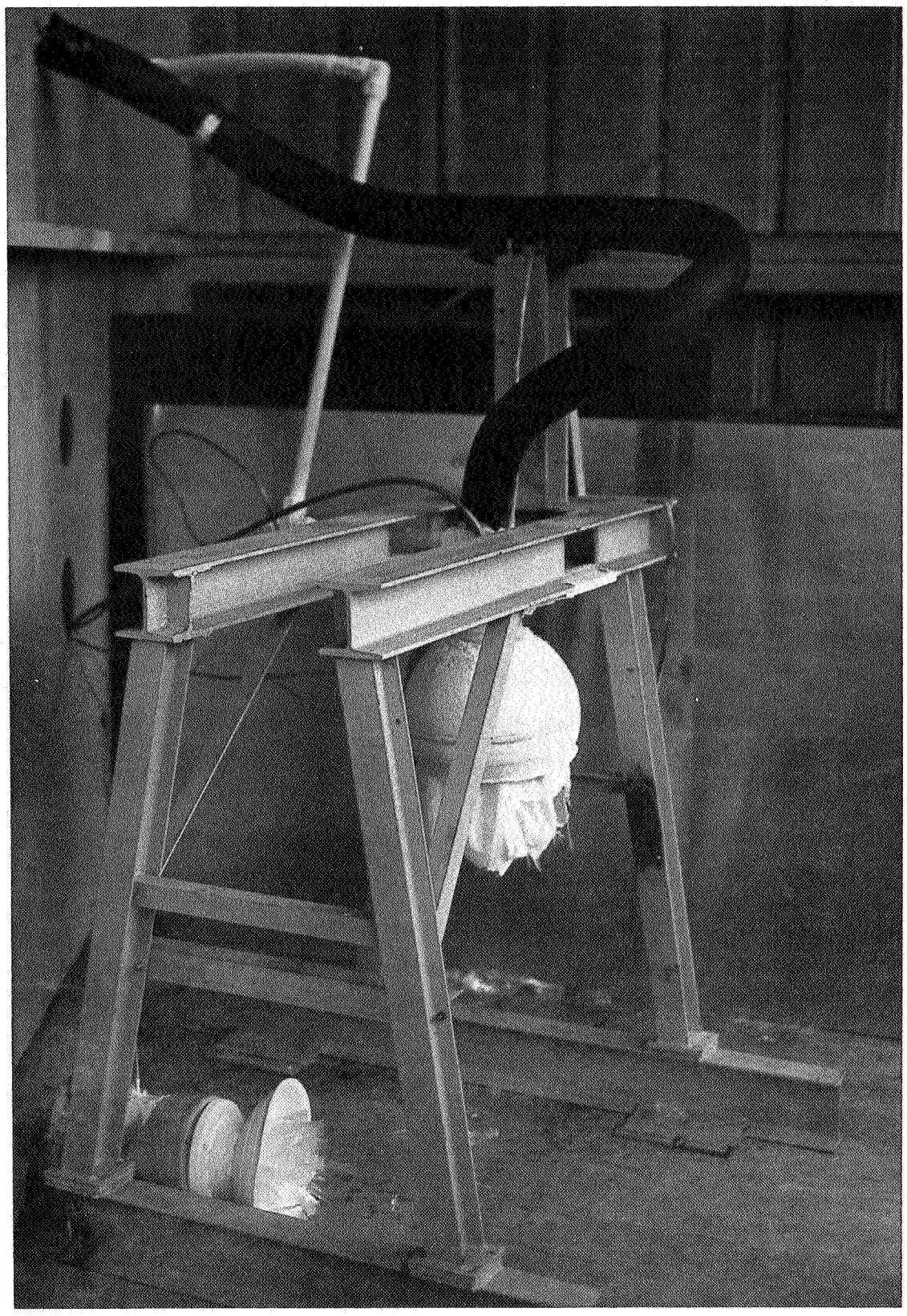

FIGURE 60 MYLAR BLADDER AFTER BURST TEST

FIGURE 61 MYLAR BLADDER AFTER BURST TEST

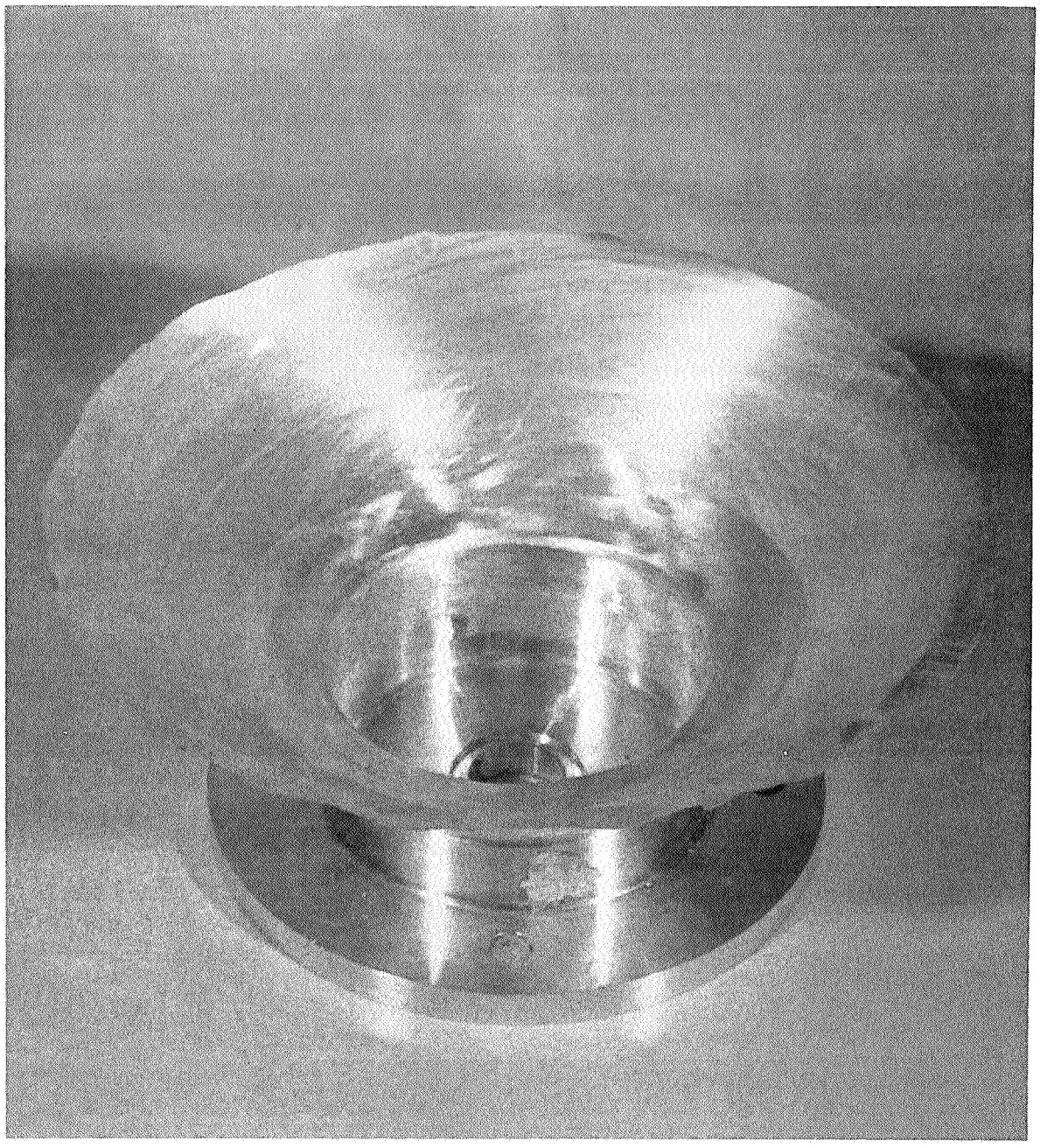

FIGURE 62 (MYLAR) BURST TANK — AFTER TEST

FIGURE 63 (MYLAR) BURST TANK — AFTER TEST

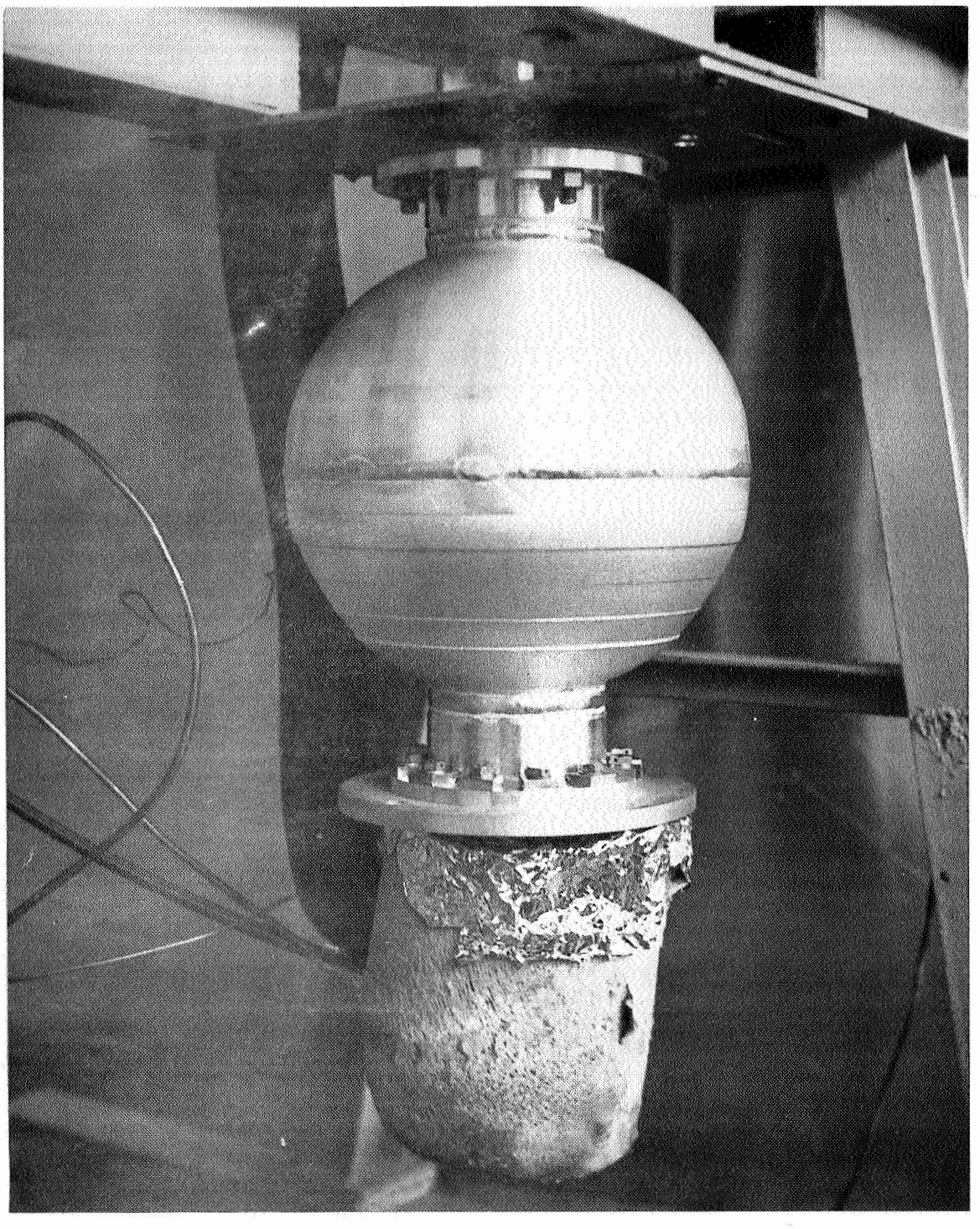

FIGURE 64 (KAPTON) BURST TANK — BEFORE TEST

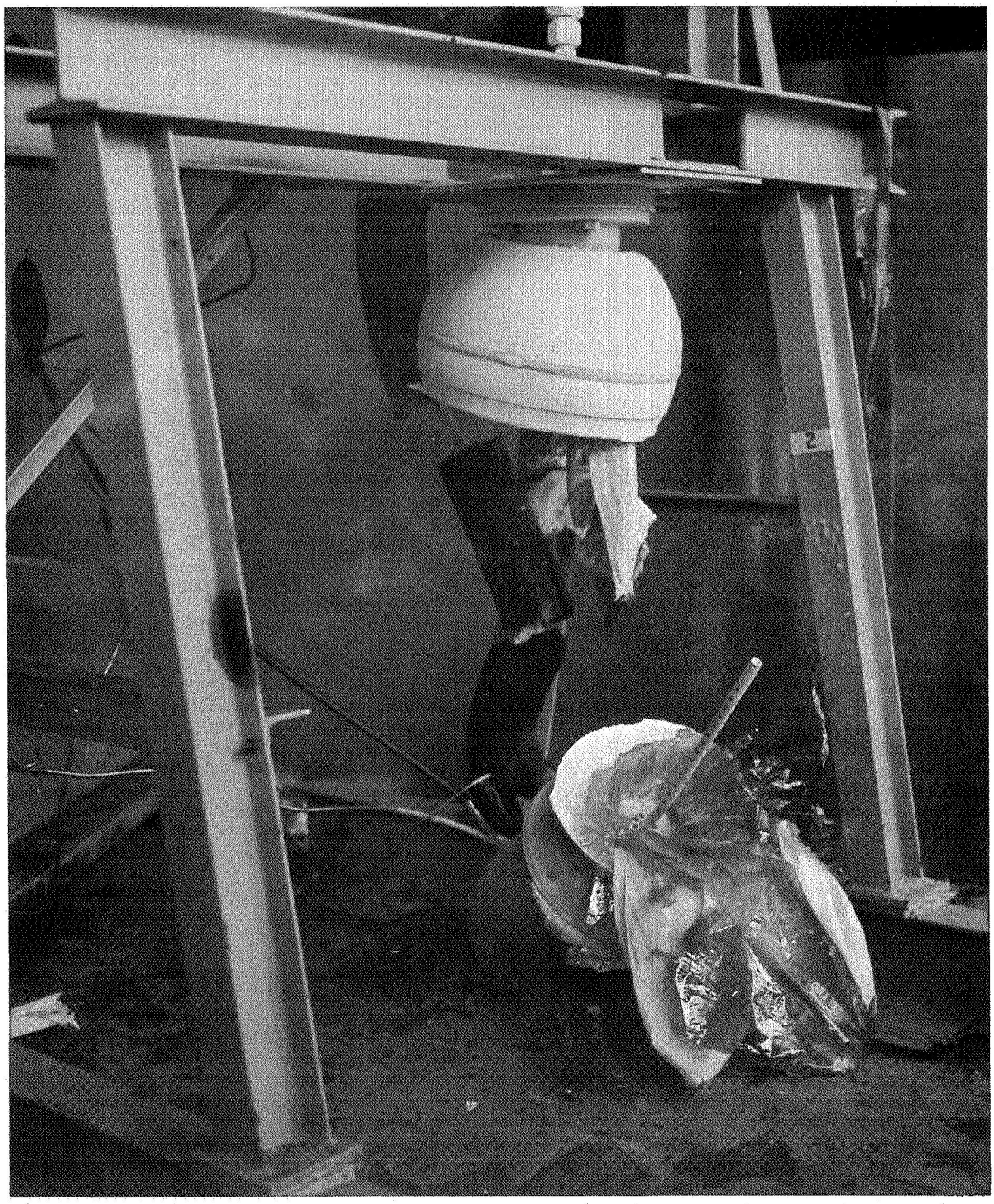

FIGURE 65 (KAPTON) BURST TANK - AFTER TEST

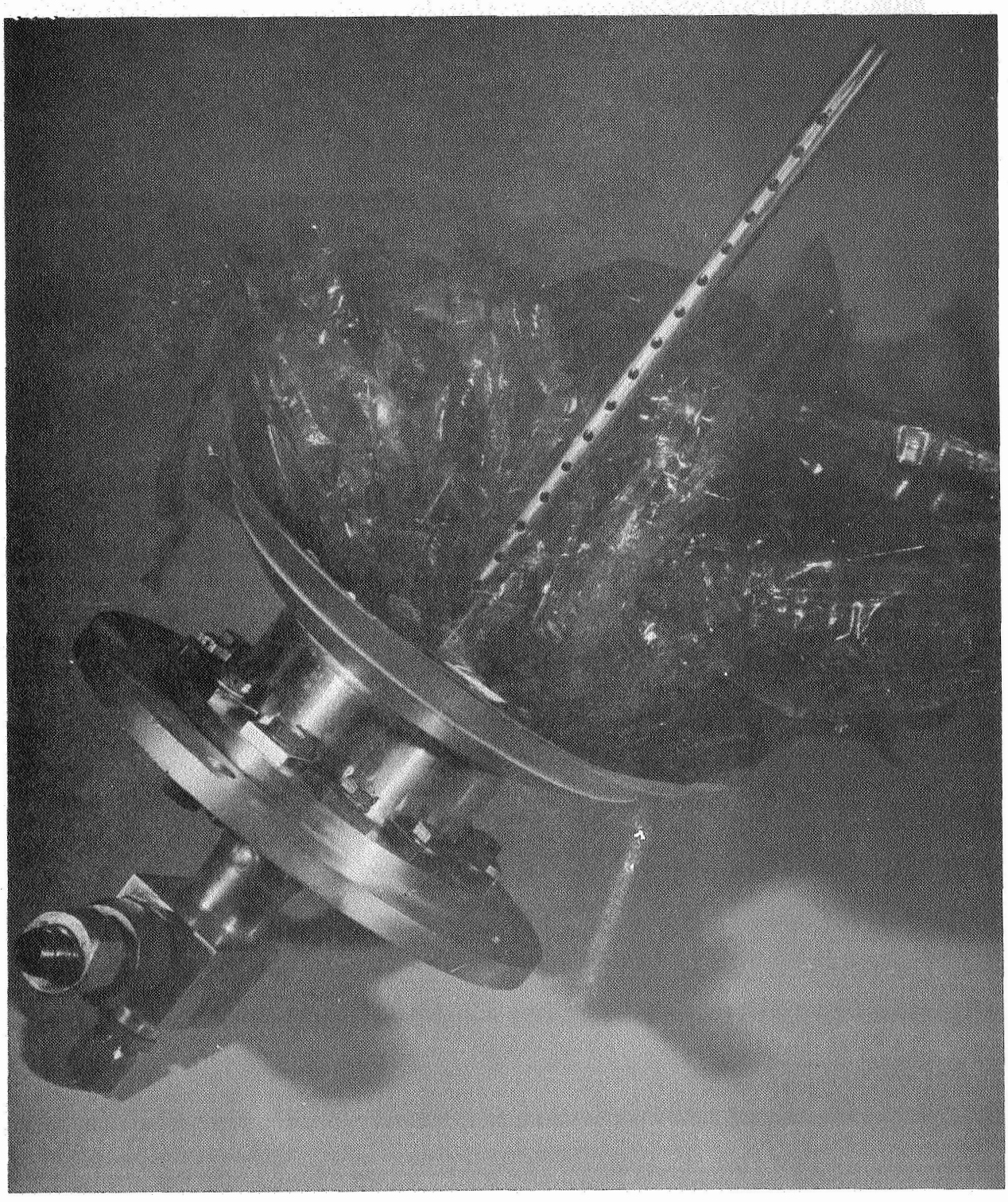

FIGURE 66 KAPTON BLADDER AFTER BURST TEST

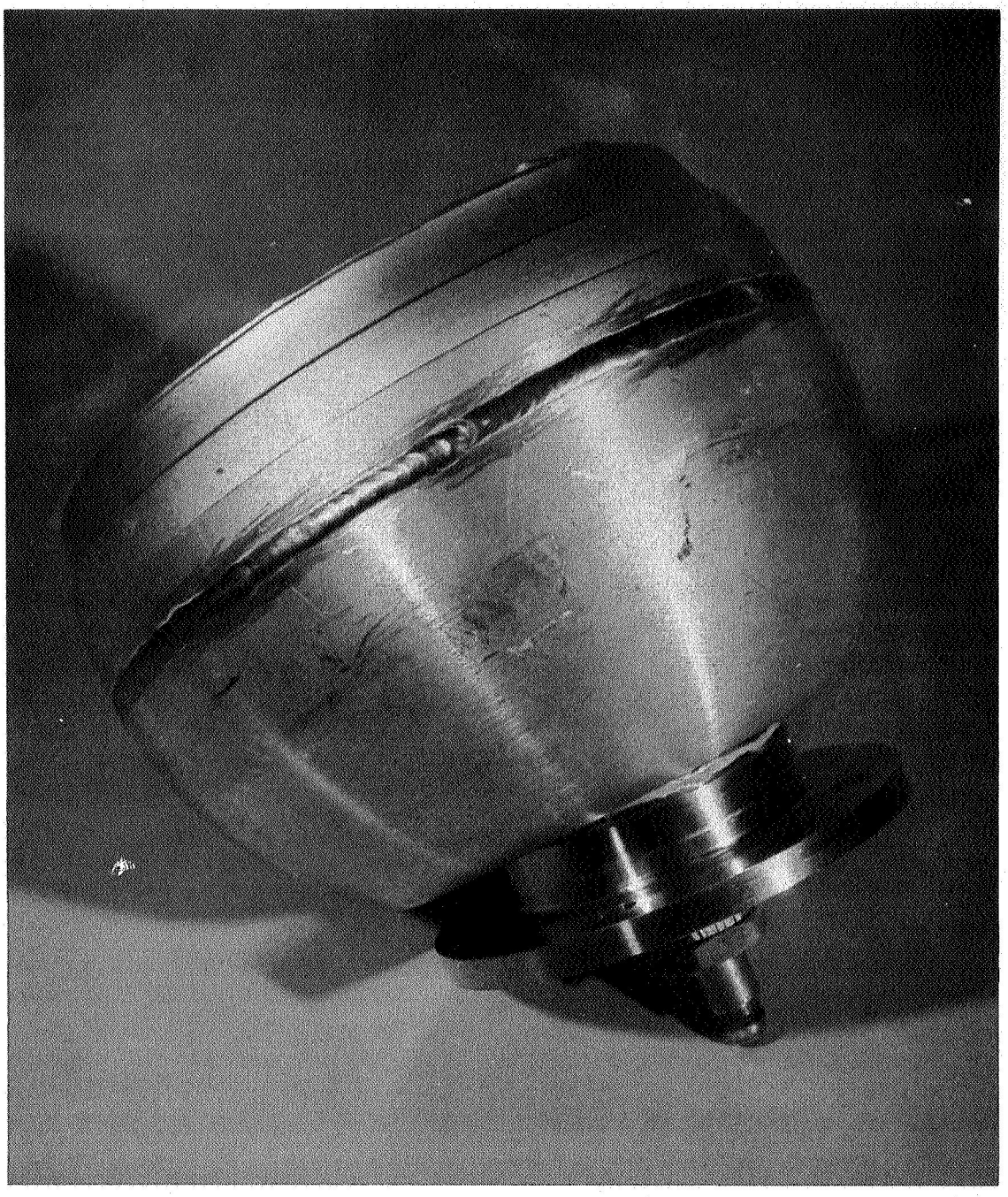

FIGURE 67 (KAPTON) BURST TANK — AFTER TEST

FIGURE 68 (KAPTON) BURST TANK — AFTER TEST

4.0 DISCUSSION OF RESULTS

4.1 EXPULSION EVALUATION

In the expulsion evaluations the 10 ply 12-gore Kapton bladders gave the best overall performance and were the only bladders to reach the program goal of 25 expulsion cycles without a major failure (i.e. leakage rate $<$ 200 cc/minute). Seventeen cycles were the maximum number of expulsion cycles that could be obtained with a Mylar film bladder.

Most of the leakage in the Kapton bladders and one of the Mylar bladders (No. 3) occurred in the stem attachment area. The method used to seal the bladders to their aluminum fittings was not reliable at cryogenic temperatures even though leak checks were made at room temperature prior to test. A slight redesign should be made in the fittings to provide a more positive seal and also to give the bladder a little more internal support. The need for this added support was evident from the vibration tests of Task III.

The failures in the film portion of the bladders did not follow any particular pattern. Most of the failures were concentrated in the stem attachment areas as would be expected since this is the ara of highest stress, but they were randomly located in this region.

The abrasion and substrate plies performed very well. There were only a few instances where the fabric seams failed due to a poor adhesive interlock with the fabric. These failures were generally 1" - 2" long and appeared to have no effect on bladder performance. Although its not conclusive from the limited tests performed, it appears that the lack of a fabric substrate ply is one of the reasons for the early failures in the 5-ply bladders.

The fill efficiency of all the bladders averaged 84% and the expulsion efficiency averaged 82%. For the 10 ply 12-gore Kapton bladders (#4, 5, and 6) the average

fill and expulsion efficiencies were 82% and 83% respectively. Tests conducted at room temperature, with water as the expelling fluid and air as the expelling gas, demonstrated that a fill efficiency of 99% and an expulsion efficiency of 98% could be obtained. Bladder No. 6 exhibited the highest fill performance and bladder No. 4 the highest expulsion efficiency. About 99% expulsion was obtained with bladder No. 4 which is equivalent to that obtained with water.

There were no signs of liquid oxygen incompatibility in any of the expulsion tests.

4.2 DYNAMIC EVALUATIONS

The magnitude and duration of the dynamic environments in Task III were representative of those which an expulsion bladder may experience in an actual system. The test demonstrated that a polymeric bladder, either Mylar or Kapton, could withstand these dynamic responses without any signs of incompatibility with the liquid oxygen propellant. The blunt impacts at 216 ft/lbs caused severe deformation of the stainless steel test tanks without causing any damage to the contained bladders. Yet these same bladder materials, when tested in Task I according to the ABMA LOX impact tests, would react in LOX with as little as 14.4 ft/lbs under direct impact. This gives indication that very little energy is absorbed by the bladder.

Both the Mylar and Kapton bladders showed signs of ignition when the tank was penetrated by a high velocity projectile. However, it should be noted that the Mylar bladder, even though charred, failed to support combustion in the oxygen atmosphere. This somewhat substantiates some of the conclusions Blackstone (Reference 5) drew from his LOX impact tests with Mylar. Namely, that Mylar does not sustain combustion very readily in a liquid oxygen atmosphere even though it chars at a relatively low impact level of energy. The Kapton bladder did support combustion after it was penetrated by a projectile. Blackstone also reported that Kapton, like Mylar, did not readily sustain combustion. The only difference between

the Mylar and Kapton ballistic penetration tests was that the projectile entered the test tank containing the Mylar bladder a distance of 1" above center while in the case of the Kapton bladder it was directly on center. It is highly probable that the slug hit above the liquid level in the case of the Mylar bladder, since the tank was only one-half full of LOX at the time of impact. Additional penetration tests need to be conducted on both materials before any firm conclusion can be drawn.

The polymeric bladders withstood, with the exception of lateral vibration, the slosh, vibration and impact loadings without any detriment to the structural integrity of the bladder. Bladder failures in the antisymmetric vibration loadings resulted from inadequate support of the bladder from the inside. This can be remedied by a slight redesign in the bladder fitting.

In summary, the program as a whole demonstrated that a Kapton bladder can be successfully expulsion cycled in liquid oxygen and withstand realistic dynamic loadings without serious impairment of its structural integrity or fear of liquid oxygen incompatibility.

5.0 CONCLUSIONS

1. Ten-ply 12-gore Kapton film bladders with 2 abrasion plies and 1 substrate ply, can withstand 25 expulsion cycles at -297° without serious functional impairment. Based on the data obtained and the results from previous programs (Refer ence 4, 6 and 8) the polymeric bladders should have approximately 10 barrier film plies. A greater number of plies, such as 20, or few plies, such as 5, may impair the performance capabilities of the bladder.

2. The current stem design, although an improvement over previous designs, needs additional refinements to provide a more positive seal and lend more support to the bladder from the underside.

3. The fabrication and quality control procedures were highly satisfactory for bladder fabrication.

4. No signs of interply inflation were noted other than that resulting from a failure of the innermost plies which permitted substantial quantities of oxygen to become trapped between barrier films. Inward mode of expulsion appears satisfactory for liquid oxygen systems.

5. The current polymeric expulsion bladder materials are capable of withstanding representative dynamic loadings which a propulsion system may experience in service. The bladder stem needs a slight modification to fulfill its role but their design does not appear to be a serious problem. By correcting the deficiencies in the stem design, the test data indicates that a polymeric expulsion bladder as part of a propulsion system, can be fabricated which will meet the expulsion and structural integrity requirements established at the onset of this program.

6.0 RECOMMENDATIONS

It is recommended that additional investigations be conducted with Kapton film bladders towards the development of a flight worthy expulsion bladder system. These investigations should encompass the following areas of study.

a. A study should be conducted to develop a LOX compatible adhesive which is suitable for bladder fabrication. This would enable Kapton bladders to be fabricated with materials which qualify to the ABMA LOX impact sensitivity test.

b. The effect of long term storage on bladder performance in fuel contamination, gas permeability and LOX compatibility needs to be established. The storage times and the limits of acceptability for each parameter need to be based on typical missions in which such expulsion devices may be used.

c. A prototype expulsion bladder system, including both the tank and bladder, should be fabricated and tested. The design and operational parameters should be selected from and the bladder performance and efficiency compared to an existing liquid oxygen propulsion system. The study should compare performance, reliability, cost, weight savings and the net system benefits. If the diameter of the prototype bladder is a factor of two greater than that of the current bladders, the effects of the scale-up should be thoroughly determined in the study. Additional qualification studies could follow if the above program reveals that a polymeric expulsion bladder will meet system performance requirements and results in a net system improvement.

7.0 REFERENCES

1. Hoggatt, J. T., "Compatibility of Polymeric Films With Liquid Oxygen," NASA CR-72134, The Boeing Company, Seattle, Washington, January 1967.

2. Key, C. F. and Riehl, W. A., "Compatibility of Materials With Liquid Oxygen," NASA TMX-985, National Aeronautics and Space Administration, August 1964.

3. "Testing Compatibility of Materials for Liquid Oxygen Systems," NASA, MSFC-SPEC-106A.

4. Pope, D. H., Penner, J. E., "Development of Cryogenic Positive Expulsion Bladders," NASA CR-72115. Beech Aircraft Corporation, Boulder, Colorado, January 1968.

5. Blackstone, W. R. et al, "Development of New Test Techniques for Determining The Compatibility of Materials with Liquid Oxygen Under Impact," AFAPL-TR-67-41 Southwest Research Institute, December 1967.

6. NASA Contract NAS-3-11192, "Development of Liquid Hydrogen Positive Expulsion Bladders, "The Boeing Company, Seattle, Washington.

7. Unpublished Data, NASA-Lewis Research Center, Cleveland, Ohio.

8. Unpublished Data, The Boeing Company, Seattle, Washington.

9. McCarty, J. L., Stephans, D. G., "Investigation of the Natural Frequencies of Fluids in Spherical and Cylindrical Tasks", NASA Technical Note D-252.

10. Budiansky, B., "Sloshing of Liquids in Circular Canals and Spherical Tanks", Journal of the Aero/Space Sciences, Volume 27, No. 3, March 1960.

11. Kana, D. D., "An Experimental Study of Liquid Surface Oscillations In Longitudinally Excited Compartmented Cylindrical and Spherical Tanks," NASA CR-545, August 1966.

12. D2-23391, "Cleaning Contamination Sensitive Parts," The Boeing Company, Seattle, Washington.

13. Bulletin T-10, "Properties and Processing of Teflon Fiber," E. I. DuPont De Nemours and Company, Wilmington, Delaware, April 1965.

DISTRIBUTION LIST

		Copies
National Aeronautics and Space Administration Lewis Research Center 21000 Brookpark Road Cleveland, Ohio 44135		
Attention:	Contracting Officer, MS 500-210	1
	Liquid Rocket Technology Branch, MS 500-209	8
	Technical Report Control Office, MS 5-5	1
	Technology Utilization Office, MS 3-16	1
	AFSC Liaison Office, MS 4-1	2
	Library	2
	Office of Reliability & Quality Assurance, MS 500-203	1
	E. W. Conrad, MS 100-1	1
National Aeronautics and Space Administration Washington, D.C. 20546		
Attention:	Code MT	1
	RPX	2
	RPL	2
	SV	1
	N. J. Mayer, RV-2	1
	A. O. Tischler, RP	1
	B. Achhammer, RRM	1
Scientific and Technical Information Facility P. O. Box 33 College Park, Maryland 20740		
Attention:	NASA Representative Code CRT	6
National Aeronautics and Space Administration Ames Research Center Moffett Field, California 94035		
Attention:	Library	1
National Aeronautics and Space Administration Flight Research Center P. O. Box 273 Edwards, California 93523		
Attention:	Library	1

		Copies
National Aeronautics and Space Administration Goddard Space Flight Center Greenbelt, Maryland 20771 Attention:	Library	1
National Aeronautics and Space Administration John F. Kennedy Space Center Langley Station Hampton, Virginia 23365 Attention:	Library	1
National Aeronautics and Space Administration Manned Spacecraft Center Houston, Texas 77001 Attention:	Library	1
National Aeronautics and Space Administration George C. Marshall Space Flight Center Huntsville, Alabama 35812 Attention:	Library	1
	Keither Chandler, R-P&VE-PA	1
	Harry L. McDaris, T-T/TR-ST	1
	John T. Shell, R-P&VE-NMR	1
	Wilbur A. Riehl, R-P&VE-MC	1
National Aeronautics and Space Administration Western Operations Office 150 Pico Boulevard Santa Monica, California 90406 Attention:	Library	1
Jet Propulsion Laboratory 4800 Oak Grove Drive Pasadena, California 91103 Attention:	Library	1
	D. D. Lawson	1
	Howard Stanford	1
Office of the Director of Defense Research & Engineering Washington, D.C. 20301 Attention:	Dr. H. W. Schulz, Office of Asst. Dir. (Chem. Technology)	1
Defense Documentation Center Cameron Station Alexandria, Virginia 22314		1

	Copies
RTD (RTNP) Bolling Air Force Base Washington, D.C. 20332	1
Arnold Engineering Development Center Air Force Systems Command Tullahoma, Tennessee 37389 Attention: AEOIM	1
Advanced Research Projects Agency Washington, D.C. 20525 Attention: D. E. Mock	1
Aeronautical Systems Division Air Force Systems Command Wright-Patterson Air Force Base, Dayton, Ohio Attention: D. L. Schmidt, Code ASRCNC-2	1
Air Force Missile Test Center Patrick Air Force Base, Florida Attention: L. J. Ullian	1
Air Force Systems Command (SCLT/Capt. S. W. Bowen) Andrews Air Force Base Washington, D.C. 20332	1
Air Force Rocket Propulsion Laboratory Edwards, California 93523 Attention: J. E. Branigan, RP-R-PT RPR RPM	1 1 1
Air Force FTC (FTAT-2) Edwards Air Force Base, California 93523 Attention: Col. J. M. Silk	1
Air Force Office of Scientific Research Washington, D.C. 20333 Attention: SREP, Dr. J. F. Masi	1
Office of Research Analyses (OAR) Holloman Air Force Base, New Mexico 88330 Attention: RRRT Maj. R. E. Brocken, Code MDGRT	1

	Copies
U. S. Air Force Washington 25, D.C. Attention: Col. C. K. Stambaugh, Code AFRST	1
Commanding Officer U. S. Army Research Office (Durham) Box CM, Duke Station Durham, North Carolina 27706	1
U. S. Army Missile Command Redstone Scientific Information Center Redstone Arsenal, Alabama 35808 Attention: Chief, Document Section Dr. W. Wharton	1 1
Bureau of Naval Weapons Department of the Navy Washington, D. C. Attention: J. Kay, Code RTMS-41	1
Commander U. S. Naval Missile Center Point Mugu, California 93041 Attention: Technical Library	1
Commander U. S. Naval Ordnance Test Station China Lake, California 93557 Attention: Code 753 W. F. Thorm, Code 4562	1 1
Commanding Officer Office of Naval Research 1030 E. Green Street Pasadena, California 91101	1
Director (Code 6180) U. S. Naval Research Laboratory Washington, D.C. 20390 Attention: H. W. Carhart	1
Picatinny Arsenal Dover, New Jersey Attention: I. Forsten, Chief Liquid Propulsion Laboratory	1

	Copies
U. S. Atomic Energy Commission Technical Information Services Box 62 Oak Ridge, Tennessee Attention: A. P. Huber, Code ORGDP Box P	1
Air Force Aero Propulsion Laboratory Research and Technology Division Air Force Systems Command United States Air Force Wright-Patterson Air Force Base, Ohio 45433 Attention: APRP (C. M. Donaldson) R. Quigley	1 1
Aerospace Corporation P. O. Box 95085 Los Angeles, California 90045 Attention: Library-Documents W. Heller	1 1
ARO, Incorporated Arnold Engineering Development Center Arnold AF Station, Tennessee 37389 Attention: Dr. B. H. Goethert Chief Scientist	1
Beech Aircraft Corporation Boulder Facility Box 631 Boulder, Colorado 80301 Attention: Douglas Pope	1
Bell Aerosystems, Inc. Box 1 Buffalo, New York 14205 Attention: Library	1
Bendix Systems Division Bendix Corporation Ann Arbor, Michigan Attention: John M. Bureger	1

	Copies
Chemical Propulsion Information Agency Applied Physics Laboratory 8621 Georgia Avenue Silver Spring, Maryland 20910	1
Lockheed-California Company 10445 Glen Oaks Blvd. Pacoima, California Attention: G. D. Brewer	1
Lockheed Propulsion Company P. O. Box 111 Redlands, California 92374 Attention: Miss Belle Berlad, Librarian	1
Lockheed Missiles & Space Company Propulsion Engineering Division (D.55-11) 1111 Lockheed Way Sunnyvale, California 94087	1
Marquardt Corporation 16555 Saticoy Street Box 2013 - South Annex Van Nuys, California 91404 Attention: Librarian	1
Martin-Marietta Corporation Martin Division Baltimore 3, Maryland Attention: John Calathes (3214)	1
McDonnell Aircraft Corporation P. O. Box 6101 Lambert Field, Missouri Attention: R. A. Herzmark	1
North American Aviation, Inc. Space & Information Systems Division 12214 Lakewood Boulevard Downey, California 90242 Attention: Technical Information Center, D/096-722 (AJ01)	1

	Copies
Northrop Space Laboratories 1001 East Broadway Hawthorne, California Attention: Dr. William Howard	1
Purdue University Lafayette, Indiana 47907 Attention: Technical Librarian	1
Radio Corporation of America Astro-Electronics Division Defense Electronic Products Princeton, New Jersey Attention: S. Fairweather	1
Republic Aviation Corporation Farmingdale, Long Island New York Attention: Dr. William O'Donnell	1
Rocket Research Corporation 520 South Portland Street Seattle, Washington 98108	1
Rocketdyne Division of North American Aviation, Inc. 6633 Canoga Avenue Canoga Park, California 91304 Attention: Library, Department 596-306	1
Rohm and Haas Company Redstone Arsenal Research Division Huntsville, Alabama 35808 Attention: Librarian	1
Space-General Corporation 777 Flower Street Glendale, California Attention: C. E. Roth	1
Stanford Research Institute 333 Ravenswood Avenue Menlo Park, California 94025 Attention: Thor Smith	1

	Copies
Lockheed Missiles & Space Company P. O. Box 504 Sunnyvale, California Attention: Technical Information Center	1
Thiokol Chemical Corporation Alpha Division, Huntsville Plant Huntsville, Alabama 35800 Attention: Technical Director	1
Thiokol Chemical Corporation Reaction Motors Division Denville, New Jersey 07834 Attention: Librarian	1
Thiokol Chemical Corporation Redstone Division Huntsville, Alabama Attention: John Goodloe	1
TRW Systems, Incorporated 1 Space Park Redondo Beach, California 90200 Attention: STL Tech. Lib. Doc. Acquisitions	1
LTV Astro Division P. O. Box 6267 Dallas, Texas 75222 Attention: Library	1
United Aircraft Corporation Corporation Library 400 Main Street East Hartford, Connecticut 06118 Attention: Library	1
United Aircraft Corporation Pratt & Whitney Division Florida Research & Development Center P. O. Box 2691 West Palm Beach, Florida 33402 Attention: Library	1

	Copies
United Aircraft Corporation United Technology Center P. O. Box 358 Sunnyvale, California 94088 Attention: Librarian	1
Curtiss-Wright Corporation Wright Aeronautical Division Woodridge, New Jersey Attention: G. Kelley	1
Douglas Aircraft Company, Inc. Santa Monica Division 3000 Ocean Park Blvd. Santa Monica, California 90405 Attention: Library	1
Fairchild Stratos Corporation Aircraft Missiles Division Hagerstown, Maryland Attention: J. S. Kerr	1
General Dynamics/Astronautics P. O. Box 1128 San Diego, California 92112 Attention: Library & Information Services (128-00)	1
Convair Division General Dynamics Corporation P. O. Box 1128 San Diego, California 92112 Attention: Mr. W. Fenning Centaur Resident Project Office	1
General Electric Company Re-Entry Systems Department P. O. Box 8555 Philadelphia, Pennsylvania 19101 Attention: F. E. Schultz	1
Grumman Aircraft Engineering Corporation Bethpage, Long Island, New York Attention: Joseph Gavin	1

		Copies
IIT Research Institute Technology Center Chicago, Illinois 60616 Attention:	C. K. Hersh, Chemistry Division	1
Air Force Material Laboratory Wright-Patterson Air Force Base, Ohio 45433 Attention:	C. G. Roach	1
	S. Litvak	1
	Lt. A. H. Birke, MANE	1
Sea-Space Systems, Inc. 1754 S. Crenshaw Blvd. Torrance, California Attention:	D. Struble	1
G. T. Schjeldahl Company Northfield, Minnesota Attention:	Library	1
Sandia Corporation P. O. Box 969 Luermore, California 94550 Attention:	Technical Library (RPT)	1
	H. Lucas	1